

530516

NASA Technical Memorandum 102857

---

# A Finite Element Procedure for Calculating Fluid-Structure Interaction Using MSC/NASTRAN

---

Mladen Chargin and Otto Gartmeier

---

(NASA-TM-102857) A FINITE ELEMENT PROCEDURE  
FOR CALCULATING FLUID-STRUCTURE INTERACTION  
USING MSC/NASTRAN (NASA) 168 p CSDL 20K

N91-16414

Unclass

G3/39 0329332

December 1990

---

# A Finite Element Procedure for Calculating Fluid-Structure Interaction Using MSC/NASTRAN

---

Mladen Chargin, Ames Research Center, Moffett Field, California  
Otto Gartmeier, Daimler-Benz AG, Stuttgart, Germany

**ORIGINAL CONTAINS  
COLOR ILLUSTRATIONS**

December 1990



National Aeronautics and  
Space Administration

**Ames Research Center**  
Moffett Field, California 94035-1000

## FOREWORD

Even though Appendix A contains a list of symbols used in this report, additional explanation is provided. In section 2,  $\partial/\partial t$  represents the time derivative, but in section 3, in the discussion of finite element modelling, ' $\dot{x}$ ' is used. For the scalar product '.' is used and for the vector product, ' $\times$ '. Vector quantities are underlined except in the finite element formulation. Some symbols are not listed in Appendix A, but these are used only locally in specific subsections and are not referenced again in any other subsection.

# CONTENTS

---

SUMMARY.....	1
1. INTRODUCTION.....	1
2. MATHEMATICAL DESCRIPTION .....	4
2.1 Structure.....	4
2.2 Fluid.....	4
2.3 Linear Fluid.....	6
2.4 Boundary Conditions .....	11
2.5 Coupled Initial Boundary Value Problem.....	14
2.6 Coupled Boundary Value Problem .....	15
3. FINITE ELEMENT MODELLING .....	17
3.1 Structure.....	17
3.2 Linear Fluid.....	17
3.3 Fluid-Structure Coupling and Symmetrization.....	20
3.4 Aspects of Solving the Coupled Fluid-Structure Equation .....	22
3.4.1 Symmetrization .....	22
3.4.2 Modal reduction .....	24
3.4.3 Residual flexibility for the fluid.....	25
4. SPECIAL FEATURES .....	29
4.1 Acoustic Absorption.....	29
4.2 Acoustic Contribution Analysis.....	31
4.3 Structure-Fluid Analogy in MSC/NASTRAN.....	33
4.4 Boundary Conditions and Their Input in MSC/NASTRAN Using the Structure-Fluid Analogy .....	35
5. DESCRIPTION OF THE ACOUSTIC PROCEDURE.....	37
5.1 Introductory Remarks.....	37
5.2 Organization and Flowchart of the Acoustic Procedure.....	37
6. DESCRIPTION OF THE USER INTERFACE.....	41



<b>6.1 Modelling Aspects</b> .....	41
6.1.1 Fluid .....	41
6.1.2 Coupling of structure and fluid .....	41
6.1.3 Use of superelements .....	42
<b>6.2 Fluid Media</b> .....	43
6.2.1 Grid point definition .....	43
6.2.2 Element definition .....	43
6.2.3 Acoustic absorption .....	43
6.2.4 Loading .....	43
<b>6.3 Uncoupled Normal Modes Analysis of Structure and Fluid (Run 1)</b> .....	44
6.3.1 Executive Control Deck .....	44
6.3.2 Case Control Deck .....	44
6.3.3 Bulk Data Deck .....	45
6.3.4 Area matrix program input/output .....	47
6.3.4.1 Input files .....	48
6.3.4.2 Output files .....	50
6.3.4.3 Absorption property interpolation .....	51
<b>6.4 Normal Modes Analysis of the Modal Coupled Fluid- Structure System (Run 2)</b> .....	53
6.4.1 Executive Control Deck .....	54
6.4.2 Case Control Deck .....	55
6.4.3 Bulk Data Deck .....	55
<b>6.5 Modal Frequency Response Analysis (Run 3.1)</b> .....	55
6.5.1 Executive Control Deck .....	56
6.5.2 Case Control Deck .....	56
6.5.3 Bulk Data Deck .....	57
<b>6.6 Modal Transient Response Analysis (Run 3.2)</b> .....	58
<b>6.7 Structural Grid Point Participation (Run 4)</b> .....	58
6.7.1 Executive Control Deck .....	59
6.7.2 Case Control Deck .....	59
6.7.3 Bulk Data Deck .....	59
6.7.4 Output .....	60

<b>7. DEMONSTRATION OF ACOUSTIC CALCULATIONS AND THEORETICAL VERIFICATION</b> .....	62
7.1.1 Description of the model .....	62
7.1.2 Theoretical solution .....	63
7.1.2.1 Coupled Eigenanalysis .....	64
7.1.2.2 Frequency response analysis .....	68
7.1.2.3 Transient response analysis .....	74

7.1.3	Finite element approximation and comparison with theoretical results.....	75
7.1.3.1	Finite element model.....	75
7.1.3.2	Uncoupled and coupled eigenanalysis.....	76
7.1.3.3	Frequency response results.....	79
7.1.3.4	Acoustic contribution analysis.....	81
7.1.3.4	Transient response.....	89
7.2	<b>Two-dimensional fluid-structure system.....</b>	<b>89</b>
7.2.1	Problem Description.....	91
7.2.2	Theoretical solution.....	92
7.2.3	Two-dimensional Nastran finite element model.....	93
7.2.4	Normal Modes Analysis - SOL 63, 70.....	94
7.2.4.1	Beam-only results.....	94
7.2.4.2	Fluid with rigid boundary results.....	95
7.2.4.3	Coupled fluid-structure modal results.....	96
7.2.5	Modal frequency response analysis - SOL 71.....	98
7.2.6	Fluid-beam grid participation factor calculation.....	101
8.	<b>VEHICLE ACOUSTIC ANALYSIS.....</b>	<b>102</b>
8.1	<b>Structural Model.....</b>	<b>102</b>
8.2	<b>Fluid Model of the Passenger Compartment.....</b>	<b>105</b>
8.3	<b>Modal Analysis of the Complete Model, Structure and Fluid.....</b>	<b>107</b>
8.4	<b>Response Analysis During Harmonic Excitation.....</b>	<b>111</b>
8.5	<b>Grid Point Participation Factor Calculation.....</b>	<b>112</b>
<b>APPENDIX A</b>		
	Notations.....	117
<b>APPENDIX B</b>		
	INPUT DECKS FOR SECTION 7.1.....	121
<b>APPENDIX B1</b>		
	Run 1 Input - One-Dimensional Piston/Tube Model.....	123
<b>APPENDIX B2</b>		
	Run 2 Input - One-Dimensional Piston/Tube Model.....	131
<b>APPENDIX B3.1</b>		
	Run 3.1 Input - One-Dimensional Piston/Tube Model.....	133
<b>APPENDIX B3.2</b>		
	Run 3.2 Input - One-Dimensional Piston/Tube Model.....	137

<b>APPENDIX B4</b>	
Run 4 Input - One-Dimensional Piston/Tube Model .....	141
<b>APPENDIX C</b>	
<b>INPUT DECKS FOR SECTION 7.2</b> .....	143
<b>APPENDIX C1</b>	
Run 1 Input - Two-Dimensional Fluid/Beam Model.....	145
<b>APPENDIX C2</b>	
Run 2 Input - Two-Dimensional Fluid/Beam Model.....	149
<b>APPENDIX C3.1</b>	
Run 3.1 Input - Two-Dimensional Fluid/Beam Model .....	151
<b>APPENDIX C3.2</b>	
Run 3.2 Input - Two-Dimensional Fluid/Beam Model .....	155
<b>APPENDIX C3.3</b>	
Run 3.3 Input - Two-Dimensional Fluid/Beam Model .....	157
<b>APPENDIX C3.4</b>	
Run 3.4 Input - Two-Dimensional Fluid/Beam Model .....	161
<b>APPENDIX C4</b>	
Run 4 Input - Two-Dimensional Fluid/Beam Model.....	165
<b>APPENDIX D</b>	
<b>INPUT DECKS FOR SECTION 8</b> .....	167
<b>APPENDIX D1</b>	
Run 1 Input - Vehicle Acoustic Analysis .....	169
<b>APPENDIX D3.1</b>	
Run 3.1 Input - Vehicle Acoustic Analysis.....	173
<b>APPENDIX D4</b>	
Run 4 Input - Vehicle Acoustic Analysis .....	175
<b>References</b> .....	177

## SUMMARY

This report is intended to serve two purposes. The first is to give a survey of the theoretical background of the dynamic interaction between a non-viscid, compressible fluid and an elastic structure. Section 1 presents a short survey of the application of finite element method (FEM) to the area of fluid-structure-interaction (FSI). Section 2 describes the mathematical foundation of the structure and fluid with special emphasis on the fluid. The main steps in establishing the finite element (FE) equations for the fluid structure coupling are discussed in section 3.

The second purpose of this report is to demonstrate the application of MSC/NASTRAN to the solution of FSI problems. Some specific topics, such as fluid structure analogy, acoustic absorption, and acoustic contribution analysis are described in section 4. Section 5 deals with the organization of the Acoustic Procedure implemented in MSC/NASTRAN. Steps which have to be performed for a complete acoustic analysis are illustrated by a flowchart. Section 6 includes the most important information that a user needs for applying the Acoustic Procedure to practical FSI problems. Beginning with some rules concerning the FE modelling of the coupled system, the NASTRAN USER DECKs for the different steps are described. The goal of section 7 is to demonstrate the use of the Acoustic Procedure with some examples. This demonstration includes an analytic verification of selected FE results. The analytical description considers only some aspects of FSI and is not intended to be mathematically complete.

Finally, section 8 presents an application of the Acoustic Procedure to vehicle interior acoustic analysis with selected results.

## 1. INTRODUCTION

In many areas of everyday engineering the interaction between structure and fluid plays an important role. Phenomena of this kind have to be considered if a structure surrounds or is embedded within a fluid. The presence of the fluid can significantly alter the behavior of a structure, and at the same time, the deformation of the structure alters the loads transmitted from the fluid. This means that there exists an interaction in both directions: the structure acts on the fluid and vice versa. These phenomena are referred to as fluid-structure interaction (FSI).

These phenomena can be divided in subareas, such as: slow viscid flow, laminar flow, turbulent flow, shallow water flow, meteorology, acoustic phenomena and FSI.

In a 1982 paper of O.C. Zienkiewicz (ref. 1) one can find a more detailed discussion of these subareas. In that paper, research progress and the advantages and drawbacks of the FEM for the solution of FSI problems are described. An overview on the use of FEM in

fluid dynamics and related areas is presented in the Finite Elements in Fluids proceedings (ref. 2).

The present description deals only with the last two areas listed above, where the fluid is considered to be compressible and inviscid.

There are many problems in everyday engineering where fluid structure interaction is present. Sound radiation into passenger compartments of automobiles and airplanes is a typical example. The main purpose of acoustic calculations is to analyze the sound transmission into the passenger compartment and the coupling mechanisms between sound conducted through solids and sound propagation in fluids (e.g., air). Through the use of these techniques one can potentially influence the design of an automobile or an airplane by identifying structural components that produce high sound pressure levels in the passenger compartment.

The calculation of sound pressure distribution in an interior domain with complex shaped boundaries (a passenger compartment of an automobile) is not possible through the use of empirical formulas. Instead, numerical solutions of initial and boundary value problems for various interior domains with different types of boundaries (acoustic soft and rigid boundaries, elastic and absorptive boundaries) are used. Although there are some restrictions, FEM is a very useful and powerful tool for solving these kinds of problems.

This report presents a unique capability to perform FSI analysis using the finite element code MSC/NASTRAN. Through the use of this added capability, MSC/NASTRAN becomes a versatile tool for acoustic and noise control analysis.

The first work in the acoustic field was done by Gladwell and Zimmermann who presented two papers in the mid 1960s (see ref. 3 and 4). These papers include finite element (FE) formulations for coupled fluid-structure vibrations. Some years after these basic developments, Craggs presented, in a series of papers dated 1970-1973 (see refs. 5,6, and 7), a variational formulation for the coupled problem in terms of fluid pressure.

Very early it was realized that the commercial finite element codes, originally developed for analyzing structural mechanics problems, could be used to analyze scalar field problems as well (see ref. 8). With FEM it is possible to investigate standing waves and the related frequencies in any complex-shaped interior domain with rigid boundaries. In order to solve eigenvalue and response problems for the coupled fluid-structure systems, it is necessary to consider the elastic as well as the absorptive boundary conditions. This task is accomplished, in this procedure, through the use of the NASTRAN DMAP language (Direct Matrix Abstraction Program) and a single Fortran program. No changes to the source code of NASTRAN were necessary.

A description of this approach for solving the FSI problems can be found, e.g., in references 9, 10, and 11. Specifically, for the applications to the interior acoustics of automobiles, refer to references 12, 13, 14 and 15.

Besides the interaction of coupled fluid-structure systems via the elastic boundary condition, sound absorption effects at the boundary also have to be considered. In the present procedure, a simple normal impedance model was developed. This model is, in general, sufficient for describing the absorption effects at the boundary in the low frequency range.

Using a special boundary condition of D.B. Bliss (ref. 16), an oblique absorption damping can be described. An application can be found in reference 17. Also, A. Craggs published some papers which dealt with the question of boundary absorption and the description of such effects using the FE technique (see refs. 17, 18, and 19).

The procedure presented here can be embedded in the standard procedure of structural analysis. The fluid medium is treated simply as another part of the structure. This allows for a simultaneous solution of the two systems, without the need for separate analysis, as is presently done in some cases.

The procedure requires the use of superelement solution sequences, but it is not necessary to define superelements. In many cases, though, it is highly desirable to use superelements because of computational efficiency.

The complete procedure consists of five steps beginning with the uncoupled modal analysis of the structure and the fluid (with rigid boundaries). Following the eigenanalysis of the coupled system, response calculations in the time or frequency domain can be carried out. Furthermore, it is possible to perform an acoustic contribution analysis identifying the influence of the structure on the sound pressure level at an interior fluid point.

It should be noted that this capability is particularly applicable to the interior problems; that is, for problems in which the fluid is contained by the structure. The exterior problem, fluid outside the structure (e.g., submarines) is very difficult to solve with the FEM. In this case, the boundary element method is more applicable.

## 2. MATHEMATICAL DESCRIPTION

In this section, a mathematical description and a mathematical derivation of the FSI phenomenon are given. Because the dynamics equations for elastic media are well known (one can find a derivation in any book on structural or continuum mechanics), the main effort will be directed at deriving and describing the mathematics of the fluid and the FSI.

### 2.1 Structure

The structural components can be formulated as

$$L(\underline{u}_s) = \underline{F}(\underline{r}, t) \quad (1)$$

where  $L$  is a partial differential operator with respect to time and space. The vector,  $\underline{u}_s$ , represents the structural displacement vector, which is a function of location  $\underline{r}$  and time  $t$ . Finally,  $\underline{F}$ , is a time-dependent load on the structure, which can be divided into an external time-dependent load  $\underline{F}_e(\underline{r}, t)$  and the influence of the fluid pressure on the structure  $\underline{F}_p(\underline{r}, t)$ . That load will manifest itself through the surface load vector

$$\underline{F}_p(\underline{r}, t) = p(\underline{r}, t)\underline{n} \quad (2)$$

where  $p$  is the unsteady fluid pressure and  $\underline{n}$  is the outward unit normal vector at the fluid-structure interface.

Note: The subscript 's' denotes structure and 'f' the fluid.

### 2.2 Fluid

The governing equations for the fluid can be obtained from most books on fluid dynamics (see ref. 19), but it is useful to offer a complete derivation of these equations in order to get a more complete understanding of the problem. Some of the following mathematical explanations were initially given in reference 20.

For an arbitrary fluid volume,  $V(t)$ , the mass balance is given by

$$\frac{d}{dt} \left( \int_{V(t)} \hat{\rho} dV \right) = \int_{V(t)} q dV \quad (3)$$

where  $\hat{\rho}$  is the density and  $q$  is the added fluid mass per unit volume and time. Reversing the order of differentiation and integration yields

$$\int_{V(t)} \left( \frac{d\hat{\rho}}{dt} + \hat{\rho} \nabla \cdot \underline{v} \right) dV = \int_{V(t)} q dV \quad (4)$$

where  $\underline{v}$  is the fluid velocity field.

Because the volume,  $V(t)$ , is arbitrary,

$$\frac{d\hat{\rho}}{dt} + \hat{\rho} \nabla \cdot \underline{v} = q \quad (5)$$

Although, when the system matrices are defined later, a Raleigh-type damping will be taken into consideration, for now the viscosity will be neglected. Internal forces acting upon a volume,  $V(t)$ , in the fluid act at the boundary,  $S(t)$ , of that volume. Furthermore, they are perpendicular to the boundary, which is a consequence of the inviscid fluid assumption. External forces are the body forces,  $b$ , (per mass unit). Conservation of linear momentum yields

$$\frac{d}{dt} \int_{V(t)} \hat{\rho} \underline{v} dV = - \int_{S(t)} \hat{p} \underline{n} dS + \int_{V(t)} \hat{\rho} \underline{b} dV + \int_{V(t)} q \underline{v}_q dV \quad (6)$$

where  $\underline{v}_q$  is the velocity of the added fluid mass.

Interchanging the order of space integration and differentiation with respect to time on the left-hand side and applying the Gauss theorem to the first term on the right-hand side of equation (6), one can obtain the following equation:

$$\int_{V(t)} \left\{ \frac{d}{dt} (\hat{\rho} \underline{v}) + \hat{\rho} \underline{v} (\nabla \cdot \underline{v}) \right\} dV = \int_{V(t)} (-\nabla \hat{p} + \hat{\rho} \underline{b} + q \underline{v}_q) dV$$

As before, the volume will again be assumed to be arbitrary, which leads to

$$\frac{d}{dt} (\hat{\rho} \underline{v}) + \hat{\rho} \underline{v} (\nabla \cdot \underline{v}) = -\nabla \hat{p} + \hat{\rho} \underline{b} + q \underline{v}_q \quad (7)$$

Using equation (4),

$$\frac{d}{dt} (\hat{\rho} \underline{v}) = \frac{d\hat{\rho}}{dt} \underline{v} + \hat{\rho} \frac{d\underline{v}}{dt} = q \underline{v} - \hat{\rho} (\nabla \cdot \underline{v}) \underline{v} + \hat{\rho} \frac{d\underline{v}}{dt}$$

Combining this result with equation (7) results in

$$\hat{\rho} \frac{d\underline{v}}{dt} = -\nabla \hat{p} + \hat{\rho} \underline{b} - q (\underline{v} - \underline{v}_q) \quad (8)$$

Equations (4) and (7) are sufficient if the fluid is an incompressible fluid and  $\hat{\rho}$  is a known and time-invariant quantity. These equations can then be solved with respect to  $\hat{p}$  and  $\underline{v}$ . If



the fluid is compressible, then one more relation containing  $\hat{\rho}$  and  $\hat{p}$  is needed. Assuming the fluid motion is independent of temperature, the additional equation (equation of state) is

$$\hat{p} = \hat{p}(\hat{\rho}) \quad (9)$$

Summarizing the results so far,

$$\left. \begin{aligned} \frac{d\hat{\rho}}{dt} + \hat{\rho} \nabla \cdot \underline{v} &= q \\ \hat{\rho} \frac{d\underline{v}}{dt} + \nabla \hat{p} &= \underline{b} - q(\underline{v} - \underline{v}_q) \\ \hat{p} &= \hat{p}(\hat{\rho}) \end{aligned} \right\} \quad (10)$$

### 2.3 Linear Fluid

In the following section, some simplifications of the physical model of the fluid described by equations (10) are introduced, because they contain effects that can be neglected for the present purpose.

The variation of the density is divided into two parts. One contains a time-dependent part,  $\rho$ , and the other contains the static part,  $\rho_f$ . Thus

$$\hat{\rho} = \rho_f + \rho$$

where  $\nabla \rho_f = 0$ . The first equation of (10) can be rewritten

$$\frac{d\rho}{dt} + \rho_f \left( 1 + \frac{\rho}{\rho_f} \right) \nabla \cdot \underline{v} = q$$

Assuming the variation in time to be small compared to the static value, that is

$$\frac{|\rho|}{\rho_f} \ll 1$$

leads to

$$\frac{d\rho}{dt} + \rho_f \nabla \cdot \underline{v} = q$$

If the second equation of (10) is dealt with in the same way, the new system equations become

$$\left. \begin{aligned} \frac{d\hat{\rho}}{dt} + \hat{\rho}_f \nabla \cdot \underline{v} &= q \\ \hat{\rho}_f \frac{d\underline{v}}{dt} + \nabla \hat{p} &= \underline{b} - q(\underline{v} - \underline{v}_q) \\ \hat{p} &= \hat{p}(\hat{\rho}) \end{aligned} \right\} \quad (11)$$

The total time derivatives of  $\rho$  and  $\underline{v}$  are

$$\begin{aligned} \frac{d\rho}{dt} &= \frac{\partial \rho}{\partial t} + \underline{v} \cdot \nabla \rho \\ \frac{d\underline{v}}{dt} &= \frac{\partial \underline{v}}{\partial t} + (\underline{v} \cdot \nabla) \underline{v} \end{aligned}$$

The convective terms in these expressions and the influence of the added fluid mass,  $q$ , on the second equation in (11) are insignificant under a certain condition. This condition occurs when the fluid velocity is considerably smaller than the speed of sound. Mathematical derivation of that simplification is not shown.

Under such a condition, from equations (11)

$$\frac{\partial \rho}{\partial t} + \rho_f \nabla \cdot \underline{v} = q \quad (12)$$

$$\rho_f \frac{\partial \underline{v}}{\partial t} + \nabla \hat{p} = \rho_f \underline{b} \quad (13)$$

Together with the equation of state, equations (12) and (13) constitute a physical model for a linearized flow.

A further simplification is possible. As was done in the case of density, the pressure is divided into two parts,  $p$  and  $p_f$  (similar notation as for  $\hat{\rho}$ ), and the equation of state is linearized

$$\hat{p} = p_f + p \approx p_f + \rho \left( \frac{dp}{d\hat{\rho}} \right) \Big|_{\hat{\rho}=\rho_f}$$

where  $p_f$  is assumed constant. Introducing a new constant

$$c_f = \sqrt{\left(\frac{dp}{d\hat{\rho}}\right)_{\hat{\rho}=\rho_f}}$$

results in

$$p = c_f^2 \rho \quad (14)$$

Equation (12) is then differentiated with respect to time

$$\frac{\partial^2 \rho}{\partial t^2} + \nabla \cdot \left( \rho_f \frac{\partial \underline{v}}{\partial t} \right) = \frac{\partial q}{\partial t}$$

Substituting equation (13) into this expression yields

$$\frac{\partial^2 \rho}{\partial t^2} + \nabla \cdot (\rho_f \underline{b} - \nabla \hat{p}) = \frac{\partial q}{\partial t}$$

In this relation,  $p$  is replaced by  $\rho$  from equation (14) and  $\hat{p}$  is replaced by  $p+p_f$  implying

$$\frac{\partial^2 \rho}{\partial t^2} = c_f^2 \nabla^2 \rho + \nabla^2 p_o - \rho_f \nabla \cdot \underline{b} + \frac{\partial q}{\partial t}$$

From the definition of  $p_f$  above, the term  $\nabla p_f$  is zero and so the final result reduces to a wave equation with source terms,

$$\frac{\partial^2 \rho}{\partial t^2} = c_f^2 \nabla^2 \rho - \rho_f \nabla \cdot \underline{b} + \frac{\partial q}{\partial t} \quad (15)$$

By using equation (14), the wave equation can be expressed in terms of the pressure

$$\frac{\partial^2 p}{\partial t^2} = c_f^2 \nabla^2 p - c_f^2 \rho_f \nabla \cdot \underline{b} + c_f^2 \frac{\partial q}{\partial t} \quad (16)$$

Returning to equations (12) and (13), the gradient operator,  $\nabla$ , is applied to the first and the partial time derivative to the second of these equations. Solving with respect to  $\underline{v}$  leads to

$$\frac{\partial^2 \underline{v}}{\partial t^2} = c_f^2 \nabla (\nabla \cdot \underline{v}) + \frac{\partial \underline{b}}{\partial t} - \frac{c_f^2}{\rho_f} \nabla q \quad (17)$$

It may be noted that

$$\nabla(\nabla \cdot \underline{v}) = \nabla^2 \underline{v} + \nabla \times (\nabla \times \underline{v})$$

For a perfect fluid, as long as the body forces are derivable from a potential function, the velocity field, once irrotational, remains irrotational. Thus

$$\nabla \times \underline{v} = 0$$

This may also be regarded as a constraint; only conservative solutions are of interest. If this constraint is imposed on equation (17), once again, the wave equation is obtained in terms of the velocity field,

$$\frac{\partial^2 \underline{v}}{\partial t^2} = c_f^2 \nabla^2 \underline{v} + \frac{\partial \underline{b}}{\partial t} - \frac{c_f^2}{\rho_f} \nabla q \quad (18)$$

If the displacement field,  $\underline{u}_f$ , of the fluid is introduced,

$$\underline{v} = \frac{\partial \underline{u}_f}{\partial t}$$

Equation (18) can be integrated with respect to time (disregarding the initial state for  $\underline{u}_f$  and  $\underline{b}$  and the convective term as before) which results in

$$\frac{\partial^2 \underline{u}_f}{\partial t^2} = c_f^2 \nabla^2 \underline{u}_f + \underline{b} - \frac{c_f^2}{\rho_f} \nabla Q \quad (19)$$

where

$$Q = \int_0^t q d\tau$$

Hence the displacement field also satisfies the wave equation.

The assumption that the velocity field is irrotational implies that the displacement field has this property also, i.e.,

$$\underline{u}_f = \nabla \psi \quad (20)$$

where  $\psi$  is a potential function to be introduced. Further, the potential associated with the body forces is expressed as

$$\underline{b} = \nabla \phi \quad (21)$$

Equation (19) yields

$$\nabla \left\{ \frac{\partial^2 \psi}{\partial t^2} - c_f^2 \nabla^2 \psi - \phi + \frac{c_f^2}{\rho_f} Q \right\} = 0$$

where the function inside the brackets is independent of position and depends on time only. Because an extra function of time can be added to  $\psi$  without changing the displacement field,  $\underline{u}_f$ , with no loss of generality

$$\frac{\partial^2 \psi}{\partial t^2} = c_f^2 \nabla^2 \psi + \phi - \frac{c_f^2}{\rho_f} Q \quad (22)$$

is obtained. Alternative formulations derived in this subsection are

$$\frac{\partial^2 \rho}{\partial t^2} = c_f^2 \nabla^2 \rho - \rho_f \nabla \cdot \underline{b} + \frac{\partial q}{\partial t} \quad (23)$$

$$\frac{\partial^2 p}{\partial t^2} = c_f^2 \nabla^2 p - c_f^2 \rho_f \nabla \cdot \underline{b} + c_f^2 \frac{\partial q}{\partial t} \quad (24)$$

$$\frac{\partial^2 \underline{v}}{\partial t^2} = c_f^2 \nabla^2 \underline{v} + \frac{\partial \underline{b}}{\partial t} - \frac{c_f^2}{\rho_f} \nabla q \quad (25)$$

$$\frac{\partial^2 \underline{u}_f}{\partial t^2} = c_f^2 \nabla^2 \underline{u}_f + \underline{b} - \frac{c_f^2}{\rho_f} \nabla Q \quad (26)$$

$$\frac{\partial^2 \psi}{\partial t^2} = c_f^2 \nabla^2 \psi + \phi - \frac{c_f^2}{\rho_f} Q \quad (27)$$

In the derivation of these equations,  $\underline{b}$  was introduced as the source of influence inside the fluid. Later, the existence of a potential,  $\phi$ , to the body forces was assumed. The relation,  $\underline{b} = \nabla \phi$ , can be introduced into equation (24), which would then lead to

$$\frac{\partial^2 p}{\partial t^2} = c_f^2 \nabla^2 (p - \rho_f \phi) + c_f^2 \frac{\partial q}{\partial t} \quad (28)$$

where  $\rho_f \phi$  can be interpreted as a prescribed pressure quantity applied inside the fluid domain.

## 2.4 Boundary Conditions

For a complete understanding of sound propagation processes it is obviously not sufficient to investigate the field equations for sound propagation. Additionally, the question "What happens at the boundary?" is of great interest.

Assuming the fluid mass inflow,  $q$ , in the neighborhood of the boundary is identically zero, the fluid close to the boundary can now be treated as a continuum. A consequence of the continuum hypothesis is that the displacement field at any time must be a continuous mapping of the initial state. Therefore, boundary particles must remain as boundary particles and interior particles remain as interior particles at all times.

The fluid boundary is divided into five different parts according to their properties. The first four types of boundary conditions are especially important for the case of interior acoustics.

- B1:** elastic boundary (fluid-structure-interaction/boundary type: Neumann)
- B2:** open boundary (with prescribed external pressure/boundary type: Dirichlet)
- B3:** rigid boundary (natural boundary condition/boundary type: Neumann)
- B4:** energy absorbing boundary (boundary type: Neumann)
- B5:** artificial boundary to imitate radiation to infinity (boundary type: mixed)

In the following paragraphs, it is desirable to formulate the boundary relations for the quantity

$$\frac{\partial v}{\partial t} \underline{n}$$

where  $\underline{n}$  is the outward normal vector to the fluid boundary.

**B1** (elastic boundary) - The motion of the structure and the normal component of the fluid motion coincide, that is

$$\underline{u}_f \cdot \underline{n} = u_{sf} \quad (29)$$

where  $\underline{u}_f$  is the fluid displacement vector and  $u_{sf}$  is the structural displacement component perpendicular to the fluid boundary. The second time derivative of equation (29) yields

$$\frac{\partial v}{\partial t} \underline{n} = \frac{\partial^2 u_{sf}}{\partial t'^2} \quad (30)$$

Using equation (13) with  $\hat{p} = p_f + p$  ( $p_f = \text{constant}$ ) and  $\underline{b} = 0$  leads to

$$\frac{\partial p}{\partial n} = -\rho_f \frac{\partial^2 u_{sf}}{\partial t^2} \quad (31)$$

**B2 (open boundary)** - The pressure at a point on the surface depends on the height of the wave created at the surface and on the external pressure,  $p_e$ .

$$p = \rho_f g (\underline{u}_f \cdot \underline{n}) + p_e \quad (32)$$

where  $\underline{n}$  is a unit vector normal to the surface in the initial state, which is independent of time. The quantity  $g(\underline{u}_f \cdot \underline{n})$  is essentially the weight of the wave created at the surface and  $g$  is the acceleration due to gravity.

Differentiating equation (32) twice with respect to time, leads to

$$\frac{\partial v}{\partial t} \cdot \underline{n} = \frac{1}{\rho_f g} \frac{\partial^2 (p - p_e)}{\partial t^2} \quad (33)$$

or

$$\frac{\partial p}{\partial n} = -\frac{1}{g} \frac{\partial^2 (p - p_e)}{\partial t^2} \quad (34)$$

**B3 (rigid boundary)** - On the surface with no waves the displacement perpendicular to the surface is assumed to be identically zero, so

$$\underline{u}_f \cdot \underline{n} = 0 \quad (35)$$

or after differentiating twice with respect to time

$$\frac{\partial v}{\partial t} \cdot \underline{n} = 0 \quad (36)$$

or

$$\frac{\partial p}{\partial n} = 0 \quad (37)$$

**B4 (absorbing boundary)** - This type of boundary is meaningful only in the frequency domain. The boundary condition belonging to this type of boundary is discussed in section 4.1.

**B5 (artificial boundary approximating radiation to infinity)** - If it is required to investigate sound radiation from an interior to an exterior domain using discrete methods, the exterior domain must be truncated. This can be achieved in different ways, for example, by infinite element techniques or boundary integral methods.

The main purpose of this report is to present the use of MSC/NASTRAN in fluid-structure-interaction problems, especially for the case of an interior fluid domain surrounded by elastic, rigid, or absorbing walls. The discussion of radiation to infinity is based on the Sommerfeld's method. This method is exact if the incident wave is perpendicular to the boundary. If the boundary is located a great distance from the sources of disturbances, it is quite accurate. The method is also easy to understand. A derivation of the necessary expressions is given below.

Assume that the boundary consists of a series of dampers. The force developed in a damper is

$$d_B \frac{\partial \underline{u}_f}{\partial t} \cdot \underline{n}$$

where  $d_B$  is the damping of the fluid on the boundary and

$$\frac{\partial \underline{u}_f}{\partial t} \cdot \underline{n}$$

is the velocity component perpendicular to the boundary. This term should equal the fluid pressure, thus

$$p + p_f = d_B \frac{\partial \underline{u}_f}{\partial t} \cdot \underline{n} \quad (38)$$

Then

$$\frac{\partial p}{\partial t} = d_B \frac{\partial^2 \underline{u}_f}{\partial t^2} \cdot \underline{n} = d_B c_f^2 \nabla (\nabla \cdot \underline{u}_f) \cdot \underline{n} \quad (39)$$

where the wave equation given by equation (26) with  $\underline{b} = 0$  and  $\nabla Q = 0$  is used. Through the use of equations (12) and (14), noting the condition that no fluid is added at the fluid structure interface, and assuming the initial state to be at rest, leads to

$$\rho_f c_f^2 \cdot \nabla \cdot \underline{u}_f = -p \quad (40)$$



Combining equations (39) and (40) results in

$$\frac{\partial p}{\partial t} = -d_B \frac{1}{\rho_f} \nabla p \cdot \underline{n} \quad (41)$$

where  $\nabla p \cdot \underline{n} = \partial p / \partial n$  is the normal derivative of the pressure at the boundary. Far away from the boundary the wave propagates at the speed of sound,  $c_f$ . Therefore,

$$\frac{\partial p}{\partial t} = -c_f \nabla p \cdot \underline{n} \quad (42)$$

is just the d'Alembert's solution to the wave equation, so

$$d_B = \rho_f c_f$$

which determines the value of the damping constant (acoustic wave resistance  $Z_0$ ). It should be noted that this quantity is exact only for the case of plane waves. Equation (42) can then be written as

$$\nabla p \cdot \underline{n} = \frac{\partial p}{\partial n} = -\frac{1}{c_f} \frac{\partial p}{\partial t} \quad (43)$$

or according to equation (13) with  $\underline{b} = 0$ , from equation (43) follows

$$\frac{\partial \underline{v}}{\partial t} \cdot \underline{n} = -\frac{1}{d_B} \frac{\partial p}{\partial t} \quad (44)$$

Note that the feature of the boundary condition as expressed in equation (43) is to transmit a right-angle incident wave.

## 2.5 Coupled Initial Boundary Value Problem

Before continuing to the discrete, i.e., FE formulation of the coupled problem, the following formulation of the problem is presented as a summary of sections 2.1 to 2.4:

STRUCTURE (see section 2.1)	FLUID (see sections 2.2 to 2.4)
<p><u>Dynamic equation of elastic media</u> (displacement formulation)</p> $L(\underline{u}_s) = \underline{F}(\underline{r}, t)$ <p>where <math>L</math> is a partial differential operator with respect to space and time, <math>\underline{u}_s</math> is the structural displacement and</p> $\underline{F}(\underline{r}, t) = \underline{F}_s(\underline{r}, t) + \underline{F}_p(\underline{r}, t)$ <p><math>\underline{F}_s(\underline{r}, t)</math> is an external time-dependent load and <math>\underline{F}_p(\underline{r}, t)</math> the fluid pressure-induced force onto the structure.</p> <p>Additionally, <u>initial and boundary conditions</u> must be given.</p>	<p><u>Wave equation</u> (see eq. 24)</p> $\frac{\partial^2 p}{\partial t^2} = c_f^2 \nabla^2 p - c_f^2 \rho_f \nabla \cdot \underline{b} + c_f^2 \frac{\partial q}{\partial t}$ <p>where <math>p</math> is the pressure depending on space and time, <math>p = p(\underline{r}, t)</math>.</p> <p><u>Boundary Conditions:</u></p> <ol style="list-style-type: none"> <li>1. Elastic boundary (B1) <math display="block">\frac{\partial p}{\partial n} = -\rho_f \frac{\partial^2 u_{sf}}{\partial t^2}</math> <p>(<math>u_{sf}</math> is the component of the structural displacement <math>\underline{u}_s</math> perpendicular to the fluid boundary).</p> </li> <li>2. Open boundary (B2) <math display="block">p = 0</math> <p>(special case: "acoustically soft").</p> </li> <li>3. Rigid boundary (B3) <math display="block">\frac{\partial p}{\partial n} = 0</math> <p>(special case: "acoustically hard").</p> </li> <li>4. Absorbing boundary (B4) (see section 4.1)</li> <li>5. Radiation condition (B5) <math display="block">\frac{\partial p}{\partial n} = -\frac{1}{c_f} \frac{\partial p}{\partial t}</math> </li> </ol> <p>Additionally <u>initial conditions</u> must be given.</p>

## 2.6 Coupled Boundary Value Problem

In order to complete the mathematical formulation of the coupled FSI problem, the steady-state version of the coupled problem discussed in section 2.5 is presented. Assume a

STRUCTURE	FLUID
<p><u>Dynamic equation of elastic media</u> (displacement formulation)</p> $L(\underline{u}_s) = \underline{F}(\underline{r})$ <p>where <math>L</math> is a partial differential operator with respect to space, <math>\underline{u}_s</math> is the structural displacement and</p> $\underline{F}(\underline{r}, t) = \underline{F}_s(\underline{r}, t) + \underline{F}_p(\underline{r}, t)$ <p>is an external time-independent load and <math>\underline{F}_s(\underline{r})</math> the fluid pressure-induced load at the structure, which is also time-independent.</p>	<p><u>Helmholtz equation</u></p> $\nabla^2 p + k^2 p = F_f(\underline{r})$ <p>where <math>p = p(\underline{r})</math>, <math>k = \omega/c_f</math> (<math>k</math>: wave number, <math>\omega</math>: radian frequency)</p> <p><u>Boundary Conditions</u></p> <ol style="list-style-type: none"> <li>1. Elastic boundary (B1) <math display="block">\frac{\partial p}{\partial n} = -\rho_f \omega^2 u_{sf}</math> </li> <li>2. Open boundary (B2) <math display="block">p = 0</math> (special case: "acoustically soft"). </li> <li>3. Rigid boundary (B3) <math display="block">\frac{\partial p}{\partial n} = 0</math> (special case: "acoustically hard"). </li> <li>4. Absorbing boundary (B4) (see section 4.1) <math display="block">\frac{\partial p}{\partial n} = -i\omega\rho_f \frac{1}{Z_n} p</math> (<math>Z_n</math>: normal impedance of the absorber). </li> <li>5. Radiation condition (B5) <math display="block">\frac{\partial p}{\partial n} = -ikp \text{ with } k = \omega/c_f</math> </li> </ol>

harmonic time dependence for the structural displacement  $\underline{u}_s(\underline{r}, t)$ , external load,  $\underline{F}_s(\underline{r}, t)$ , pressure-induced load  $\underline{F}_p(\underline{r}, t)$ , and pressure  $p(\underline{r}, t)$ . The sources inside the fluid will be summed in  $\underline{F}_f(\underline{r}, t)$  and assumed to have a harmonic time dependence also. For simplicity, the notations for the time-independent quantities and the operator  $L$  are the same as in the time-dependent case.

### 3. FINITE ELEMENT MODELLING

The content of this section relates to the discretization of the equations derived in the previous section using FEM. In the fluid domain, the FE formulation is derived using the pressure as an independent variable. A reformulation is carried out using the weak form and Galerkin's method of choosing the test functions. In the first step, some notes referring to the discretization of the structure are presented.

#### 3.1 Structure

As stated in section 2.1 the structural behavior is governed by

$$L(\underline{u}_s) = \underline{F}(r, t) \quad (45)$$

with

$$\underline{F}(r, t) = \underline{F}_e(r, t) + \underline{F}_p(r, t)$$

where  $\underline{F}_e$  is an external load and  $\underline{F}_p$  is the fluid pressure load on the structure.

A discretized formulation for the structure yields, in matrix notation,

$$[M_s]\{\ddot{U}\} + [D_s]\{\dot{U}\} + [K_s]\{U\} = \{L_s^e\} + \{L_f\} \quad (46)$$

where  $[M_s]$ ,  $[D_s]$ , and  $[K_s]$  are the structural mass, damping, and stiffness matrix, respectively.  $\{U\}$  is the structural displacement vector,  $\{L_s^e\}$  is the load vector due to external structural loads, and  $\{L_f\}$  is the load vector due to the coupling effects.

In the derivation of equation (46) the test functions and the trial functions are of the same type, although they may differ from the ones used for the fluid domain. That is why this function is designated by a subscript 's', i.e.,  $N_s$  and the function set by  $\{N_s\}$ . Thus the coupling vector,  $L_f$ , between the structural and the fluid domain is

$$L_f = \int_{B_1} N_s \cdot \underline{n} p dS \quad (47)$$

#### 3.2 Linear Fluid

Referring to equation (24), the following form of the wave equation is used as a starting point:

$$\frac{\partial^2 p}{\partial t^2} = c_f^2 \nabla^2 p + c_f^2 \frac{\partial q}{\partial t} - c_f^2 \rho_f \nabla \cdot \underline{b} \quad (48)$$

Multiplying equation (48) by a test function (or "variation")  $w=w(x,y,z)$  and integrating over the total fluid domain volume,  $V$ , results in

$$\int_V w \frac{\partial^2 p}{\partial t^2} dV - c_f^2 \int_V w \nabla^2 p dV = c_f^2 \int_V w \frac{\partial q}{\partial t} dV - c_f^2 \rho_f \int_V w \nabla \cdot \underline{b} dV \quad (49)$$

Applying Green's first formula to the second integral in equation (49) yields

$$\int_V w \nabla^2 p dV = \int_S w (\nabla p) \cdot \underline{n} dS - \int_V (\nabla w) \cdot (\nabla p) dV$$

where  $S$  is the boundary of  $V$  and  $\underline{n}$  is the outward normal of  $S$ . Inserting this expression in equation (49) leads to

$$\int_V w \frac{\partial^2 p}{\partial t^2} dV + c_f^2 \int_V (\nabla w) \cdot (\nabla p) dV = c_f^2 \int_S w (\nabla p) \cdot \underline{n} dS + c_f^2 \int_V w \frac{\partial q}{\partial t} dV - c_f^2 \rho_f \int_V w \nabla \cdot \underline{b} dV \quad (50)$$

Noting that  $\hat{p} = p_0 + p$  ( $p_0 = \text{constant}$ ) from equation (13) one obtains

$$\nabla p = -\rho_f \frac{\partial \underline{v}}{\partial t} + \rho_f \underline{b}$$

Reformulate the first and the third integral on the right side of equation 50. It becomes

$$\begin{aligned} c_f^2 \int_S w (\nabla p) \cdot \underline{n} dS - c_f^2 \rho_f \int_V w \nabla \cdot \underline{b} dV &= -c_f^2 \rho_f \int_S w \frac{\partial \underline{v}}{\partial t} \cdot \underline{n} dS + c_f^2 \rho_f \int_S w \underline{b} \cdot \underline{n} dS - c_f^2 \rho_f \int_V w \nabla \cdot \underline{b} dV \\ &= -c_f^2 \rho_f \int_S w \frac{\partial \underline{v}}{\partial t} \cdot \underline{n} dS + c_f^2 \rho_f \int_V \nabla w \cdot \underline{b} dV \end{aligned}$$

The next step is to split the surface integral in equation (50) into the four boundary parts, (B1, B2, B3, B5) discussed in section 2.4. To that end, note the reformulated integrals above. Splitting of the surface integrals leads to

$$c_f^2 \rho_f \int_{B_1} w \frac{\partial \underline{v}}{\partial t} \cdot \underline{n} dS = c_f^2 \rho_f \int_{B_1} w \frac{\partial^2 u_d}{\partial t^2} dS \quad (51)$$

$$c_f^2 \rho_f \int_{B_2} w \frac{\partial v}{\partial t} \cdot \underline{n} dS = \frac{c_f^2}{g} \int_{B_2} w \frac{\partial^2 (p - p_e)}{\partial t^2} dS \quad (52)$$

$$c_f^2 \rho_f \int_{B_3} w \frac{\partial v}{\partial t} \cdot \underline{n} dS = 0 \quad (53)$$

$$c_f^2 \rho_f \int_{B_5} w \frac{\partial v}{\partial t} \cdot \underline{n} dS = c_f \int_{B_5} \frac{\partial p}{\partial t} dS \quad (54)$$

Now, equation (50) is transformed to the following form:

$$\left. \begin{aligned} \int_V w \frac{\partial^2 p}{\partial t^2} dV + c_f^2 \int_V (\nabla w) \cdot (\nabla p) dV &= -c_f^2 \rho_f \int_{B_1} w \frac{\partial^2 u_{sf}}{\partial t^2} dS + \frac{c_f^2}{g} \int_{B_2} w \frac{\partial^2 (p - p_e)}{\partial t^2} dS \\ -c_f \int_{B_5} w \frac{\partial p}{\partial t} dS + c_f^2 \int_V w \frac{\partial q}{\partial t} dV - c_f^2 \rho_f \int_V (\nabla w) \cdot \underline{b} dV \end{aligned} \right\} \quad (55)$$

If there are no body forces and no external applied pressure,  $p_e$ , equation (55) reduces to

$$\left. \begin{aligned} \int_V w \frac{\partial^2 p}{\partial t^2} dV + c_f^2 \int_V (\nabla w) \cdot (\nabla p) dV &= -c_f^2 \rho_f \int_{B_1} w \frac{\partial^2 u_{sf}}{\partial t^2} dS + \frac{c_f^2}{g} \int_{B_2} w \frac{\partial^2 p}{\partial t^2} dS \\ -c_f \int_{B_5} w \frac{\partial p}{\partial t} dS + c_f^2 \int_V w \frac{\partial q}{\partial t} dV \end{aligned} \right\} \quad (56)$$

The discretization of equation (55) is carried out by expanding the pressure,  $p$ , in terms of FE basis functions or shape functions, each one associated with a unique nodal point. The shape functions in the fluid domain are designated by a subscript  $f$ , i.e.,  $N_f$ , and the function set by  $\{N_f\}$ .

The discretization process of the pressure,  $p$ , leads to the expression

$$p(\underline{x}, t) = \sum_j N_f^j(\underline{x}) P_j(t) \quad (57)$$

The summation is over the number of shape functions and  $P_j(t)$  is the value of the pressure at the associated nodal point at time,  $t$ .

Finally, the standard Galerkin formulation with

$$w \in \{N_f\}$$

is applied to equation (56) and noting equation (57), gives the discretized form of equation (55)

$$[M_f]\{\ddot{P}\} + [D_f]\{\dot{P}\} + [K_f]\{P\} = -\{L_s\} + \{L_q\} + \{L_b\} + \{L_e\} \quad (58)$$

where  $\{P\}$  is the column vector of the unknown nodal values of the pressure, and

$$\begin{aligned} (M_f)_{ij} &= \int_V N_f^i N_f^j dV + \frac{c_f^2}{g} \int_{B_2} N_f^i N_f^j dS \\ (D_f)_{ij} &= c_f \int_{B_2} N_f^i N_f^j dS \\ (K_f)_{ij} &= c_f^2 \int_V (\nabla N_f^i) (\nabla N_f^j) dV \\ (L_s)_i &= c_f^2 \int_{B_1} N_f^i \ddot{u}_{sf} dS \\ (L_q)_i &= c_f^2 \int_V N_f^i \frac{\partial q}{\partial t} dV, \quad (L_b)_i = c_f^2 \rho_f \int_V (\nabla N_f^i) \cdot \underline{b} dV \\ (L_e)_i &= \frac{c_f^2}{g} \int_S N_f^i \frac{\partial^2 p_e}{\partial t^2} dS \end{aligned}$$

are the elements of the matrices  $[M_f]$ ,  $[D_f]$ ,  $[K_f]$ , and the vectors  $\{L_s\}$ ,  $\{L_q\}$ ,  $\{L_b\}$ , and  $\{L_e\}$  where  $i$  is the row and  $j$  is the column index.

The vector  $\{L_s\}$  is responsible for the coupling of the fluid with the structure and represents the action of the structure on the fluid surface. The counterpart of  $\{L_s\}$  is  $\{L_f\}$  (see eq. 47), which describes the action of the fluid on the structure.

### 3.3 Fluid-Structure Coupling and Symmetrization

Following the developments in sections 3.1 and 3.2, a matrix equation of the coupled system using equations (46) and (58) can be written. As mentioned above, the coupling between structure and fluid is fixed by the coupling terms  $\{L_f\}$  and  $\{L_s\}$  on the right-hand side of equations (46) and (58) respectively.

$\{L_f\}$  is a function of the fluid pressure and  $\{L_s\}$  is a function of the structural displacement. All other vectors on the right-hand side of equations (46) and (58) are true load vectors.

The definition of  $\{L_s\}$  and  $\{L_f\}$  is

$$(L_s)_i = c_f^2 \rho_f \int_{B_1} N_f^i \ddot{u}_{sf} dS$$

and

$$(L_f)_i = \int_{B_1} \underline{N}_s^i \cdot \underline{n} p dS$$

Because

$$u_{sf} = \underline{u}_s \cdot \underline{n} = \underline{N}_s^j \cdot \underline{n} U_s^j$$

where the nodal index,  $j$ , runs through the set of structural trial functions, results in

$$\{L_s\} = [M_c] \{\ddot{U}_s\}$$

where

$$(M_c)_{ij} = c_f^2 \rho_f \int_{B_1} N_f^i \underline{N}_s^j \cdot \underline{n} dS$$

Similarly,

$$p = \sum_j N_f^j P$$

and thus

$$\{L_f\} = [K_c] \{P\}$$

where

$$(K_c)_{ij} = \int_{B_1} \underline{N}_s^i \cdot \underline{n} N_f^j dS$$

Only those structural degrees of freedom that are perpendicular to the fluid boundary need to be considered. The same is valid for the fluid degrees of freedom, i.e., only the pressure nodes along the structure, that are linked to the structure, need to be considered.

The assembled system of equations is

$$\begin{bmatrix} M_s & 0 \\ M_c & M_f \end{bmatrix} \begin{bmatrix} \ddot{U} \\ \ddot{P} \end{bmatrix} + \begin{bmatrix} D_s & 0 \\ 0 & D_f \end{bmatrix} \begin{bmatrix} \dot{U} \\ \dot{P} \end{bmatrix} + \begin{bmatrix} K_s & -K_c \\ 0 & K_f \end{bmatrix} \begin{bmatrix} U \\ P \end{bmatrix} = \begin{bmatrix} L_s^e \\ L_q + L_b + L_e \end{bmatrix} \quad (59)$$

It is obvious that  $M_c = c_f^2 \rho_f K_c^T$ .

If the second row of equation (59) is multiplied by the factor

$$1/\chi$$



another form of equation (59) can be obtained, where  $\chi = c_f^2 \rho_f$  is the bulk modulus. For the sake of brevity, the same notation for  $M_f, D_f, K_f, L_q, L_b, L_e$  as in equation (59) is used which leads to

$$\begin{bmatrix} M_s & 0 \\ -C^T & M_f \end{bmatrix} \begin{bmatrix} \ddot{U} \\ \ddot{P} \end{bmatrix} + \begin{bmatrix} D_s & 0 \\ 0 & D_f \end{bmatrix} \begin{bmatrix} \dot{U} \\ \dot{P} \end{bmatrix} + \begin{bmatrix} K_s & C \\ 0 & K_f \end{bmatrix} \begin{bmatrix} U \\ P \end{bmatrix} = \begin{bmatrix} L_s^e \\ L_q + L_b + L_e \end{bmatrix} \quad (60)$$

where  $C$  (Coupling Matrix) is the matrix  $-K_c$  from equation (59).

Consider the following interesting aspects of equation (60). Assume that the acoustic frequencies are all greater than the maximum structural frequency of interest. In this case, the fluid can be considered to be incompressible. This corresponds to letting the bulk modulus,  $\chi$ , be infinite. This leads to  $M_f$  and  $D_f \Rightarrow 0$ .

It is easy to see that for this case the coupled system can now be completely described in terms of structural nodal displacements only. That is, equation (60) reduces to its structural part, where an additional mass term reflects the total effect of the incompressible fluid on the response of the structure.

It is interesting to observe that the assumptions of incompressible, small deformation behavior (the latter assumption was made for the acoustic approximation) of the fluid eliminates the need for a coupled solution. The presence of the fluid is entirely reflected by the additional mass term for the structure.

### 3.4 Aspects of Solving the Coupled Fluid-Structure Equation

#### 3.4.1 Symmetrization

For the solution of the general FSI problem, matrix equation (60) has to be solved. But an important feature of the above equation is its lack of symmetry, i.e., the system has unsymmetric mass and stiffness matrices. This can present some difficulties in extracting the eigenvalues and in the calculation of the dynamic response of the system.

Eigenvalue equation of the coupled system can be obtained if the right-hand side of equation (60) is replaced by a zero vector,  $D_s = D_f = 0$ , and harmonic time-dependence of  $U(t)$  and  $P(t)$  is assumed, i.e.,

$$U(t) = U \exp(i\omega t)$$

and

$$P(t) = P \exp(i\omega t)$$

respectively. The vectors  $U$  and  $P$  are now dependent only on the nodal position. The eigenvalue problem of the coupled system leads to the following nonsymmetric equation:

$$\left( \begin{bmatrix} K_s & C \\ 0 & K_f \end{bmatrix} - \omega^2 \begin{bmatrix} M_s & 0 \\ -C^T & M_f \end{bmatrix} \right) \begin{bmatrix} U \\ P \end{bmatrix} = \begin{bmatrix} 0 \\ 0 \end{bmatrix} \quad (61)$$

Equation (61) is costly to solve and it is difficult to obtain eigenvalues for large systems. With regard to practical problems, the existing capabilities of MSC/NASTRAN are not suitable for solving systems of the type in equation (61). Furthermore, it can be shown that the eigenvalues of the coupled system in equation (61) are real. The nature of the problem suggests a symmetric formulation for equation (61). A symmetric form can be obtained directly by using the displacement formulation for the fluid (ref. 9). This approach has a major drawback because of an increase in the number of unknowns, especially in three-dimensional applications. In the literature one can find many descriptions of symmetrization procedures for equations (61) and (60), see references 21-28. The method used in the Acoustic Procedure presented here is described in references 25 and 28. The characteristic feature of this method is that the symmetrization is accomplished by replacing the vector  $P$  in equation (60) by a vector  $Q$  given by

$$P = \dot{Q}$$

This vector is, except for a multiplicative constant, the velocity potential used in fluid dynamics.

A symmetric form of equation (60) is obtained, if the second row of equation (60) is multiplied by -1, integrated with respect to time,  $t$ , and finally  $\{P\}$  is replaced by  $\{\dot{Q}\}$ . The result is the following system:

$$\begin{bmatrix} M_s & 0 \\ 0 & -M_f \end{bmatrix} \begin{bmatrix} \ddot{U} \\ \ddot{Q} \end{bmatrix} + \begin{bmatrix} D_s & C^T \\ C & -D_f \end{bmatrix} \begin{bmatrix} \dot{U} \\ \dot{Q} \end{bmatrix} + \begin{bmatrix} K_s & 0 \\ 0 & -K_f \end{bmatrix} \begin{bmatrix} U \\ Q \end{bmatrix} = \begin{bmatrix} L_s \\ -G \end{bmatrix} \quad (62)$$

where

$$G(t) = \int_0^t (L_q + L_b + L_e) d\tau$$

The disadvantage of this symmetrization is, that in case of the eigenvalue calculation, it leads to an additional symmetric but fictitious damping matrix, which makes it necessary to use complex eigenvalue methods. This situation can be avoided by applying the following matrix transform:

$$T = \begin{bmatrix} K_s M_s^{-1} & 0 \\ C^T M_s^{-1} & I_f \end{bmatrix} \quad (63)$$

where  $I_f$  is a unit matrix with the same size as  $K_f$ . Multiplying equation (61) from the left by equation (63) results in

$$\left( \begin{bmatrix} K_s M_s^{-1} K_s & -K_s M_s^{-1} C \\ -C^T M_s^{-1} K_s & K_f + C^T M_s^{-1} C \end{bmatrix} - \omega^2 \begin{bmatrix} K_s & 0 \\ 0 & M_f \end{bmatrix} \right) \begin{bmatrix} U \\ P \end{bmatrix} = \begin{bmatrix} 0 \\ 0 \end{bmatrix} \quad (64)$$

In practice, the systems represented by equations (62) and (64) are very large. There exists a method that can reduce the expense in solving these systems. It involves the use of modal reduction.

### 3.4.2 Modal reduction

For very large problems it is computationally attractive to apply modal reduction for the purpose of reducing the size of the analysis. In this case, both the fluid and the structure are possible candidates for this operation.

Applying modal reduction to the structure (for the modes of the structure in vacuo) and to the fluid (for the modes of the fluid in a rigid container) results in the equations listed in the following table:

	Structure (s)	Fluid (f)
Variables	$U = \phi_s \xi_s$	$P = \phi_f \xi_f$
Modal mass	$m_s = \phi_s^T M \phi_s$	$m_f = \phi_f^T M \phi_f$
Modal damping	$d_s = \phi_s^T D \phi_s$	$d_f = \phi_f^T D \phi_f$
Modal stiffness	$k_s = \phi_s^T K \phi_s$	$k_f = \phi_f^T K \phi_f$
Modal excitation	$f_s = \phi_s^T L_s^e$	$g_f = \phi_f^T G$

The matrices  $\phi_s$  and  $\phi_f$  represent the modal matrices of structure and fluid respectively. In general, both are rectangular matrices, where the number of rows is equal to the number of physical degrees of freedom and the number of columns is equal to the number of modes used in the analysis.

Following the transformation process given in the table above, equations (62) and (64) are converted to a set of "modally coupled" equations, where the coupling is represented by the "modal coupling matrix"

$$\zeta = \phi_f^T C \phi_s \quad (65)$$

The resulting equation of motion for the modal coupled system is

$$\begin{bmatrix} m_s & 0 \\ 0 & -m_f \end{bmatrix} \begin{bmatrix} \ddot{\xi}_s \\ \ddot{\xi}_f \end{bmatrix} + \begin{bmatrix} d_s & \zeta^T \\ \zeta & -d_f \end{bmatrix} \begin{bmatrix} \dot{\xi}_s \\ \dot{\xi}_f \end{bmatrix} + \begin{bmatrix} k_s & 0 \\ 0 & -k_f \end{bmatrix} \begin{bmatrix} \xi_s \\ \xi_f \end{bmatrix} = \begin{bmatrix} f_s \\ -g_f \end{bmatrix} \quad (66)$$

The eigenvalue equation for the coupled modal system is

$$\left( \begin{bmatrix} k_s m_s^{-1} k_s & -k_s m_s^{-1} \zeta \\ -\zeta^T m_s^{-1} k_s & k_f + \zeta^T m_s^{-1} \zeta \end{bmatrix} - \omega^2 \begin{bmatrix} k_s & 0 \\ 0 & m_f \end{bmatrix} \right) \begin{bmatrix} \xi_s \\ \xi_f \end{bmatrix} = \begin{bmatrix} 0 \\ 0 \end{bmatrix} \quad (67)$$

Assuming a harmonic time-dependence for structural displacement and pressure, the following frequency response equation is obtained from equation (66):

$$\left[ \begin{bmatrix} k_s & 0 \\ 0 & -k_f \end{bmatrix} - \omega^2 \begin{bmatrix} m_s & 0 \\ 0 & -m_f \end{bmatrix} + i\omega \begin{bmatrix} d_s & \zeta \\ \zeta & -d_f \end{bmatrix} \right] \begin{bmatrix} \xi_s \\ \xi_f \end{bmatrix} = \begin{bmatrix} f_s \\ -g_f \end{bmatrix} \quad (68)$$

### 3.4.3 Residual flexibility for the fluid

If the modal reduction is used, the analyst is alerted to the possible effects of mode truncation inherent in the method. Enhancements can be made to the above equations of motion by adding terms for the fluid model residuals. This addition compensates for the omission of high frequency fluid modes. Normally, high frequency modes respond "statically" and residual flexibility accounts for their static behavior (ref. 30).

The derivation of the residual flexibility terms is done in terms of an unsymmetric formulation (see eq. (60)). For simplicity the damping matrices in equation (60) are ignored because they have no impact on the final result. Likewise, for simplicity, assume that there are no body forces, no added fluid mass and no external time-dependent pressure, i.e.,  $\underline{b} = 0$ ,  $q = 0$ ,  $p_e = 0$ . Therefore, from equation (60) one obtains

$$\begin{bmatrix} M_s & 0 \\ -C^T & M_f \end{bmatrix} \begin{Bmatrix} \ddot{U} \\ \ddot{P} \end{Bmatrix} + \begin{bmatrix} K_s & +C \\ 0 & K_f \end{bmatrix} \begin{Bmatrix} U \\ P \end{Bmatrix} = \begin{Bmatrix} L_s^e \\ 0 \end{Bmatrix} \quad (69)$$

After transforming the lower part of equation (69) to modal coordinates, the "fluid part" yields the following equation:

$$m_f(\ddot{\xi}_f + [\omega_f^2]\xi_f) = \phi_f C^T \ddot{U} \quad (70)$$

where  $[\omega_f^2] = m_f^{-1} k_f$  is a diagonal matrix and  $\omega_f^2$  are the fluid eigenvalues. The matrices  $m_f$  and  $k_f$  are modal mass and stiffness matrices of the fluid. The next step is to separate the fluid modes in the following manner:

$$\phi_f = [\phi_f^0 | \phi_f^e | \phi_f^t] \quad (71)$$

where

$\phi_f^0$  : "zero" modes with  $\omega_f^0 = 0$

$\phi_f^e$  : "elastic" modes with  $\omega_f^e > 0$

$\phi_f^t$  : "truncated" modes with  $[\omega_f^{t2}]\xi_f^t \gg \ddot{\xi}_f^t$

In the same manner the quantities,  $\xi_f$ ,  $m_f$ , and  $[\omega_f^2]$  can be separated, i.e.,

$$\xi_f = \begin{bmatrix} \xi_f^0 \\ \xi_f^e \\ \xi_f^t \end{bmatrix}, m_f = \begin{bmatrix} m_f^0 & & \\ & m_f^e & \\ & & m_f^t \end{bmatrix}, [\omega_f^2] = \begin{bmatrix} \omega_f^0 & & \\ & \omega_f^e & \\ & & \omega_f^t \end{bmatrix} \quad (72)$$

Then, from equation (70) the following is obtained:

$$\xi_f^0 = (m_f^0)^{-1} \phi_f^{0T} C^T U \quad (73)$$

$$\xi_f^e = (m_f^e)^{-1} [s^2 + \omega_f^{e2}]^{-1} \phi_f^{eT} C^T \ddot{U} \quad (74)$$

$$\xi_f^t = (m_f^t)^{-1} [\omega_f^{t2}]^{-1} \phi_f^{tT} C^T \ddot{U} \quad (75)$$

where the following have been used: case (a)  $\ddot{U} = s^2 U$  and  $\ddot{\xi}_f^0 = s^2 \xi_f^0$ , case (b)  $\ddot{\xi}_f^e = s^2 \xi_f^e$ , and case (c) the condition  $[\omega_f^{t2}]\xi_f^t \gg \ddot{\xi}_f^t$ .

Using equations (71), (72), (73) through (75), and  $P = \phi_f \xi_f$ , the following expression is obtained:

$$P = \phi_f^0 (m_f^0)^{-1} \phi_f^{0T} C^T U + \phi_f^e (m_f^e)^{-1} [s^2 + \omega_f^{e2}]^{-1} \phi_f^{eT} C^T \ddot{U} + Z_f^t C^T \ddot{U} \quad (76)$$

where

$$Z_f^i = \phi_f^i (m_f^i [\omega_f^{i2}])^{-1} \phi_f^{iT} \quad (77)$$

represents the residual flexibility.

Now, equation (76) can be solved for  $Z_f^i$  by separating the static from the dynamic part of the pressure, i.e.,

$$P = P^s + P^d$$

Set  $s = 0$  (i.e.,  $\ddot{P} = 0$ ) and get

$$P^s = \phi_f^0 (m_f^0)^{-1} \phi_f^{0T} C^T U + \phi_f^0 (m_f^0)^{-1} [s^2 + \omega_f^{02}]^{-1} \phi_f^{0T} C^T \ddot{U} + Z_f^i C^T \ddot{U} \quad (78)$$

Multiply equation (78) by  $K_f$  and note that the exact static solution is known from equation (69):

$$K_f P^s = C^T \ddot{U} \quad (79)$$

Furthermore, for zero modes

$$K_f \phi_f^0 = 0$$

Then from equation (78), the following expression is obtained:

$$K_f Z_f^i = -K_f \phi_f (m_f)^{-1} [\omega_f^{-2}] \phi_f^T \quad (80)$$

By constraining zero modes, equation (80) can be solved directly for  $Z_f^i$ , i.e.,

$$Z_f^i = -\phi_f (m_f)^{-1} [\omega_f^{-2}] \phi_f^T \quad (81)$$

Further define

$$Z_f^{0i} = \phi_f^0 (m_f^0)^{-1} \phi_f^{0T} \quad (82)$$

Using equation (82), the following is obtained from equation (76)

$$P = \phi_f \xi_f + Z_f^{0i} C^T U + Z_f^i C^T \ddot{U} \quad (83)$$

Combine equations (70) and (83) with the upper half of equation (69) and transform to structural modes to obtain

$$\begin{bmatrix} m_s + \bar{Z}_f' & 0 \\ -\zeta^T & m_f \end{bmatrix} \begin{bmatrix} \ddot{\xi}_s \\ \ddot{\xi}_f \end{bmatrix} + \begin{bmatrix} k_s + \bar{Z}_f^{0t} & \zeta \\ 0 & k_f \end{bmatrix} \begin{bmatrix} \xi_s \\ \xi_f \end{bmatrix} = \begin{bmatrix} f_s \\ 0 \end{bmatrix} \quad (84)$$

where

$$\bar{Z}_f' = \phi_s^T C Z_f' C^T \phi_s \text{ and } \bar{Z}_f^{0t} = \phi_s^T C Z_f^{0t} C^T \phi_s$$

This section is concluded by noting that if there is an excitation in the fluid the residual flexibility terms to be added are given by the following two equations

$$\bar{Z}_f' = \phi_s^T C (K_f^{-1} - \phi_f m_f^{-1} \omega_f^{-2} \phi_f^T) \phi_s \quad (85)$$

$$\bar{Z}_f^{0t} = \phi_s^T C (\phi_f m_f^{-1} \phi_f^T) C^T \phi_s \quad (86)$$

After symmetrization, this addition leads to an equation which has the following form:

$$\begin{bmatrix} m_s + \bar{Z}_f' & 0 \\ 0 & -m_f \end{bmatrix} \begin{bmatrix} \ddot{\xi}_s \\ \ddot{\xi}_f \end{bmatrix} + \begin{bmatrix} d_s & \zeta^T \\ \zeta & -d_f \end{bmatrix} \begin{bmatrix} \dot{\xi}_s \\ \dot{\xi}_f \end{bmatrix} + \begin{bmatrix} k_s + \bar{Z}_f^{0t} & 0 \\ 0 & -k_f \end{bmatrix} \begin{bmatrix} \xi_s \\ \xi_f \end{bmatrix} = \begin{bmatrix} f_s \\ -g_f \end{bmatrix} \quad (87)$$

## 4. SPECIAL FEATURES

### 4.1 Acoustic Absorption

The effect of an absorbing wall in an acoustic cavity can be modelled in two ways, depending on the nature of the absorption. If the absorption is due to a porous material then special porous elements must be used. The porous elements have to model the behavior of a flexible porous material under certain assumptions regarding the structure of the material. At the present state of the program, such elements are not available. The other possibility is to model the absorbing wall, both in the case of a porous material or in a general type of absorption, by using the impedance formulation of the absorber. In order to obtain a boundary condition in this case, the boundary condition for boundary B1 (see section 2.4, eq. 31) can be rewritten by the use of a relation between pressure,  $p$ , and the normal fluid velocity,  $v_n = \partial u_{sf} / \partial t$ , at the wall

$$p = Z_n \frac{\partial u_{sf}}{\partial t} \quad (88)$$

to give

$$\frac{\partial p}{\partial n} = -i\omega\rho_f \frac{1}{Z_n} p \quad (89)$$

To use the impedance for modelling absorptive boundaries, the value of  $Z_n$  has to be determined as a function of the radian frequency,  $\omega$ . In some cases an analytical expression can be formulated, whereas in others, the values can be obtained from experimental measurements. In the latter case, the so-called "standing wave tube" is used, which can be used to measure the (normal) impedance  $Z_n$  (see ASTM E1050-85A)

$$Z_n = Z_1 + iZ_2 \quad (90)$$

where  $Z_1$  is usually called the **specific acoustic resistance** and  $Z_2$  the **specific acoustic reactance**.

If the absorber is connected to an elastic boundary, the boundary condition can be expressed as

$$\frac{\partial p}{\partial n} = -i\omega\rho_f \left( v_n + \frac{p}{Z_n} \right) \quad (91)$$

A surface with a "large" impedance,  $|Z_n| \Rightarrow \infty$ , is considered to be "acoustically hard." A surface with a "small" impedance,  $|Z_n| \Rightarrow 0$ , is considered to be "acoustically soft." Relat-



ing to equation (91), the first case leads to the elastic condition in section 2.6, where  $\underline{v}_n = \partial u_{sf} / \partial t$ , while the second case leads to  $p = 0$ , i.e., "pressure release."

If the enclosed acoustic domain is discretized with finite elements, the equations of motion are obtained as described in section 3. However, the damping matrix,  $D$  (see equations (60) and (62)), has to be complemented by the boundary absorption,  $D_z$ . It is easy to see, that  $D_z$  is given by

$$D_z = \frac{1}{Z_n} A_z \quad (92)$$

where  $A_z$  is the matrix representing those parts of the boundary which are acting as absorbers.

For a lumped approximation,  $D_z$  is null except for terms corresponding to the grid point location of the absorber material.

The Area Matrix Program generates the matrix  $A_z$ . With an additional input of the material property of the absorber, it also generates the damping matrix,  $D_z$ . Usually, the impedance property of the absorber is described by the **specific acoustic admittance** defined by

$$\beta = \frac{Z_0}{Z_n} \quad (93)$$

where  $Z_0 = \rho_f c_f$  is the wave resistance for plane waves in the fluid. It should be noted that  $Z_0$  is a real quantity only in the case of plane waves, because there is no phase shift between pressure,  $p$ , and the velocity,  $\underline{v}$ , of the fluid particles, if the fluid is inviscid and homogeneous.

Using equation (90), the following expression is derived from equation (93)

$$\beta = \gamma + i\sigma \quad (94)$$

where

$$\gamma = \frac{Z_0}{|Z_n|^2} Z_1 \quad \text{and} \quad \sigma = -\frac{Z_0}{|Z_n|^2} Z_2 \quad (95)$$

where  $Z_n$  is defined by equation (90). Therefore, instead of equation (92), the following expression is obtained for the damping matrix,  $D_z$ :

$$D_z = \frac{1}{Z_0} (\gamma + i\sigma) A_z \quad (96)$$

That is, as input of the absorber's material property, the quantities  $\gamma$  and  $\sigma$  are used, which are defined by equation (95). They determine the specific acoustic admittance defined by equation (94).

The condition for the validity of the normal impedance is that only plane, normal incident sound waves will be correctly damped. If this condition is violated then reflections will occur.

It is possible that reflections may, in some cases, corrupt the solution and the results are not what the analyst expects. To avoid this situation, it is possible for some problems to estimate when sound waves, originating from a source, are plane. Nevertheless, it is questionable whether the impedance model really does represent the absorbing surface correctly. There are examples where this model is completely confusing.

But these reservations, which can be theoretically proven, are diminished by the experience of others especially with regard to applications in automobile interior acoustics (ref. 14).

An improvement for the simple impedance model implemented in the present Acoustic Procedure is possible, if instead of equation (88), the following condition proposed by D.B. Bliss (ref. 16) is used

$$p + B(\omega)\nabla_b^2 p = \underline{v}_n Z_n \quad (97)$$

where  $\nabla_b$  is the gradient operator on the absorbing boundary (B4) and (B5).

$$B(\omega) = \frac{1}{k(\omega)^2}$$

is the so-called **bulk-reacting coefficient** and  $k(\omega)$  is the complex wave number. The condition in equation (97) can be applied to describe the boundary absorption effects. This procedure was implemented in MSC/NASTRAN by Burfeindt (ref. 15).

## 4.2 Acoustic Contribution Analysis

This section presents a brief description of the calculation procedure for determining the contribution of different parts of the structure to the sound pressure level at any point in the fluid domain. A more detailed presentation is given in reference 31.

The modal solution method provides valuable information regarding the structural and modal participation in the acoustic response. The **acoustic modal participation** at the interior points,  $\{P_i\}$ , can be calculated by

$$\{P\} = [\phi_f] \{\xi_f\} = \sum_{i=1}^{n_f} \{P_i\} (= \xi_{fi} \phi_{fi}) \quad (98)$$

where  $n_f$  is the total number of acoustic modes used in the analysis. Each vector  $\{P_i\}$  represents the contribution to the acoustic response from the acoustic mode,  $i$ , or the modal acoustic participation factor.

The **structural modal participation factor** can be calculated for a harmonic solution of radian frequency,  $\omega$ , as follows. First, the equation of motion is solved for the fluid modal vector:

$$\{\xi_f\} = [z2] (\omega^2 [\zeta] \{\xi_s\}) \quad (99)$$

where  $[\zeta]$  is the modal coupling matrix defined by equation (65) and

$$[z2] = (-\omega^2 [m_f] + [k_f])^{-1} \quad (100)$$

is the acoustic modal frequency response function, which is included also in equation (67). Substituting equation (99) into  $P = \phi_f \xi_f$  results in

$$\{P\} = \omega^2 [\phi_f] [z2] [\zeta] \{\xi_s\} = \sum_{j=1}^{n_s} P_j \quad (101)$$

where  $n_s$  is the total number of structural modes. Note that each vector  $P = \{P_j\}$  represents the contribution of the structural mode  $j$  to the acoustic response or the structural modal participation factor.

The **boundary panel participation** for a boundary panel  $b$  is basically the collective structural modal participation of all the structural nodes on that panel. The  $[C_b]$  matrix, which is the coupling matrix due to panel  $b$ , has to be computed and the global coupling matrix  $[C]$  will be the assembly of all panels in the structure. Once the  $[C_b]$  are known, equation (65) can be written as

$$[\zeta] = [\phi_f]^T \sum_{b=1}^{n_b} [C_b] [\phi_s] \quad (102)$$

which when substituted in equation (102) becomes

$$P = \omega^2 [\phi_f] [z2] [\phi_f]^T \sum_{b=1}^{n_b} [C_b] [\phi_s] \{\xi_s\} = \sum_{b=1}^{n_b} \{P_b\} \quad (103)$$

where  $n_b$  is the total number of boundary panels. Note that each  $\{P_b\}$  vector represents the contribution of boundary panel  $b$  to the acoustic response.

### 4.3 Structure-Fluid Analogy in MSC/NASTRAN

Since there are at present no "fluid elements" in MSC/NASTRAN, the analogy between the structure and fluid equations has to be used. The following theoretical development is reproduced from reference 23. Rewrite equation (16) neglecting the source terms and expressing  $c_f$  in terms of the bulk modulus  $\chi$  and density  $\rho_f$  of the fluid. The following form of the wave equation (in Cartesian coordinates) is obtained:

$$\frac{\partial}{\partial x} \left( \frac{1}{\rho_f} \frac{\partial p}{\partial x} \right) + \frac{\partial}{\partial y} \left( \frac{1}{\rho_f} \frac{\partial p}{\partial y} \right) + \frac{\partial}{\partial z} \left( \frac{1}{\rho_f} \frac{\partial p}{\partial z} \right) = \frac{1}{\chi} \frac{\partial^2 p}{\partial t^2} \quad (104)$$

An analogous equation in structural mechanics is the equation for the equilibrium of stresses in a particular fixed direction:

$$\frac{\partial \sigma_{xx}}{\partial x} + \frac{\partial \tau_{xy}}{\partial y} + \frac{\partial \tau_{xz}}{\partial z} = \rho_s \frac{\partial^2 u_{xx}}{\partial t^2} \quad (105)$$

where  $u_{xx}$  is the structural displacement in the  $x$  direction,  $\sigma_{xx}$ ,  $\tau_{xy}$ , and  $\tau_{xz}$  are stress components and  $\rho_s$  is the structural mass density.

In order to establish the acoustic-structural analogy, let

$$u_{xx} = p \quad (106)$$

$$\rho_s = \frac{1}{\chi} \quad (107)$$

$$\sigma_{xx} = \frac{1}{\rho_f} \frac{\partial p}{\partial x} = -\ddot{u}_{fx} \quad (108)$$

$$\tau_{xy} = \frac{1}{\rho_f} \frac{\partial p}{\partial y} = -\ddot{u}_{fy} \quad (109)$$

$$\tau_{xz} = \frac{1}{\rho_f} \frac{\partial p}{\partial z} = -\ddot{u}_{fz} \quad (110)$$

where the second forms of equations (108), (109), and (110) are obtained from equation (10) with  $\underline{b} = 0$  and  $q = 0$  and where  $\ddot{u}_x$  is the  $x$ -component of fluid acceleration, etc.

In order to complete the analogy, note that, if structural displacement components  $u_y$  and  $u_z$  are set equal to zero, the general stress-strain relationship provided by the MSC/NASTRAN MAT9 material card is

$$\begin{Bmatrix} \sigma_{xx} \\ \tau_{xy} \\ \tau_{xz} \end{Bmatrix} = \begin{bmatrix} G_{11} & G_{14} & G_{16} \\ & G_{44} & G_{46} \\ sym & & G_{66} \end{bmatrix} \begin{Bmatrix} \epsilon_{xx} \\ \gamma_{xy} \\ \gamma_{xz} \end{Bmatrix} \quad (111)$$

where  $G_{ij}$  is an element of the 6x6 elastic material matrix, and the strain-displacement relationships are:

$$\left. \begin{aligned} \epsilon_{xx} &= \frac{\partial u_{xx}}{\partial x} \\ \gamma_{xy} &= \frac{\partial u_{yx}}{\partial y} \\ \gamma_{xz} &= \frac{\partial u_{zx}}{\partial z} \end{aligned} \right\} \quad (112)$$

Therefore, if

$$\left. \begin{aligned} G_{11} = G_{44} = G_{66} &= \frac{1}{\rho_f} \\ G_{14} = G_{16} = G_{46} &= 0 \end{aligned} \right\} \quad (113)$$

equations (111), (112), and (106) will produce equations (108), (109), and (110) exactly. The other components of the  $[G_{ij}]$  may be set to any values, including zero, since  $\epsilon_{yy}$ ,  $\epsilon_{zz}$ , and  $\gamma_{yz}$  are all zero. Equations (107) and (113) indicate the manner in which the MAT9 card should be filled out. Note that several MAT9 cards may be used to represent the fluids where  $\rho_f$  and  $\chi$  vary with position in the fluid. The basic coordinate system should be used to define components of displacement and also the material coordinate system. (The symbol 0 (zero) must be inserted for CORDM on the PSOLID card.)

Note that, from equations (108), (109), and (110), normal NASTRAN stress data recovery will produce the accelerations components within the fluid, with a change in sign.

#### 4.4 Boundary Conditions and Their Input in MSC/NASTRAN Using the Structure-Fluid Analogy

In section 2.4 boundary conditions are discussed in a more mathematical sense. The purpose of this section is to present a method of implementing the boundary conditions for the fluid with regard to FSI calculations using MSC/NASTRAN.

1. At free surfaces (open boundaries), set  $u_x = p = 0$  by means of an SPC card.
2. At rigid walls, take no action. The acoustic boundary condition,

$$\frac{\partial p}{\partial n} = n_x \frac{\partial p}{\partial x} + n_y \frac{\partial p}{\partial y} + n_z \frac{\partial p}{\partial z} = 0 \quad (114)$$

where  $n_x$ ,  $n_y$ , and  $n_z$  are the direction cosines of the normal, implies an analogous structural boundary condition

$$f_x = n_x \sigma_{xx} + n_y \tau_{xy} + n_z \tau_{xz} = 0 \quad (115)$$

where  $f_x$  is the  $x$ -component of traction at the boundary. Satisfaction of equation (115) requires only that no structural forces be applied to grid points on the boundary.

3. At a surface where the pressure is a known function of time, set

$$u_x = p(t)$$

using the large mass method described in the MSC/NASTRAN Application Manual.

4. At a surface where the normal component of the displacement,  $u_{fn}$ , velocity,  $\dot{u}_{fn}$ , or acceleration,  $\ddot{u}_{fn}$ , is known, apply a grid point load

$$F_x = A_i \ddot{u}_{fn}(t) \quad (116)$$

where  $A_i$  is the area associated with the grid point  $i$ . Equation 116 follows from equations (108), (109), (110), and (115). Note that  $u_{fn}$ ,  $\dot{u}_{fn}$ , and  $\ddot{u}_{fn}$  must be inward to the fluid.

5. At a surface where the pressure and the normal velocity are linearly related, i.e., where

$$p = -W\dot{u}_{,n} \quad (117)$$

connect a CDAMP2 element to  $u_{,x}$  with a damping coefficient

$$D_w = \frac{A_i}{W} \quad (118)$$

where, again,  $A_i$  is the area associated with the grid point  $i$ .

6. Boundary conditions for other cases can easily be worked out. For example, if

$$p = -\mu u_{,n} \quad (119)$$

connect a scalar mass,  $M = A_i/\mu$  to the boundary grid point  $i$ .

## **5. DESCRIPTION OF THE ACOUSTIC PROCEDURE**

### **5.1 Introductory Remarks**

This section presents the summary of the capabilities of the Acoustic Procedure to perform FSI analysis using MSC/NASTRAN. It is specifically aimed at the acoustic and noise control analysis for the interior acoustic domains, e.g., passenger cabins in automobiles and aircraft.

The goal of this development is to treat the fluid medium simply as another part of the structure. This allows for a simultaneous solution of the two systems, without the need for a separate analysis, as is presently done in some cases. The only difference between the standard MSC/NASTRAN dynamic analysis and the Acoustic Procedure is the addition of some Direct Matrix Abstraction Programs (DMAP) and a single FORTRAN program.

The procedure requires the use of superelement solution sequences, but it is not necessary to define superelements. In many cases, though, it is highly desirable to use superelements. Since MSC/NASTRAN currently does not have special fluid elements, Structure-Fluid Analogy (see section 4.3) is used. This capability is particularly applicable to the interior problems; that is, for problems in which the fluid is contained by the structure. The exterior problem, fluid outside the structure (e.g., submarine) is very difficult to solve with FEM. In this case boundary element methods are more suitable.

### **5.2 Organization and Flowchart of the Acoustic Procedure**

The analysis capabilities that have been developed include the following:

1. Uncoupled normal modes analysis of the structure and the fluid, SOL 63
2. Normal modes analysis of the "modal coupled" fluid-structure system, SOL 70 (see section 3.4)
3. Modal frequency response analysis of the coupled system, SOL 71
4. Modal transient response analysis of the coupled system, SOL 72
5. Absorption damping for the fluid medium (attention: only normal impedance, see section 4.1)
6. Calculation of the structure grid point participation factors in the generation of the pressure at any specified point in the fluid (see section 4.2)

The Acoustic Procedure consists of five NASTRAN runs. Figure 1 illustrates the sequence of these runs during the process of an acoustic calculation.



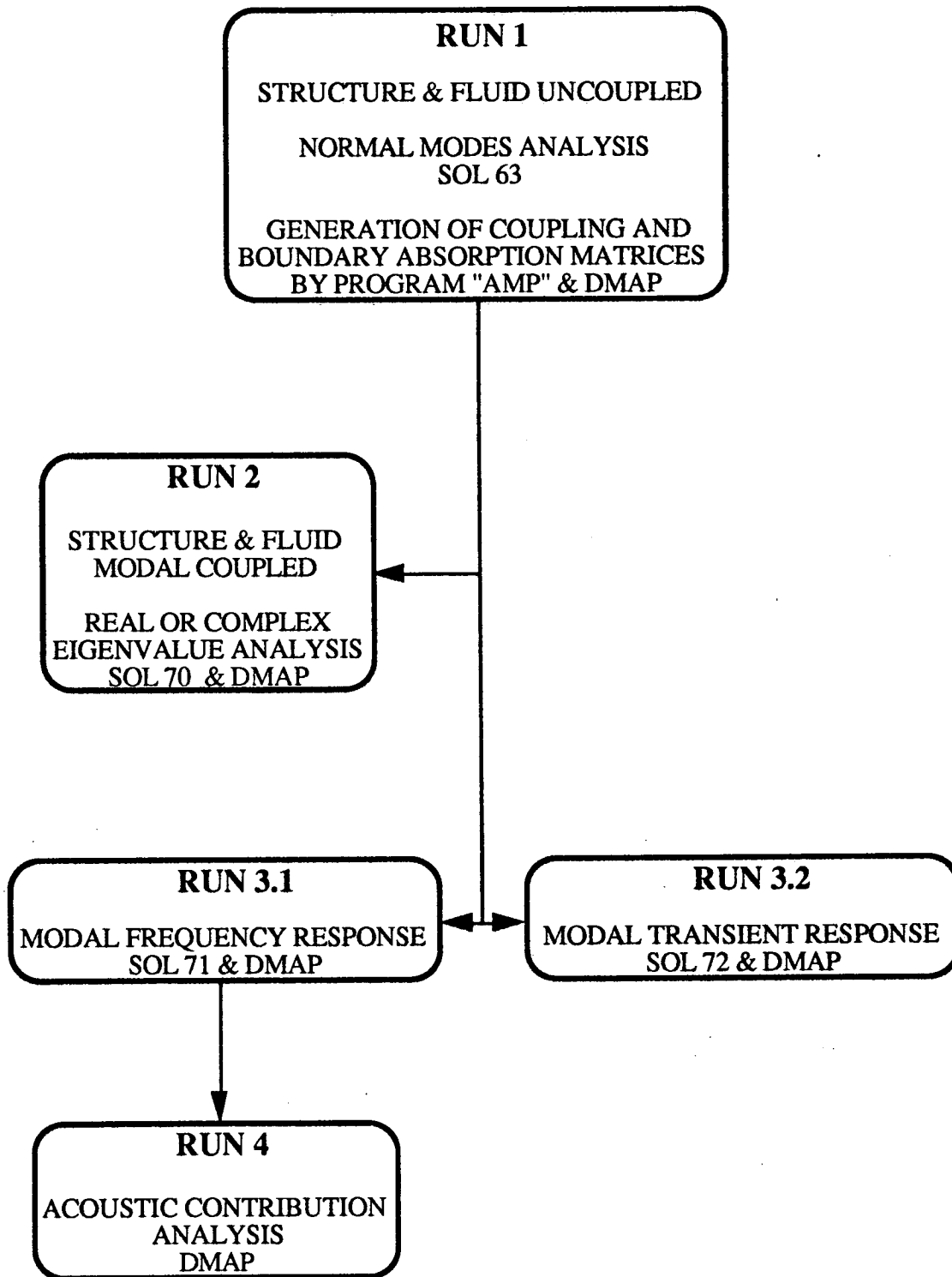


Figure 1. Acoustic procedure flowchart.

The most costly run is the first run (see fig. 1). This run contains the FE models of structure and fluid, the definition of the coupling and absorbing areas, and the absorber proper-

ties. The coupling matrix and the absorber matrices are formed by the Fortran program AMP (Area Matrix Program), which is also involved in Run 1, see figure 1. Run 2 is the cheapest run and the user has to decide if it should be executed. To better understand the coupling effects, Run 2 should be carried out. The response Runs 3.1 and 3.2 can be performed immediately after Run 1. Run 4 (Acoustic Contribution Analysis) is carried out as a restart of Run 3.1.

To get an idea of the CPU time, three examples of different size, i.e., with different number of degrees of freedom (DOF), are presented.

Example 1: This problem is a simple piston/tube model described in section 7.1. It consists of only 25 structural nodes and 16 QUAD4 elements. It has 1275 fluid nodes and 800 HEXA8 elements.

Example 2: The following problem is described in Section 7.2 and it is a two-dimensional model composed of 17 nodes and 16 BAR elements for the structure and 313 nodes and 128 QUAD8 elements for the fluid.

Example 3: This example involves a solution of a complex automobile structure composed of 6 superelements. There are 46000 grids and 51000 assorted elements in the structure model and 800 grids and 700 solid elements in the fluid.

Table 1. CPU time (sec) for acoustic analysis (CRAY YMP)			
Run	Example 1	Example 2	Example 3
1	33.3	10.9	15066.0
2	2.9	2.3	633.6
3.1	8.4	6.1	1954.4
3.2	5.8	3.4	-
4	10.5	1.0	47.6

In figure 1, the runs which have to be performed during an acoustic analysis were presented. Figure 2 shows the essential steps in acoustic analysis. These steps include the modelling of the structure and fluid, defining the areas of coupling and absorption, frequency and time response calculations, and so on.

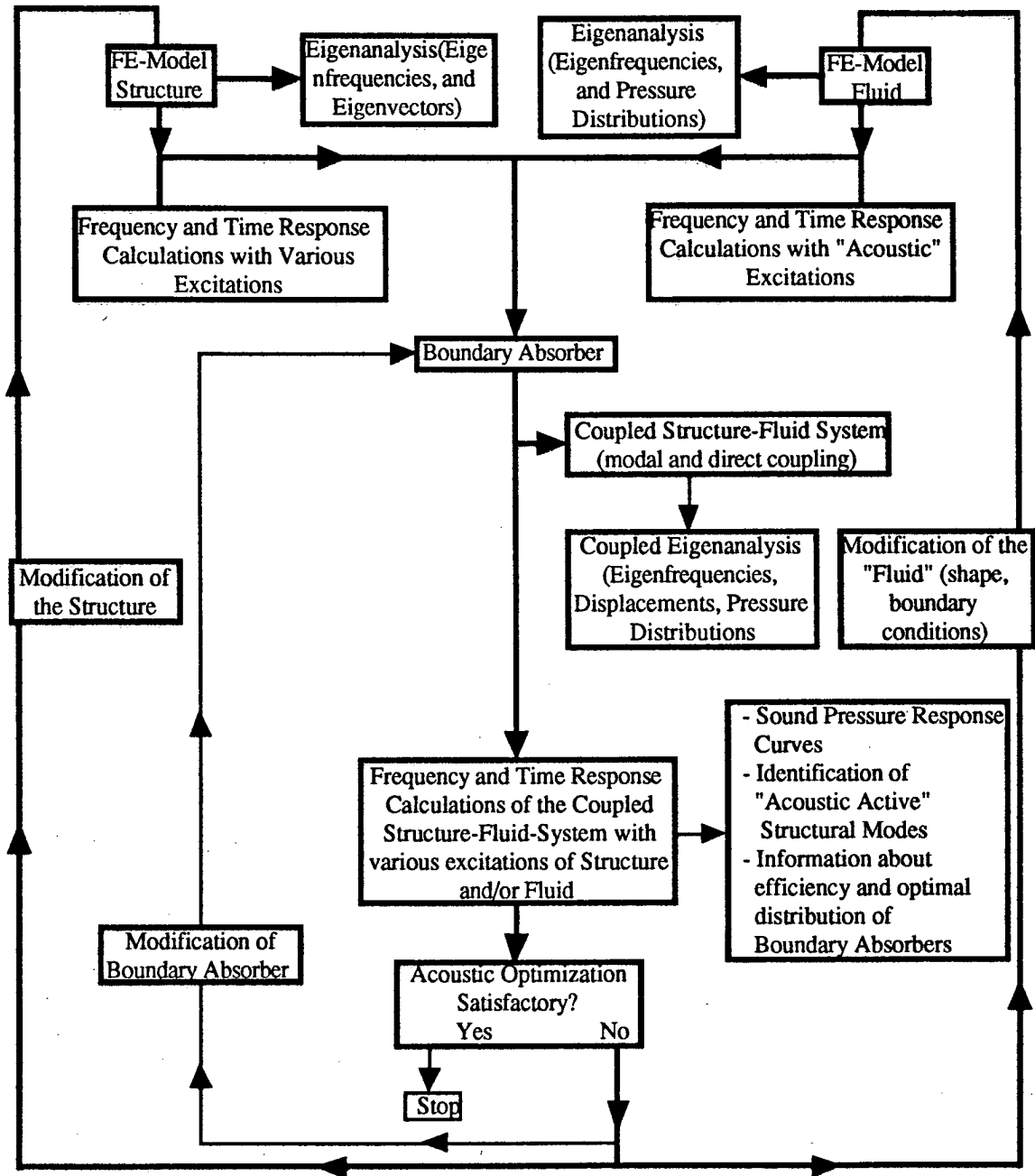


Figure 2. Possible analysis steps in the acoustic procedure.

## 6. DESCRIPTION OF THE USER INTERFACE

### 6.1 Modelling Aspects

#### 6.1.1 Fluid

In the building of a finite element model certain aspects must be considered. The acoustic problem is a dynamic problem, hence the variation of the pressure field, both in time and space, has to be incorporated into the model. For the sake of simplicity, the discussion is restricted to the spatial variation of the pressure. From the basic Helmholtz equation, it can be shown that for a one-dimensional problem,

$$p(x) = a_1 \cos kx + a_2 \sin kx$$

where  $k = \omega/c_f$ . To obtain the behavior indicated in this equation, the finite element mesh has to be able to reproduce a sinusoidal variation. Since this variation is dependent upon the frequency, because of the wave number,  $k$ , it is clear that the size of the elements must be compatible with the wavelength of the highest frequency of interest.

Given an upper frequency limit for a specific problem, the size of the elements can be deduced. If  $ND$  nodes are required to discretize a wavelength, then the distance between any two nodes should be

$$D = \frac{2\pi}{ND \cdot k} \quad (120)$$

and the maximum size of an element side is of course  $2 \cdot D$ . Depending on the type of analysis and the desired accuracy, the value of  $ND$  can be selected as

$$6 < ND < 12 \quad (121)$$

If the mesh is too coarse, the stiffness of the fluid will be exaggerated. It should be noted that the rule of thumb given above is applicable to any dynamic analysis problem.

#### 6.1.2 Coupling of structure and fluid

For the case in which the fluid interacts with a flexible structure, the considerations in section 6.1.1 must be applied to the finite element model of the structure as well as to the modelling of the interface coupling between the fluid and structure. Special attention has to be given to the interface where, in general, two systems with large differences in wave length are coupled to each other, see figure 3.

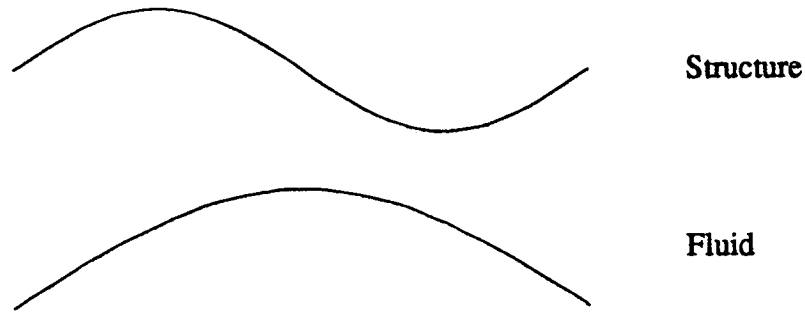


Figure 3. Comparison of wave length.

The most obvious approach in this situation is to use the same fine mesh in both the fluid and the structure. But for most situations, this would result in many unnecessary nodes in the fluid. Thus, it is desirable to use a different mesh size in the fluid and in the structure even at the interface. This approach gives rise to a discretization error because the effect of the structure upon the fluid is smoothed (assuming the situation in fig. 3). However, since this effect is not very important for the strength of interaction, it is acceptable. An interface similar to that shown in figure 4 would thus be possible.

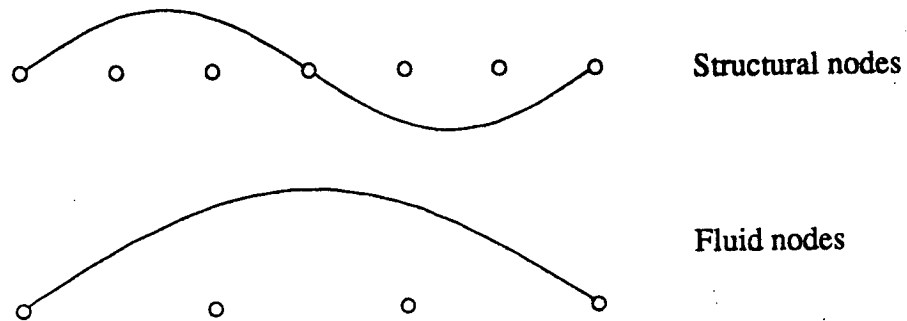


Figure 4. Discretization at the interface between fluid and structure.

It should be noted, though, that the above approach is by no means generally valid and the equations (120) and (121) must be considered for the fluid and the structure (ref. 32).

### 6.1.3 Use of superelements

One of the unique capabilities of this procedure is the capability to use superelements. In many large problems, especially for dynamic analysis, the use of superelements can significantly reduce the cost of the analysis. There is no limitation on the use of superelements for fluid-structure coupling as long as the fluid model is in the residual structure. Any superelement can be in contact with the fluid, regardless of the number of superelement levels used. Currently, secondary superelements are not supported. Any superelement that is in contact with the fluid must be a primary superelement.

## 6.2 Fluid Media

### 6.2.1 Grid point definition

The fluid media geometry is described by the use of the standard GRID and element connectivity cards. The fluid grid points should be distinguished from structural points by numbering the fluid points in a different range. Thus, partition between the two systems is easier to specify. The fluid grid points have "stiffness" and "mass" properties at only one of the six DOF at a grid. The user can specify the active DOF by constraining all other DOFs except that which is to be used. Typically, the T1 DOF is used (T1 is the NASTRAN notation for the DOF in  $x$ -direction). Where the displacement coordinate system for the fluid grid point references a cylindrical or spherical coordinate system, it is required that the T3 DOF (DOF in  $z$ -direction) must be the active DOF.

### 6.2.2 Element definition

The fluid medium can be modeled with any MSC/NASTRAN elements (in the three-dimensional case, e.g., HEXA, PENTA, and TETRA elements). It is recommended that the user specify the consistent mass for the fluid. This leads to better results in practice.

<p><b>Caution:</b> On the PSOLID card (property definition for solids) Integration Option 2 should be used for VERSION V65.</p>
---

### 6.2.3 Acoustic absorption

The absorption capability has been provided and is defined by the DMIG input. DMIG matrices are generated by the AMP. Provision has been made to define frequency dependent absorption. For transient response analysis boundary absorption cannot be used since the derivation shown in section 4.1 is valid only in the frequency domain.

### 6.2.4 Loading

The loading of the fluid is generally analogous to that used in structural mechanics analysis. Several types of loading can be specified for the fluid model:

1. Constant enforced pressure at the grid points
2. Frequency or time dependent enforced pressure at the grid points
3. Acoustic source characterized by a volumetric flow rate

The pressure can be enforced in the same manner as structural base excitations, i.e., "large mass" approach or Lagrange multiplier method. The volumetric flow rate is specified via standard structural load specification. Owing to the symmetrization of equations of motion

in section 3.4, the forces applied directly to the fluid first have to be integrated in time and then multiplied by -1.0. The resulting load is applied in the usual way.

### 6.3 Uncoupled Normal Modes Analysis of Structure and Fluid (Run 1)

This run is based on solution sequence, SOL 63, of MSC/NASTRAN. In general, the superelement capability is available to the user of the acoustic package. The input listing of Run 1 is shown in Appendix B1.

**Caution:** If superelements are used, the following limitations (mentioned in section 6.1.3) must be observed:

1. The whole fluid model must be in the residual structure.
2. Any superelement that has any interior grid points that are in contact with the fluid must be in primary superelement. It cannot be an identical or a mirror image, i.e., secondary superelement.
3. Fluid grid points must be "reasonably" coincident with an adjacent structure grid point. Coincidence is defined, see section 6.3.4.1, by the AMP parameter, TOL 1. (Remember: An unconnected fluid surface grid point is assumed to have a  $\partial p / \partial n = 0$  boundary condition, i.e., rigid wall).

#### 6.3.1 Executive Control Deck

The DMAP alter must be inserted following the SOL 63 call. This instruction is in general automatically fulfilled by the actual machine-dependent procedure, i.e., no user action is necessary. If the analysis is performed in multiple steps, the DMAP alter must be present during the residual structure processing. It is recommended that the alter program be included for processing of all upstream superelements. There are no other special instructions.

#### 6.3.2 Case Control Deck

During the residual structure processing the user is required to do the following:

1. Specify a **LOADSET = xx** to select an **LSEQ** card in the Bulk Data Deck. **LSEQ** will be described in the discussion of the Bulk Data Deck.
2. Define **SET yy = I thru J** such that all fluid grid points are in the range of **I** to **J**. This set can include any number of nonexistent grid points.

3. Specify **DISP ( . . . ) = ALL** for all superelements that have any interior grid points in contact with the fluid.
4. Define two subcases for Fluid-Structure Interaction. Note that there is ordinarily only one subcase for the residual structure processing. The first subcase contains the **PARTN = yy**, where **yy** references the **SET yy** defined above and a **METHOD** card selecting an eigenvalue extraction method for the structure only. The second subcase contains only the **METHOD** card for selecting the eigenvalue extraction method for the fluid.

### 6.3.3 Bulk Data Deck

The structural model is defined in the usual way. The fluid model is defined in the same way with one exception. The material property cards define the bulk modulus and the density of the fluid. For two-dimensional elements use the **MAT2** and for three-dimensional elements use the **MAT9** cards. Due to the analogy described in section 4.3, the density of the fluid is

$$1/\chi$$

and the  $G_{ii}$  entries are

$$1/\rho_f$$

Use of the parameter **PARAM, COUPMASS** requires some consideration. This parameter selects the consistent mass formulation. If the user does not wish to use the consistent mass for all the elements in the model, the parameter can be specified in the Case Control Deck. Specifically, if the superelements are used then the **COUPMASS** can be specified for any superelement. In any case the **PARAM, COUPMASS** should be used for the residual since the fluid is in the residual structure.

**Caution:** The parameter specification must be placed in the first subcase and not in the second subcase of the residual.

The two unique remaining items for the fluid model are the specification of the pressure load data to help define the 1) coupling areas (=> coupling matrix) and 2) absorbing areas (=> absorption matrix) of the fluid surface. The definition of these areas takes place in the two-dimensional case by **FORCE** cards and in the three-dimensional case by **PLOAD2** or **PLOAD4** cards.



**Caution:** The pressure magnitude must be 1.0 and its direction must be inward to the fluid. If one wishes to use PLOAD2 cards the areas have to be described by uniformly oriented surface elements, where the orientation is prescribed by the direction of the surface normal using, e.g., the right-hand-rule. If an error is made in the definition of the direction, it can be corrected later in the AMP Input (see section 6.3.4.1).

The first pressure (force) load defined must be applied to the surface of the fluid in contact with the structure.

The absorption areas are defined by specifying pressure loads on the surfaces at which absorption material is in contact with the fluid. Note that the absorption area may be internal to the fluid, such as a seat in the automobile acoustic cavity. Each pressure load with a different Set Id (Id: Identification) represents a separate absorption area. The order number for these areas is specified on the LSEQ card.

The format of the LSEQ card is

LSEQ	SID	AID	LID
------	-----	-----	-----

The SID is selected by the LOADSET = SID in the Case Control Deck. The AID entry defines the order of the load vectors representing the total surface area and the absorption areas. The LID represents the Set Id of the applied pressure (force) loads. Each LID is associated with a specific AID. Therefore, the absorption areas are numbered by their association with the AID entry.

**Caution:** The pressure load applied to the surface of the fluid in contact with the structure ( $\Rightarrow$  coupling matrix) must have the lowest numbered AID.

Example:

Let  $S_B$  be the total (discretized) surface of the fluid,  $S_{BC}$  the total surface of the fluid coupling with the structure and  $I_{BC1}$  through  $J_{BC1}$  the element numbers of  $S_B$ . Assume  $S_{BC}=S_B$ , i.e., the whole surface is coupling. Further, let  $S_{BA}$  be the total absorbing area of the fluid surface with  $S_{BA} \subset S_B$  consisting of  $m$  different subareas  $S_{BA1}, S_{BA2}, \dots, S_{BAm}$ . The element numbers belonging to these subareas are  $I_{BA1}$  through  $J_{BA1}, I_{BA2}$  through  $J_{BA2}, \dots, I_{BAm}$  through  $J_{BAm}$ .

PLOAD2 and LSEQ Input					
Coupling surface					
PLOAD2	LID <sub>BC1</sub>	1.0	I <sub>BC1</sub>	THRU	J <sub>BC1</sub>
LSEQ	SID	AID <sub>BC1</sub>	LID <sub>BC1</sub>		
Absorbing areas					
PLOAD2	LID <sub>BA1</sub>	1.0	I <sub>BA1</sub>	THRU	J <sub>BA1</sub>
PLOAD2	LID <sub>BA2</sub>	1.0	I <sub>BA2</sub>	THRU	J <sub>BA2</sub>
.	.	.	.	.	.
.	.	.	.	.	.
.	.	.	.	.	.
PLOAD2	LID <sub>BA<sub>m</sub></sub>	1.0	I <sub>BA<sub>m</sub></sub>	THRU	J <sub>BA<sub>m</sub></sub>
LSEQ	SID	AID <sub>BA1</sub>	LID <sub>BA1</sub>		
LSEQ	SID	AID <sub>BA2</sub>	LID <sub>BA2</sub>		
.	.	.	.		
.	.	.	.		
.	.	.	.		
LSEQ	SID	AID <sub>BA<sub>m</sub></sub>	LID <sub>BA<sub>m</sub></sub>		

In this example each absorbing subarea  $S_{BA1}$ ,  $S_{BA2}, \dots, S_{BA_m}$  is also a coupling area, i.e., it is  $S_{BAi} \subset S_{BC}$  ( $i = 1, \dots, m$ ).

In this example, the assumption was:  $S_{BC} = S_B$ . If there are subareas of  $S_B$  that are not coupled, then  $S_{BC} \subset S_B$  and according to this situation the element numbers, which determine the coupling area, have to be changed on the PLOAD2 card for this case.

Other combinations of coupling and absorbing areas have to be handled in a similar way.

#### 6.3.4 Area matrix program input/output

Before any of the response analysis can be performed the AMP must be executed. The purpose of AMP is to generate the coupling matrix (or matrices) between the structure and the fluid. It also generates the absorption matrix (or matrices) if they are to be included in the analysis.

### 6.3.4.1 Input files

There are two input files for AMP that by default are defined to be Fortran Units 14 and 15. The data which are assigned to these files are generated by MSC/NASTRAN SOL 63 Normal Modes Analysis of the structure and the fluid. These data consist of the following MSC/NASTRAN data blocks:

```

OUTPUT2   PFS,  CSTM,PGF,   SEID,PGA//0/V,Y,CSTMOUT=11  $
OUTPUT2   GPLS,SILS,BGPDTS           //0/V,Y,GEOMOUT=12  $
    
```

During the SOL 63 run (Run 1, see fig. 1) five data blocks are written to Fortran Unit 11 and three data blocks are written to Fortran Unit 12 by default. As can be seen in the above DMAP statements these default values can be redefined by specifying parameters CSTMOUT and GEOMOUT.

During the AMP run, data blocks PFS, CSTM, PGF, SEID, and PGA are assigned to Fortran Unit 14. Data blocks GPLS,SILS, and BGPDTS are assigned to Fortran Unit 15. The contents of these data blocks are as follows:

Name	Contents
PFS	This is the partition vector that separates the fluid grid points from the structure grid points in the residual.
CSTM	Coordinate System Transformation Matrices.
PGF	This file contains the areas associated with each fluid grid point that is on the interface with the structure model.
SEID	Contains the Superelement ID's if there are superelements in the analysis.
PGA	This file contains the absorption data. Each column of this matrix defines a different absorption area.
GPLS	Grid Point List Table.
SILS	Scalar Index List Table.
BGPDTS	Basic Grid Point Definition Table that defines the locations of all the grid points in the model.

The direct input to the AMP program is input at the terminal or Unit 5. The input is relatively simple and will be described by the order of appearance. The input is assumed to be in free format, meaning that the data are separated by a comma or a blank.

RECORD NO. 1 - TOL1, TOL2 (real, real)	
TOL1	If the fluid and structure grid points are within the distance less than TOL1 then they are considered to be coincident.
TOL2	In general, the area matrix terms have components in x,y, and z directions ( $A_x, A_y, A_z$ ). The total area then is simply $A_i = \sqrt{A_x^2 + A_y^2 + A_z^2}$ . If for any of the area components, $A_i/A_i < TOL2$ then $A_i$ will be ignored, i.e., $A_i = 0$ ( $i = x,y,z$ ). Usually, TOL2 is equal to 0.

RECORD NO. 2 - IFF, FF (integer, real)	
IFF	Identifies which of the structural DOFs will be used as the pressure DOF. If the $T_i$ DOF is used as pressure DOF, then $IFF = i$ ( $i = 1,2,3$ ), e.g., T1 is the DOF in x direction.
FF	Defines the multiplier for the area matrix terms. Used primarily to reverse the sign of the surface normal, which must be inward to the fluid, if one made an error. Usually, FF is equal to 1.0.

RECORD NO. 3 - ANS (character)	
ANS	Y or N, i.e., Yes or No. If Yes, then the user will be requested in the next record to specify the search region for the determination of fluid to structure grid points match. In some cases, by specifying the search region, the computational effort may be reduced. In most cases this has been found not to be very significant.

RECORD NO. 4 - XL,XU,YL,YU,ZL,ZU (reals), required only if ANS=Y	
The above six numbers define a rectangular region in the basic coordinate system. They provide the lower (L) and upper (U) bounds for each coordinate direction X, Y, and Z.	

The following records are required only if there are absorption areas. The AMP will print out the number, NCOL, of unique absorption areas that it has found from the PGA data block.

RECORD NO. 5 - (NR(I), I = 1, NCOL) (integers)	
NR(I)	If $NR(I) < 0$ the absorption data will not be generated for I'th region. If $NR(I) > 0$ the absorption data will be generated for I'th region. If all $NR(I) < 0$ no further input is required.

<b>RECORD NO. 6 - NF (integer)</b>	
NF	Specifies the number of frequencies at which the absorption data will be provided. This is required if absorption is defined as a function of frequency. If a constant value of absorption is desired, set NF = 1.

<b>RECORD NO. 7 - (F(I), I = 1, NF) (reals)</b>	
F(I)	Frequencies at which the absorption data will be provided. Note that the absorption data for all retained regions must be supplied for all the frequencies even though some regions may not have frequency dependent absorption properties.

<b>RECORD NO. 8 - RHOC (real)</b>	
RHOC	Value representing the product of the density, $\rho_f$ , and the speed of sound, $c_f$ , for the fluid medium (see section 4.1, constant $Z_o$ in eq. 93).

The following NF records are repeated for every absorption area that is active. At most this number will be NCOL. Note, that in Record 5 any or all absorption areas can be ignored.

<b>RECORD NO. 9 - CR(I), CI(I) (reals)</b>	
•	•
•	•
•	•
<b>RECORD NO. 9+(NF-1) - CR(NF), CI(NF) (reals)</b>	
CR(I)	Real part of the specific acoustic admittance.
CI(I)	Complex part of the specific acoustic admittance. See eqs. 93, 94, and 95 in section 4.1.

### 6.3.4.2 Output files

Three files are generated by the AMP program. By default, they are written to Fortran Units 16, 19, and 20. Data contained in these files are as follows:

- UNIT 16: MSC/NASTRAN DMI cards that define the coupling matrices, describing the coupling area of the fluid surface. There will be as many different names for the DMI matrices as there are superelements that have any internal points connecting to the fluid model. If there are absorption areas, then this file will also contain the DMIG cards that describe the damping properties for each absorption area. All absorption areas are grouped into one DMIG matrix. Since absorption matrices can be frequency dependent, there will be as many unique DMIG matrices as there

are frequencies at which the the absorption properties are defined. This file is required in SOL 70, 71, and 72.

- UNIT 19: MSC/NASTRAN Case Control Set card definition, SET 911= $n_1, n_2, n_3, \dots, n_n$  where  $n_i$ 's represent fluid grid points that are on the surface of the fluid mesh and in contact with the structure. This file will be used in the calculation of the Grid Point Participation Factors.
- UNIT 20: This file contains some DMAP statements. These statements redefine the names of the DMI matrices (area matrices) that are stored in the data base. It changes the names from that of "DMIxxxx 0 0" to "AREA 0 xxxx," where xxxx is some integer value and the other two values are the data block qualifiers. This file is required in the SOL 70, 71, and 72.

#### 6.3.4.3 Absorption property interpolation

Generally, absorption properties are frequency dependent (see section 4.1). The dependency is significant and cannot be ignored. To accommodate this phenomenon, a provision has been made to allow the user to specify any curve that defines the properties as a function of frequency. There is a capability in the FRRD2 module (Frequency Response for Aeroelastic Analysis) that uses a spline technique to interpolate any complex matrix quantity. The user is required only to specify matrices of complex quantities as a function of frequency. This capability originally was intended for the interpolation of aerodynamic matrices. Owing to this fact, a very special form of spline interpolation is used. The user must understand this spline form, so that the absorption function can be properly defined.

This interpolation technique is best illustrated in figure 5.

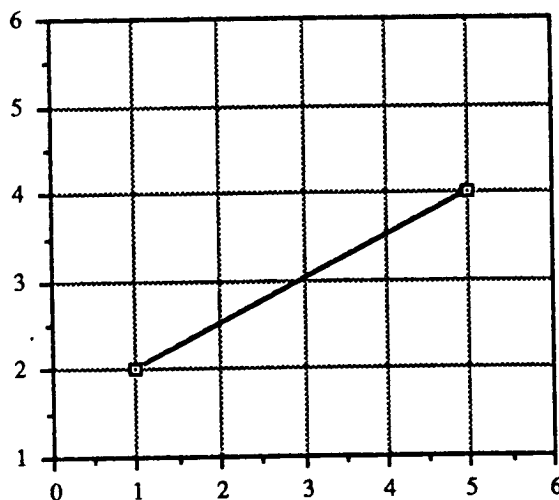


Figure 5(a). Interpolation technique.

In this figure a simple line, defined by two points, is shown. The absorption is a complex quantity and this line represents the same variation versus frequency for both the real and the imaginary components. Figure 5(b) illustrates the behavior of MSC/NASTRAN spline interpolation.

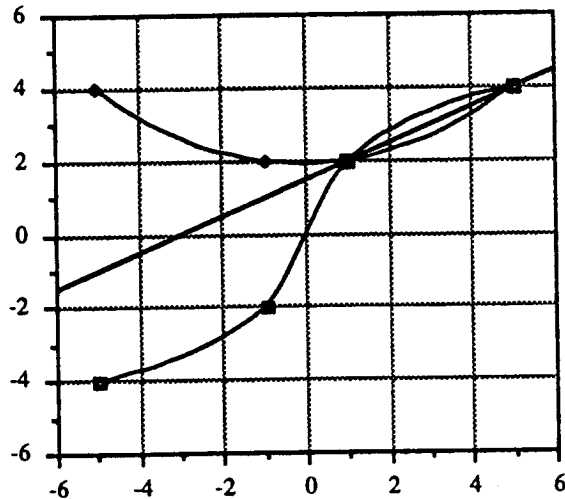


Figure 5(b). Behavior of MSC/NASTRAN spline interpolation.

For the real component the zero slope at zero frequency is assumed, i.e., the curve is symmetric about the y-axis. For the imaginary component the assumption is made that the function value is zero at zero frequency, i.e., the curve is antisymmetric about the y-axis. Obviously, the resultant interpolation of the real and complex quantities does not produce the correct result. To remedy this problem, additional input is required. This problem can be avoided by specifying a slope of the curve at the first frequency value. The slope can be defined implicitly by specifying two points spaced closely together as shown in figure 5(c). The resultant interpolation is shown in figure 5(d).

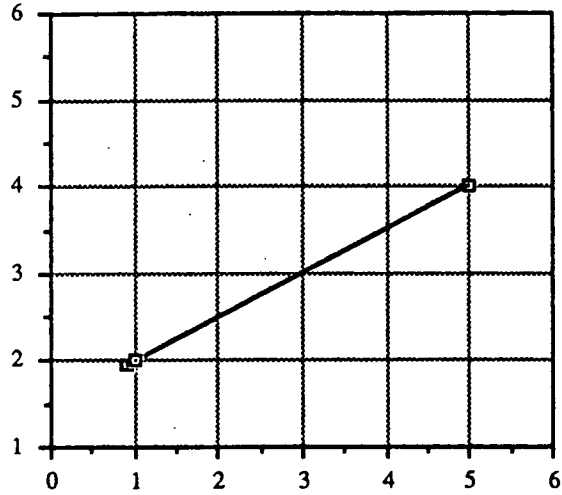


Figure 5(c). Slope defined implicitly by specifying two points spaced closely together.

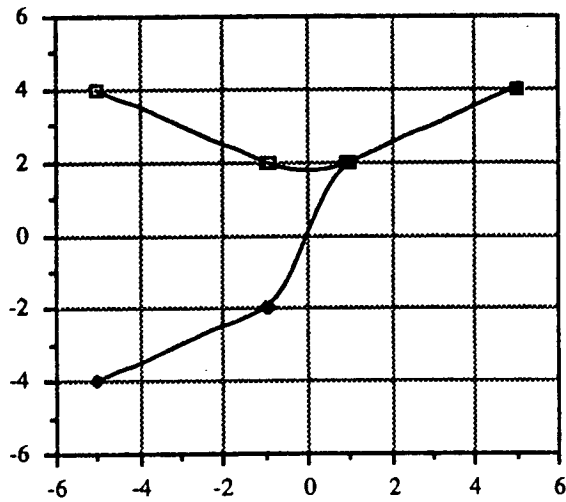


Figure 5(d). Resulting interpolation.

Caution: The absorption should not be defined at zero frequency because MSC/NASTRAN divides the function value by frequency when interpolating the imaginary part of the absorption quantity.

#### 6.4 Normal Modes Analysis of the Modal Coupled Fluid-Structure System (Run 2)

This analysis is performed only if the coupled Fluid-Structure-Interaction (FSI) modes are required. In this case both the structure and the fluid are represented by their respective



modal coordinates, calculated during Run 1 (SOL63). This is, compared to Run 1, a rather quick and simple calculation, since the problem size is generally very small. Even though SOL 70 is used, the DMAP program allows the user to calculate the real eigenvalues of the coupled system if there are no actual damping matrices. In that case a different symmetric formulation is used where the coupling terms are no longer in the damping matrix (see section 3.4, e.g., eq. (64)). Before executing the MSC/NASTRAN analysis the AMP must be run in order to prepare coupling (DMI input) and also, if required, absorption (DMIG input) data. The input to AMP for this case is

```

RECORD NO: 1:   TOL1 = 1., TOL2 = 0.

RECORD NO: 2:   IFF = 1, FF = 1.

RECORD NO: 3:   ANS = N

RECORD NO: 5:   NR(I) = -1 (I=1,...,NCOL) means:
                 -1,-1,...,-1 (NCOL "times" -1 or NCOL*-1)

```

The Record 5 implies that no absorption matrices will be generated. Input listing of Run 2 is shown in Appendix B2.

#### 6.4.1 Executive Control Deck

1. It is required that the downstream data base from SOL 63 be assigned to the read-only data base, DBSET 15.
  - NASTRAN DBSET 1=(DB01, DB15), DBSET 2=(DB01, DB15)
  - NASTRAN DBSET 15=(DB15)
2. Include a small DMAP program (DMAP.DAT) generated by AMP, fetched from UNIT 20. This usually is done by a merge utility, which varies with the computer system used.
3. Include one of two DMAP alter programs; one is used for the real and the other is used for the complex eigenvalue analysis. The real eigenvalue analysis capability has been provided for the case with no damping terms.

Both DMAP programs are inserted following the SOL 70 call. This instruction is, in general, automatically accomplished by the actual machine-dependent procedure and needs no additional user action.

### 6.4.2 Case Control Deck

1. Specify **SET xx = 0, SEMG = xx**.
2. Select the usual output requests, i.e., structural or fluid grid points for, e.g., plotting deformed shapes.
3. Select eigenvalue extraction method, either **METHOD = yy** or **CMETHOD = zz**, depending on the selection of real or complex eigenvalue analysis.

Where **xx**, **yy**, and **zz** are some user-specified integer numbers.

### 6.4.3 Bulk Data Deck

Specify the following parameters:

1. **PARAM, DLOAD, -1**
2. **PARAM, RESDUAL, -1**  
Caution: see parameter description NASTRAN USER'S MANUAL Vol II.
3. **PARAM, LMODES, xx**; where **xx** > sum of modes for the fluid and the structure from Run 1 (SOL 63). **PARAM, LFREQ** and **PARAM, HFREQ** must not be used.
4. **PARAM, SMALL, EPS**; where **EPS** is used to filter the modal area matrix terms. If any area matrix term,  $A_{ij}$ , divided by the largest  $|A_{ij}|$  is smaller than **EPS**, then that  $A_{ij}$  is discarded. If  $(A_{ij}.lt. A_{ijmax}) A_{ij} = 0$ . Default for **EPS** is 1.E-6.

Additionally, the user must specify the eigenvalue extraction method, either **EIGR** or **EIGC** depending on the type of solution. Using the computer system merge utility, include the contents of file on UNIT 16. This file includes the area matrix defined on DMI/DMIG cards.

## 6.5 Modal Frequency Response Analysis (Run 3.1)

This is probably the most commonly used analysis technique for FSI calculations. Like the coupled modes solution, this analysis is also restarted from SOL 63 data base (Run 1). Before executing this analysis, the AMP must be run to generate the required files (DMI, DMIG, DMAP.DAT) as described in section 6.4. The input to AMP for this case is, e.g.,

RECORD NO: 1: TOL1 = 1., TOL2 = 0.

RECORD NO: 2: IFF = 1, FF = 1.

RECORD NO: 3: ANS = N

RECORD NO: 5: NO ABSORPTION  
NR(I) = -1 (I=1,...,NCOL) means:  
-1,-1,...,-1 (NCOL "times" -1 or NCOL\*-1)

ABSORPTION:  
NR(I) = 1 (I=1,...,NCOL) means:  
1,1,...,1 (NCOL "times" 1) or NCOL\*1

Input listing of Run 3.1 is shown in Appendix B3.1.

### 6.5.1 Executive Control Deck

1. It is required that the downstream data base from SOL 63 be assigned to the read-only data base, DBSET 15.

- NASTRAN DBSET 1=(DB01, DB15) , DBSET 2=(DB01, DB15)
- NASTRAN DBSET 15=(DB15)

2. Insert a small DMAP program (DMAP.DAT) generated by the AMP.

3. Insert a DMAP Alter Program for Frequency Response.

Both DMAP programs are inserted following the SOL 71 statement. This statement is, in general, satisfied automatically by the machine-dependent procedure and needs no additional user action.

### 6.5.2 Case Control Deck

No special instruction must be observed.

Exception: If pressure response curves at fluid grid points  $GPF_i$  ( $i = 1, 2, \dots$ ) are required, the user must use the following Case Control cards:

```
SET pp = GPF1,GPF2,...  
VELO = pp  
.  
.  
.  
Plot request:  
XYPLOT VELO / GPFi(T1RM).
```

Where  $pp$  is some user specified integer number.

### 6.5.3 Bulk Data Deck

Specify the following parameters:

1. **PARAM, DLOAD, -1**
2. **PARAM, NORF, -1**; no residual flexibility for the fluid.
3. **PARAM, LMODES, XX**; see section 6.4.3)
4. **PARAM, SMALL, EPS**; see section 6.4.3)

There are two possible methods for specifying the modal damping for the structure and fluid. The first method is to use the TABDMP1 Bulk Data card. In this case, the fluid modal damping is defined in the third quadrant, i.e., frequency and damping values must be input with a negative sign. The second method is to input the modal damping via the DMI cards. Damping can be specified for each structure and fluid mode, as output from Run 1, via DMI cards. One DMI card is assigned to each mode that has modal damping. The number of the DMI card must be the same as the number of that mode. Using the DMI input, the DMAP program generates modal damping matrices TGDMP5 and TGDMPF for structure and fluid respectively, which are added to the total modal damping matrix of the modal coupled system.

The following example illustrates the modal damping input via DMI cards: Let  $n_s$  be structural modes and  $n_f$  fluid modes calculated in Run 1. Some of the modes are damped and some are not damped.

Fluid:

DMI, TGDMPF, 0, 2, 1, 1, 1, $n_f$				
		Mode No.		Modal Dmp.
DMI	TGDMPF	1	1	0.03
DMI	TGDMPF	2	1	0.03
DMI	TGDMPF	3	1	0.03
•	•	•	•	•
•	•	•	•	•
DMI	TGDMPF	n	1	0.03

Structure:

DMI,TGDMPS,0,2,1,1,,1, $n_s$				
		Mode No.		Modal Dmp.
DMI	TGDMPS	1	1	0.06
DMI	TGDMPS	2	1	0.03
.	.	.	.	.
.	.	.	.	.
DMI	TGDMPS	9	1	0.0
DMI	TGDMPS	10	1	0.02
.	.	.	.	.
.	.	.	.	.
DMI	TGDMPS	21	1	0.0
DMI	TGDMPS	22	1	0.04
.	.	.	.	.
.	.	.	.	.
DMI	TGDMPS	n	1	0.0

**Caution:** The modal damping is input as % of critical modal damping, where 3% is specified as 0.03.

### 6.6 Modal Transient Response Analysis (Run 3.2)

In many respects, this analysis is very similar to the frequency response analysis so it will not be described in detail. The difference in the two analysis methods are the same as for any other non-FSI analysis, i.e., **FREQ** versus **TSTEP**, **RLOADi** versus **TLOADi**, etc. Furthermore, a special DMAP Alter Package is used and no absorption damping is allowed.

### 6.7 Structural Grid Point Participation (Run 4)

Before executing this run, the frequency response analysis, Run 3.1, must have been successfully completed. The output from this run is a very useful diagnostic tool in the acoustic analysis. With this output the user can pinpoint the source that causes a pressure rise or fall at any point in the interior of the fluid domain. Since one is usually concerned with the structure surrounding a fluid, this information can be beneficial in the redesign of the part of the structure that causes a noise problem.

### 6.7.1 Executive Control Deck

1. It is required that the downstream data base from SOL 63/SOL 71 be assigned to the read-only data base, DBSET 15.

```
NASTRAN DBSET    1=(DB01, DB14, DB15)
NASTRAN DBSET    2=(DB01, DB14, DB15)
NASTRAN DBSET    15=(DB14, DB15)
```

2. Insert a DMAP alter program

The Grid Point Participation DMAP Alter Program is automatically inserted by the machine dependent procedure and no user action is necessary.

### 6.7.2 Case Control Deck

1. Insert the file SET.DATA (SET 911) from UNIT 19, which contains the fluid points that are coupled to the structure.

2. DISP = 911

3. Input of frequencies for which the participation factor should be calculated

```
SET xx = F1, F2, F3, . . . , Fn
OFREQ  = xx
```

The input frequencies  $F_1, F_2, F_3, \dots, F_n$  should be approximately equal to the frequencies used in Run 3.1 (SOL 71).

### 6.7.3 Bulk Data Deck

1. User Instruction for calculating the participation factor at fluid grid point  $GID_i$  (CID is the DOF which determines the pressure; usually it is  $CID = 1$  (see description of Run 1).

```
DMIG, PDOF, 0, 6, 1, 0
DMIG, PDOF, GIDi, CID, , GIDi, CID, 1.0
```

2. If one only wants the real displacement output set

```
PARAM, REAL, 0
```

#### 6.7.4 Output

The output from this run requires some explanation because it is not immediately obvious. This output describes the contribution of the structural grid points to the generation of the pressure anywhere in the interior of the fluid domain. Obviously, the only structural grid points that can contribute to the pressure in the fluid domain are the points on the interface to the fluid. The AMP establishes the relationship between the fluid and structural points on the interface. In general, one structural grid point is "connected" to a closest single fluid grid point. In other words, there is a one-to-one correspondence between the fluid and structural grid points on the interface. The goal of this output is to provide a numerical as well as a graphical representation of structural grid participation factors.

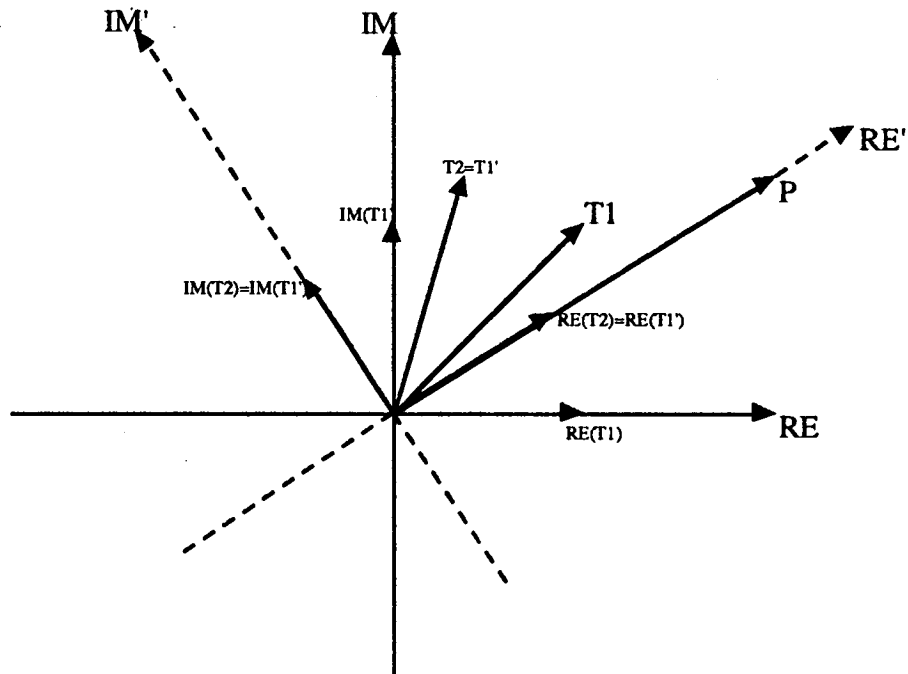
In most typical applications of this acoustic procedure (such as aircraft or automobile noise studies), the structural mesh will usually be much finer than the corresponding fluid mesh, therefore, only some of the structural points on the interface will be "connected" to the fluid surface. Also, the structural mesh on the interface may contain a number of different types of elements. It is very difficult to graphically (contour plots, etc.) present the participation information on such a mesh. The fluid mesh is usually composed of three-dimensional elements and it is easy to plot contours on the outside surface of the fluid domain. To facilitate the graphical display, the output of the structural grid participation factors is transferred to the corresponding fluid grid points as produced by the AMP. The results of this operation can be seen in section 8.

The output of this analysis looks like the usual SORT1 "Complex Displacement Vector" output for frequency response. It is generated for a user-specified interior fluid point,  $GID_i$ , at each frequency,  $F_i$  ( $i = 1, 2, \dots, NF$ ), input in the Case Control Deck (see above). The contribution to the pressure at interior fluid point,  $GID_i$ , influenced by the participation points, is given. The participation points are the structural points on the interface, but in the output they are labeled by the corresponding fluid point on the interface as explained above.

COMPLEX DISPLACEMENT VECTOR (REAL/IMAGINARY)				
Participation Point ID	T1	T2	T3	R1
PGP <sub>i</sub> (i=1,2,..,N <sub>C</sub> )	RE(T1) IM(T1)	RE(T2) IM(T2)	RE(T3) IM(T3)	R1 0
•	•	•	•	•
•	•	•	•	•
•	•	•	•	•

$N_C$  is the number of fluid coupling points on the interface and they are listed in SET 911.

1. Listed under the heading T1 is the real (RE(T1)) and the imaginary (IM(T1)) components of all participating points  $PGP_i$  ( $i=1, \dots, N_C$ ). If all the terms are added, the actual pressure at frequency  $F_i$  for the selected fluid point,  $GID_i$ ,  $CID$ , will be obtained.
2. Under the heading T2 each term in T1 is rotated in the complex plane such that the real term is in the direction of the resultant pressure vector (for point  $GID_i$ ) and the imaginary term will be at  $90^\circ$  to that vector (see fig. 3). The new coordinate system is labeled by ( ' ).



Note the sign of RE(T2): + means "contribute" to pressure p  
- means "subtract" from pressure p.

3. Under the T3 heading the output is simply the vector

$$T3 = \frac{T2}{\|P\|}$$

which gives the fraction of the contribution for each point. Note that only the real term of T2 contributes to the resultant pressure.  $\|P\|$  is the magnitude of the pressure vector.

4. Under the R1 heading, the output is the same as the T3 except that each term is normalized by the largest real term.



## 7. DEMONSTRATION OF ACOUSTIC CALCULATIONS AND THEORETICAL VERIFICATION

### 7.1 A One-Dimensional Example

#### 7.1.1 Description of the model

Generally, it is very difficult to obtain theoretical solutions for practical problems of FSI. Such solutions are necessary to evaluate the results and the accuracy of the finite element analysis. A simple Fluid-Structure System for which an analytic solution exists will be used to verify the finite element results and to demonstrate most of the capabilities of the acoustic procedure presented here. Owing to his expertise in the mathematics of acoustics, all the equations in this section were derived and solved by the second author.

The system consists of a straight air-filled tube with quadratic cross section. One end of the tube is closed by a rigid wall ( $|Z_n| = \infty$ ), or by an absorbing wall ( $0 < |Z_n| < \infty$ ), and the other end has a moveable piston supported by a spring-damper-system.  $Z_n$  is the normal impedance of the boundary. Additionally, the piston surface can be chosen to be absorbing. A more general situation is to introduce flexible walls on both ends of the tube (with or without absorbers) which can be done by a simple spring-damper system.

The natural frequency of a one-degree-of-freedom spring-damper-piston system is assumed to be close to that of the air with a fixed piston in order to create an interaction between the air and the structure. In view of response calculations, the piston can be loaded by an external force. The model is shown in the figure 6.

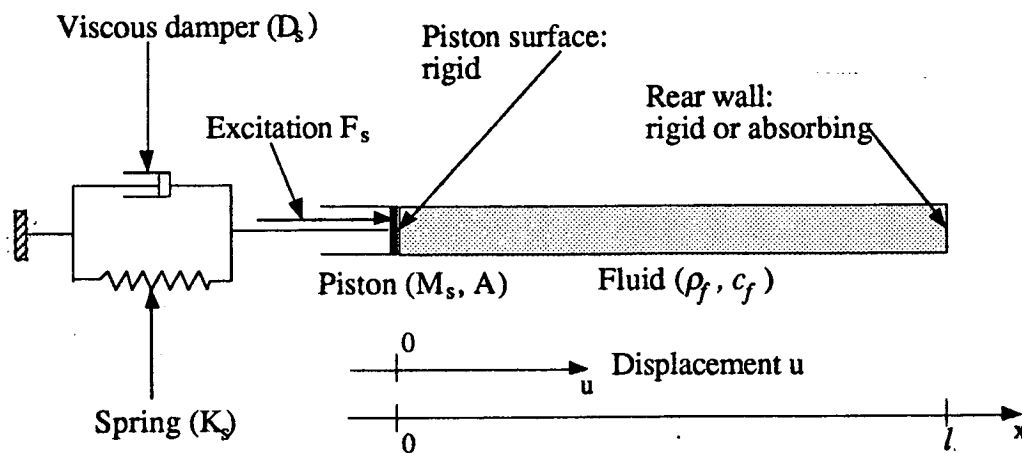


Figure 6. Spring-damper-piston-tube system.

The following table gives the physical properties which are necessary to describe the coupled system.

Table 2. Physical properties		
Spring-damper-piston system (Structure)		
area of piston cross section	$A$	0.000625 m
spring stiffness	$K_s$	7474.75 N/m
mass of piston	$M_s$	0.01 kg
viscous damping	$D_s$	0.50 kg/s
external load	$F_s$	2.1885 N
Air-filled tube (Fluid)		
length of tube	$l$	1.25 m
area of tube cross section	$A$	0.000625 m
speed of sound (air)	$c_f$	344 m/s
density of air	$\rho_f$	1.205 kg/m
bulk modulus	$\chi$	142594.17 N/m
specific acoustic resistance	$Z_1 = \text{Re } Z_n$	228 kg/m <sup>2</sup> s
specific acoustic reactance	$Z_2 = \text{Im } Z_n$	-1456 kg/m <sup>2</sup> s

Remark: Because  $l \gg \sqrt{A}$ , it is sufficient to describe the wave propagation in the tube by a one-dimensional wave equation along the longitudinal axis,  $x$ -axis, of the tube.

### 7.1.2 Theoretical solution

The equation of motion of the damped spring-piston system is given by

$$M_s \ddot{u}(t) + D_s \dot{u}(t) + K_s u(t) = F(t) \quad (122)$$

$M_s$ ,  $D_s$ , and  $K_s$  are mass, viscous damping, and stiffness of the system. The displacement of the piston in  $x$ -direction is  $u$ . The exciting force,  $F(t)$ , consists of an external part,  $F_s(t)$ , acting on the piston and a part,  $F_p(t)$ , induced by the fluid pressure on the piston surface. Discussion is restricted to the steady-state case, i.e., piston displacement, pressure, and exciting force are all assumed to be harmonic in time. Therefore, the following boundary value problem, equation (123), has to be solved:

Structure	Fluid
$(K_s - \omega^2 M_s + i\omega D_s)u = F_s + F_p$ <p>with <math>F_p = -Ap(0)</math>.</p>	$\frac{d^2}{dx^2} p(x) + k^2 p(x) = 0 \quad (k = \omega/c_f)$ <p>Boundary Conditions:</p> <ol style="list-style-type: none"> <li><math>x = 0</math>:  <math display="block">\frac{\partial p}{\partial x} = \rho_f \omega^2 u.</math></li> <li><math>x = l</math>: <math display="block">\frac{\partial p}{\partial x} = \alpha \left( -i\omega \rho_f \frac{1}{Z_n} p \right),</math></li> </ol> <p>with <math>\alpha = 0</math>: rigid, <math>\alpha = 1</math>: absorbing.  <math>Z_n</math> is the impedance of the absorber (see section 4.1)</p>

In the following, several formulas will be presented for

1. coupled eigenvalues
2. pressure distribution in the tube along the  $x$ -axis belonging to these eigenvalues
3. expressions for the piston displacement,  $u = u(v)$ , and pressure,  $p(x, v)$ , in the tube at location  $x$

All these formulas will depend on the excitation frequency. The derivation of the formulas is elementary, therefore, details can be omitted. A more detailed mathematical investigation of some FSI questions can be found in reference 33.

#### 7.1.2.1 Coupled Eigenanalysis

With  $D_s = 0$ ,  $F_s = 0$ , and  $\partial p/\partial x = 0$  at  $x = l$ , from equation (123) follows the eigenvalue problem of the the spring-piston-tube system. In order to obtain the eigenvalue equation, first obtain solutions of the fluid boundary value problem of the form

$$p(x, k) = C_1 \cos kx + C_2 \sin kx$$

where  $C_1$  and  $C_2$  have to be determined from the boundary conditions, elastic at  $x = 0$  and rigid at  $x = l$ .

Using  $k = \omega/c_f$ ,  $\omega = 2\pi\nu$ , and  $Z_0 = c_f \rho_f$ , the following expression is obtained

$$p(x, v) = 2\pi Z_0 u v \left( \tan \frac{2\pi l}{c_f} v \right)^{-1} \left\{ \left( \tan \frac{2\pi l}{c_f} v \right) \left( \sin \frac{2\pi v}{c_f} x \right) + \left( \cos \frac{2\pi v}{c_f} x \right) \right\} \quad (124)$$

and from that

$$p(0, \nu) = 2\pi Z_0 \mu \nu \left( \tan \frac{2\pi l}{c_f} \nu \right)^{-1} \quad (125)$$

Combining the structural part of equation (123) with equation (125) yields a transcendental equation for the frequencies,  $\nu = \nu_j$  ( $j = 1, 2, 3, \dots$ ), of the coupled system,

$$\tan \frac{2\pi l}{c_f} \nu = \frac{Z_0 A}{2\pi M_s} \cdot \frac{\nu}{\nu^2 - \nu_s^2} \quad (126)$$

where  $\nu_s$  is the frequency of the spring-piston system (see eq. 127). Table 3 shows the frequencies of the uncoupled and coupled structure-fluid system. The calculation is based on the data shown in table 2.

Table 3. Coupled and uncoupled frequencies (in Hz)		
Spring-Piston System	Tube (air-filled)	Coupled System
137.6	137.6	128.3345
		147.1835
	275.2	
	412.8	
	550.4	

Note that the frequencies of the spring-piston system and the air-filled tube with rigid boundary at  $x = 0$  and  $x = l$  were calculated from

$$\nu_s = \frac{1}{2\pi} \sqrt{\frac{K_s}{M_s}} \quad \text{and} \quad \nu_f^{(n)} = n \frac{c_f}{2l} \quad (n = 1, 2, 3, \dots) \quad (127)$$

It can be seen from table 3 that the interaction between the spring-piston system and the air in the tube, with rigid boundary at  $x = l$ , leads to a considerable shift in the frequency,  $\nu_s$ , of the spring-piston system and  $\nu_f^{(1)}$  of the fluid. Clearly, as  $j$  increases, the frequency shift,  $\nu_j - \nu_f^{(j-1)}$  ( $j = 3, 4, 5, \dots$ ), tends to zero. Moreover, the coupling increases the fluid frequencies, i.e.,  $\nu_f^{(j-1)} < \nu_j$  if  $j > 2$ .

In figure 7, equation (126) is solved graphically by the intersection of two curves

$$y_1(\nu) = \tan \frac{2\pi l}{c_f} \nu \quad y_2(\nu) = \frac{Z_0 A}{2\pi M_s} \cdot \frac{\nu}{\nu^2 - \nu_s^2} \quad (128)$$

in the case  $v_s = v_f^{(1)}$ . This clearly shows the effect of coupling described above.

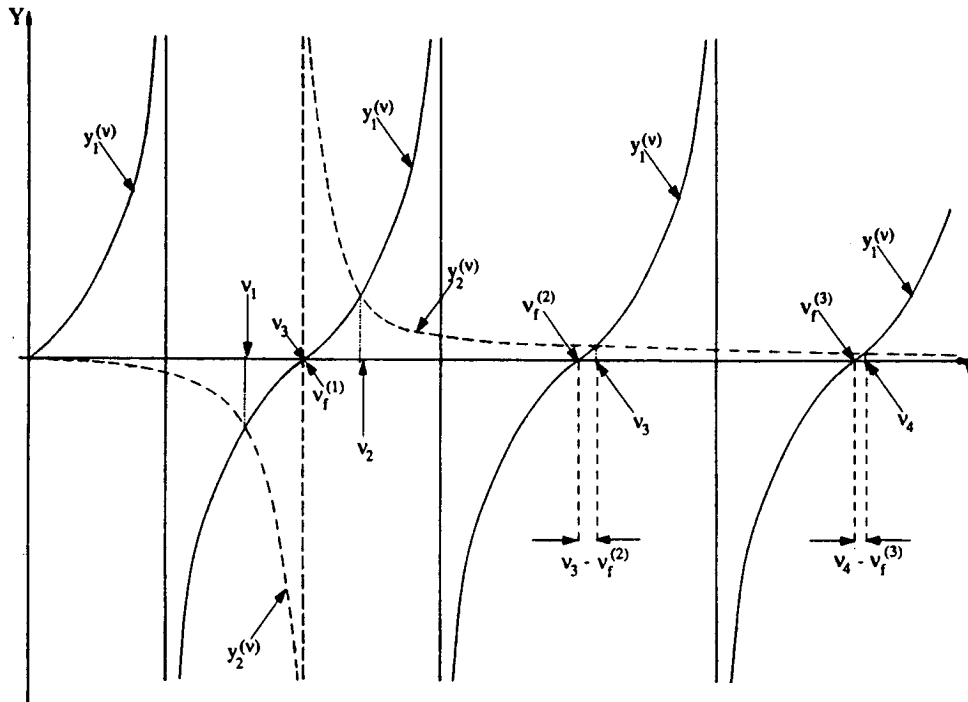


Figure 7. Graphical determination of coupled frequencies.

In the uncoupled case, i.e., rigid boundary at  $x = 0$  and at  $x = l$ , the stationary pressure distribution is given by

$$p_n^{uc}(x) = \text{const.} \cos\left(\frac{2\pi v_f^{(n)}}{c_f} x\right), \quad n = 1, 2, 3, \dots \quad (129)$$

In comparison with equation (129) for the coupled case, the following pressure distribution is obtained (see eq. 124):

$$p_j(x) = \text{const.} v_j \left(\tan \frac{2\pi l}{c_f} v_j\right)^{-1} \left\{ \left(\tan \frac{2\pi l}{c_f} v_j\right) \left(\sin \frac{2\pi v_j}{c_f} x\right) + \left(\cos \frac{2\pi v_j}{c_f} x\right) \right\}, \quad j = 1, 2, \dots \quad (130)$$

As above,  $v_f^{(n)}$  ( $n = 1, 2, 3, \dots$ ) are the frequencies of the standing waves in the rigid bounded tube and  $v_j$  ( $j = 1, 2, 3, \dots$ ) represent the coupled eigenfrequencies. Both groups of frequencies are listed in table 3.

Because of condition 1. in equation (123), the coupling also changes the pressure gradient at  $x = 0$ . For the first two coupled modes

$$\left. \frac{dp_1}{dx} \right|_{x=0} < 0, \quad \left. \frac{dp_2}{dx} \right|_{x=0} > 0 \quad (131)$$

In comparison, for the uncoupled case at the rigid boundary,  $x = 0$ , the pressure gradient is null.

It is obvious that the position of the pressure node, i.e., values for which the pressure is zero, is also influenced by the coupling. These values can be calculated from equation (130) and compared to the corresponding pressure node positions of the standing waves in the tube with rigid boundaries at  $x = 0$  and  $x = l$ . There is a significant shift of the pressure node position,  $x_j^o$  ( $j = 1, 2$ ), especially for coupled modes 1 and 2, compared to  $l/2$ , which is the pressure node position of the first standing wave in the rigid tube. These effects are shown in figure 8.

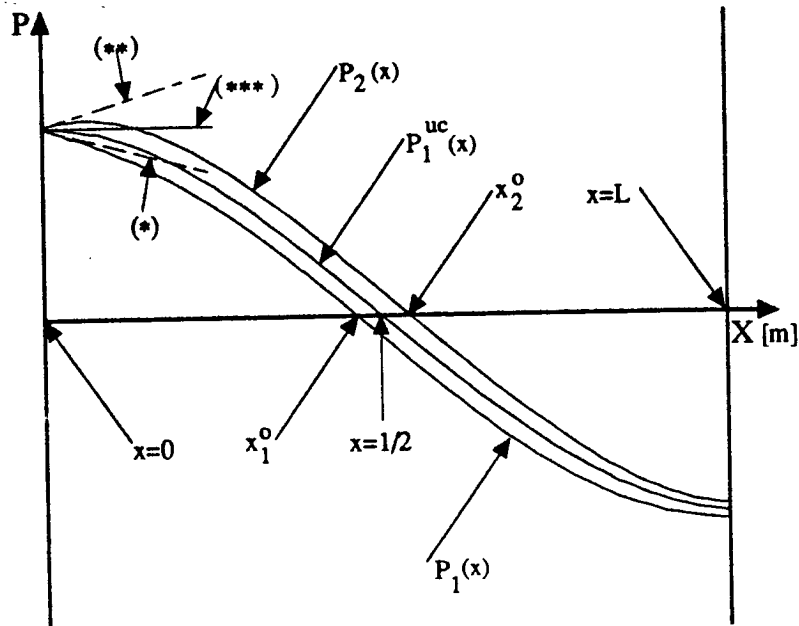


Figure 8. Pressure distribution,  $p_j(x)$ , for coupled modes  $j = 1, 2$ , compared to  $p_n^{uc}(x)$ , of the first standing wave ( $n = 1$ ) in a rigid tube.

Coupled case : (\*)  $\left. \frac{dp}{dx} \right|_{x=0} < 0$ ,      (\*\*)  $\left. \frac{dp}{dx} \right|_{x=0} > 0$

Uncoupled case ("uc") : (\*\*\*)  $\left. \frac{dp}{dx} \right|_{x=0} = 0$

### 7.1.2.2 Frequency response analysis

To get the response (piston displacement  $u$  and pressure  $p$ ) of the coupled system, the boundary value problem, equation (123), has to be solved. Starting with a formulation for the pressure function, equation (124), an elementary calculation yields  $u(\nu)$  for the piston displacement and  $p(x, \nu)$  for the pressure in the tube. The following two expressions result:

$$u(\nu) = \frac{f_{M_s}}{\xi_1^2 + \xi_2^2} (\xi_1 - i\xi_2) \quad (132)$$

and

$$p(x, \nu) = 2\pi Z_0 \nu \frac{f_{M_s}}{\xi_1^2 + \xi_2^2} \left\{ \left[ \xi_1 \left( \Gamma_1 \cos \frac{2\pi\nu}{c_f} x + \sin \frac{2\pi\nu}{c_f} x \right) + \xi_2 \Gamma_2 \cos \frac{2\pi\nu}{c_f} x \right] + i \left[ \xi_1 \Gamma_2 \cos \frac{2\pi\nu}{c_f} x - \xi_2 \left( \Gamma_1 \cos \frac{2\pi\nu}{c_f} x + \sin \frac{2\pi\nu}{c_f} x \right) \right] \right\} \quad (133)$$

respectively, where

$$\left. \begin{aligned} \xi_1 &= (\nu_s^2 - \nu^2) + \frac{AZ_0}{2\pi M_s} \Gamma_1 \nu \\ \xi_2 &= \frac{D_s + AZ_0 \Gamma_2}{2\pi M_s} \nu \\ f_{M_s} &= \frac{F_s}{4\pi^2 M_s} \end{aligned} \right\} \quad (134)$$

$$\left. \begin{aligned} \Gamma_1 &= \frac{\frac{1}{2} [1 - \alpha^2 (\sigma^2 + \gamma^2)] \sin \frac{4\pi l}{c_f} \nu + \alpha \sigma \cos \frac{4\pi l}{c_f} \nu}{\left( \sin \frac{2\pi l}{c_f} + \alpha \sigma \cos \frac{2\pi l}{c_f} \nu \right)^2 + \alpha^2 \gamma^2 \left( \cos \frac{2\pi l}{c_f} \nu \right)^2} \\ \Gamma_2 &= \frac{\alpha \gamma}{\left( \sin \frac{2\pi l}{c_f} + \alpha \sigma \cos \frac{2\pi l}{c_f} \nu \right)^2 + \alpha^2 \gamma^2 \left( \cos \frac{2\pi l}{c_f} \nu \right)^2} \end{aligned} \right\} \quad (135)$$

$$\left. \begin{aligned} \alpha &= \begin{cases} 0 & : \text{boundary at } x = l \text{ is rigid} \\ 1 & : \text{boundary at } x = l \text{ is absorbing} \end{cases} \\ \gamma &= \frac{Z_0 Z_1}{Z_1^2 + Z_2^2}, \quad \sigma = -\frac{Z_0 Z_1}{Z_1^2 + Z_2^2} \\ Z_0 &= \rho_f c_f, \quad Z_1 = \text{Re } Z_n, \quad Z_2 = \text{Im } Z_n \end{aligned} \right\} \quad (136)$$

It is useful to present the response results, i.e., piston displacement,  $u(\nu)$ , and pressure,  $p(x, \nu)$ , in the tube, in terms of absolute values,  $|u(\nu)|$ ,  $|p(x, \nu)|$ , and of their phase shifts,  $\varphi_s(\nu)$  and  $\varphi_f(x, \nu)$ , due to the exciting force

$$F_s(t) = F_s \cdot \exp(i \cdot 2\pi\nu t)$$

From equation (132) one obtains

$$|u(\nu)| = \frac{f_{M_s}}{(\xi_1^2 + \xi_2^2)^{1/2}} \quad (137)$$

and

$$\tan \varphi_s(\nu) = -\frac{\xi_2}{\xi_1} \quad (138)$$

Analogously equation (133) yields

$$|p(x, \nu)| = 2\pi Z_0 \nu \frac{f_{M_s}}{\xi_1^2 + \xi_2^2} \left\{ \left[ \xi_1 \left( \Gamma_1 \cos \frac{2\pi\nu}{c_f} x + \sin \frac{2\pi\nu}{c_f} x \right) + \xi_2 \Gamma_2 \cos \frac{2\pi\nu}{c_f} x \right]^2 + \left[ \xi_1 \Gamma_2 \cos \frac{2\pi\nu}{c_f} x - \xi_2 \left( \Gamma_1 \cos \frac{2\pi\nu}{c_f} x + \sin \frac{2\pi\nu}{c_f} x \right) \right]^2 \right\}^{1/2} \quad (139)$$

and

$$\tan \varphi_f(x, \nu) = \frac{\xi_1 \Gamma_2 \cos \frac{2\pi\nu}{c_f} x - \xi_2 \left( \Gamma_1 \cos \frac{2\pi\nu}{c_f} x + \sin \frac{2\pi\nu}{c_f} x \right)}{\xi_1 \left( \Gamma_1 \cos \frac{2\pi\nu}{c_f} x + \sin \frac{2\pi\nu}{c_f} x \right) + \xi_2 \Gamma_2 \cos \frac{2\pi\nu}{c_f} x} \quad (140)$$

The solution for a rigid boundary at  $x = l$  can be obtained by setting  $\alpha = 0$  (see eq. (136)) in equations (134) and (135). Then the coefficients  $\Gamma_1$  and  $\Gamma_2$  are reduced to

$$\Gamma_1 = 1 / \tan \frac{2\pi l}{c_f} \nu, \quad \Gamma_2 = 0 \quad (141)$$

It is straightforward to derive the response formulas for this case from equations (137) through (140) using equation (141); therefore, the details will not be shown.

The following figures include the graphs of the expressions for the piston displacement  $|u(\nu)|$ , the pressure  $|p(x, \nu)|$ , dependent on  $\nu$  with fixed  $x$ . Furthermore, the phase shifts  $\varphi_s(\nu)$  and  $\varphi_f(x, \nu)$  are also shown.



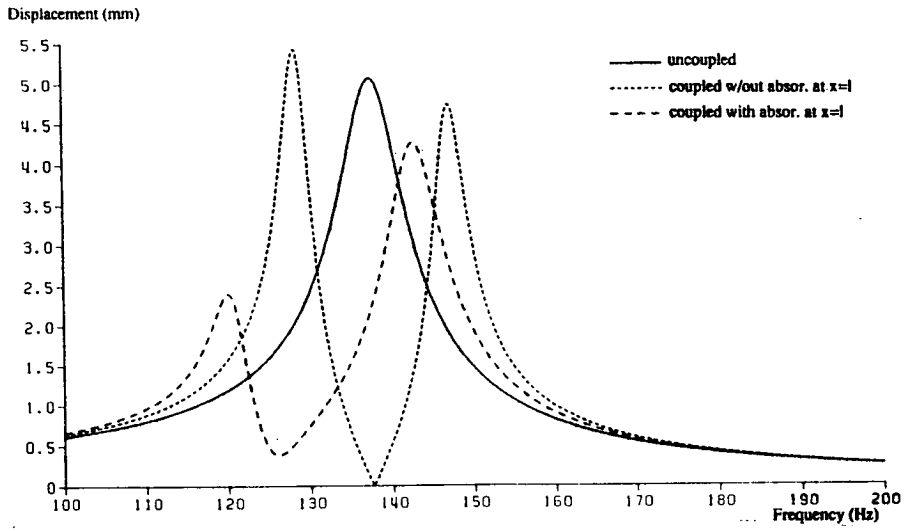


Figure 9. Piston displacement.

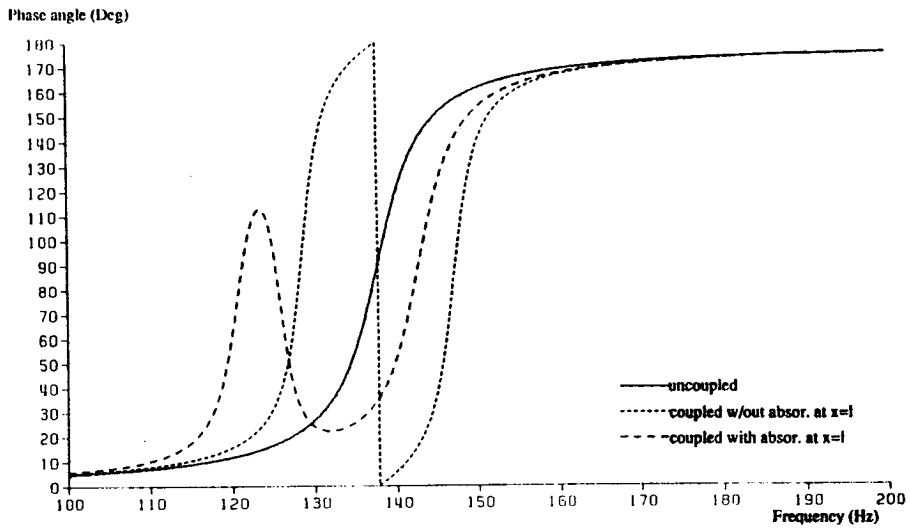


Figure 10. Phase shift  $\phi_s(\nu)$  of the piston motion.

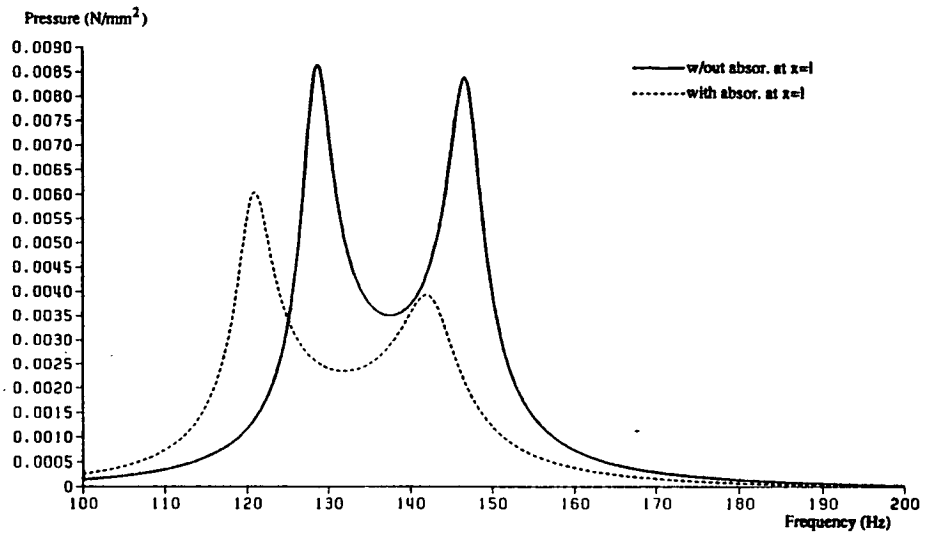


Figure 11. Pressure response curves at  $x = 0$  (i.e., piston surface).

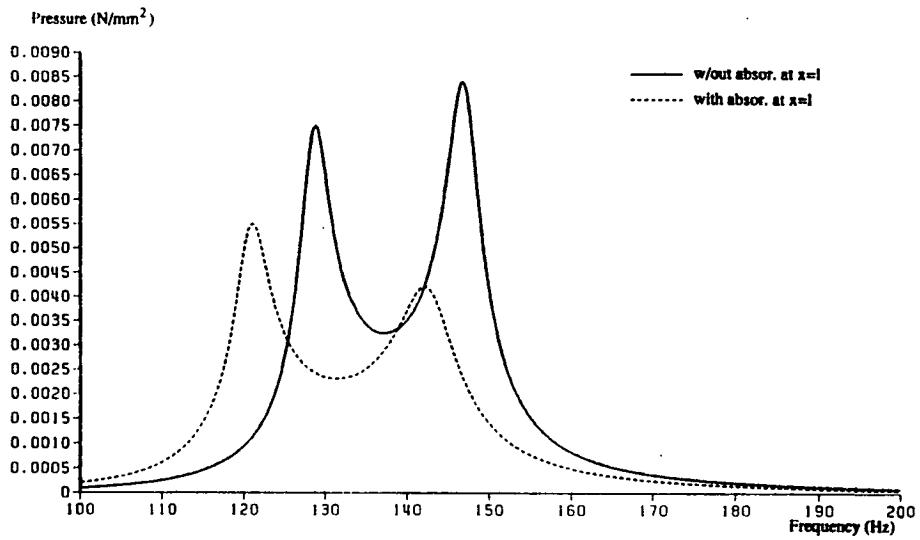


Figure 12. Pressure response curves at  $x = 0.15$  m.

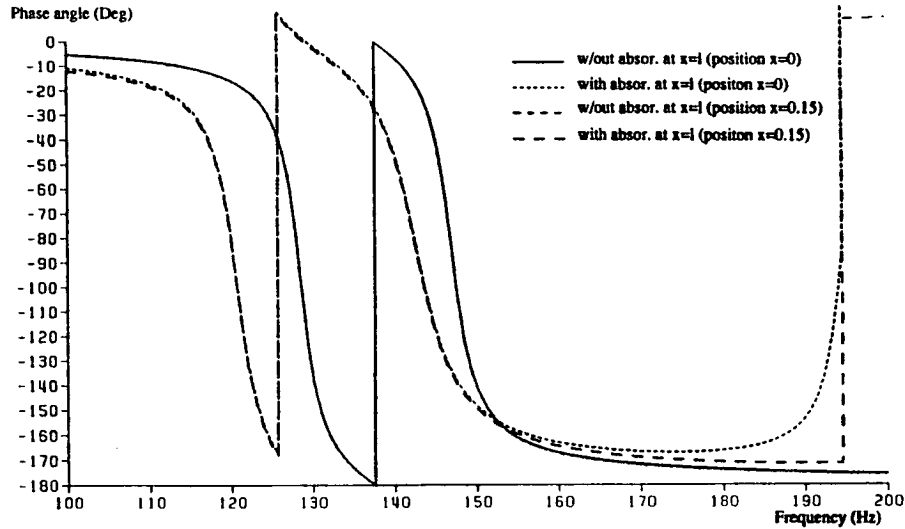


Figure 13. Phase shift  $\phi_f(x, \nu)$  of the pressure response.

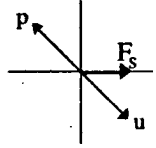
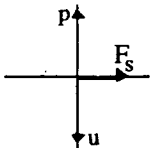
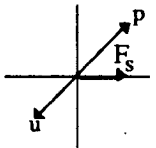
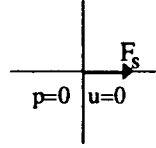
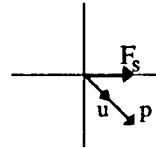
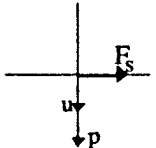
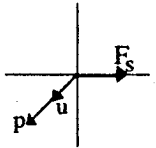
Figures 9 through 13 exhibit the characteristic phenomena caused by the interaction of the piston and fluid in the tube. The discussion of these phenomena is restricted to the following remark: In the frequency range from  $\nu_f^{(1)}/2$  to  $3\nu_f^{(1)}/2$ , neglecting absorption at  $x = l$ , from figure 10, the phase shift,  $\phi_s(\nu)$ , for the coupled case jumps from  $180^\circ$  to  $0^\circ$  at  $\nu = \nu_f^{(1)}$ . On the other hand, figure 9 shows that  $|u(\nu_f^{(1)})| = 0$ . That means the piston does not move if the excitation frequency is  $\nu = \nu_f^{(1)}$ . This effect occurs because the pressure-induced force,  $F_p = -Ap(0, \nu)$  (see eq. (123)), is moving in the direction opposite to the exciting force,  $F_s(t) = F_s \exp(i2\pi\nu t)$  and  $|F_p| = |F_s(t)|$  if  $\nu = \nu_f^{(1)}$ .

The pressure on the piston surface depends on the piston displacement expressed by the following equation:

$$p(0, \nu) = 2\pi Z_o \Gamma_1 \nu u(\nu) \quad (142)$$

which follows from equation (133) with  $x = 0$ ,  $\Gamma_2 = 0$  and equation (132). The factor,  $\Gamma_1$ , given by equation (141), in equation (142) causes  $p(x, 0) \uparrow u(\nu)$  for  $\nu_f^{(1)}/2 < \nu < \nu_f^{(1)}$  and  $p(x, 0) \downarrow u(\nu)$  for  $\nu_f^{(1)} < \nu < 3\nu_f^{(1)}/2$ . For the first two coupled frequencies the terms  $u(\nu)$  and  $p(0, \nu)$  are purely imaginary. An analogous statement is valid for  $x > 0$ .

Table 4 shows the phase relation between exciting force,  $F_s(t)$  at  $t = 0$ , the piston displacement,  $u(\nu)$ , and the pressure,  $p(0, \nu)$ , on the piston surface.

Table 4. Phase relation between $F_s(t)$ , $u(v)$ , and $p(0, v)$				
	$v_f^{(1)}/2 < v < v_1$	$v = v_1$	$v_1 < v < v_f^{(1)}$	$v = v_f^{(1)}$
Re u	>0	=0	<0	=0
Im u	<0	<0	<0	=0
Re p	<0	=0	>0	=0
Im p	>0	>0	>0	=0
				
	$v_f^{(1)} < v < v_2$	$v = v_2$	$v_2 < v < 3v_f^{(1)}/2$	
Re u	>0	=0	<0	
Im u	<0	<0	<0	
Re p	>0	=0	<0	
Im p	<0	<0	<0	
				

In closing, the pressure distribution,  $|p(x, v)|$ , in the tube as a function of  $x$  at selected frequencies is presented (see figs. 14 and 15). There is a significant difference in the location of the minimal pressure which depends on parameter  $v$ . Positions,  $x$ , can be determined by using equation (139).

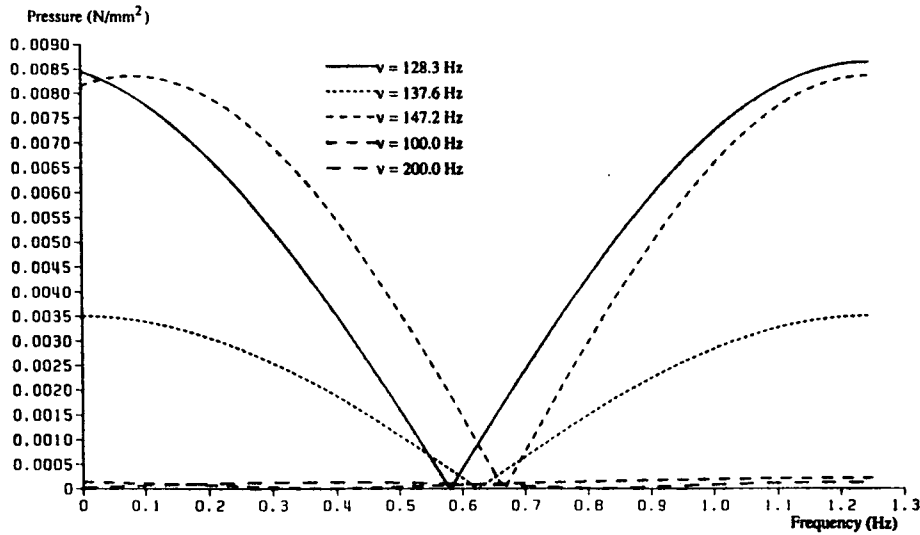


Figure 14. Pressure in the tube for ( $\nu = 100, 128.33, 137.6, 147.2,$  and  $200$  Hz) without absorption at  $x = l$ .

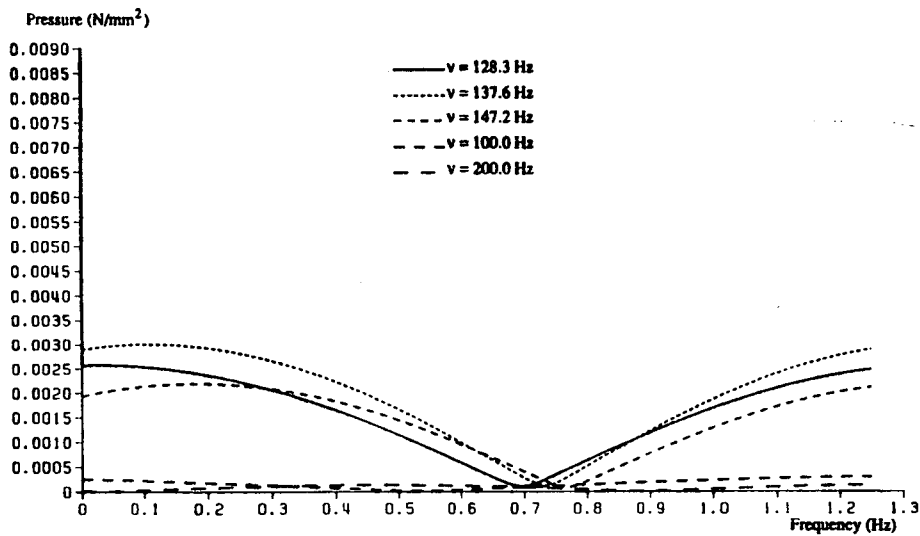


Figure 15. Pressure in the tube for ( $\nu = 100, 128.33, 137.6, 147.2,$  and  $200$  Hz) with absorption at  $x = l$ .

### 7.1.2.3 Transient response analysis

This type of response analysis is more complicated than the one investigated in section 7.1.2.2. The mathematical description of the solution procedure requires significant elaboration, therefore it will not be presented.

### 7.1.3 Finite element approximation and comparison with theoretical results

The coupled fluid-structure system introduced in section 7.1 is approximated by a suitable finite element model, which can be a one-, two-, or a three-dimensional. The theoretical description and solution of the coupled problem is based on the assumption that the coupled system is one-dimensional.

This assumption is sufficient because the condition,  $l \gg \sqrt{A}$ , where  $l$  is the length of the tube and  $A$  is the area of the cross section, is fulfilled. Therefore, it is appropriate to describe the coupled spring-piston-tube system by a one-dimensional finite element model. In reality most problems are three-dimensional. Consequently, a three-dimensional model is used for the FE approximation. It is left to the reader to describe the coupled system by a one-dimensional finite element model.

In the following sections, the finite element model of the spring-piston-tube system is described first. Subsequently, the finite element results for the usual types of analysis are presented. These analyses consist of 1) uncoupled and coupled eigenanalysis of the spring-piston-tube system, and 2) frequency response analysis. In many cases, transient response analysis can be performed by transforming the problem to the frequency domain via the Fourier transform. Then the same solution scheme can be used.

The finite element results were calculated by applying modal and direct (or physical) coupling of structure (spring-piston system) and fluid (air in the tube) and compared to theoretical results, which were presented in section 7.1.2. Equations (67) and (68) were used for the modal coupling and equations (62) and (64) for direct coupling (see section 3.4).

A detailed description of the NASTRAN runs can be found in Appendix B. NASTRAN user decks (Executive, Case and Bulk Data Deck) are shown for all runs. The background can be found in section 6 (sections 6.3 through 6.7). Various cases of boundary absorption input data are presented.

#### 7.1.3.1 Finite element model

The fluid in the tube is modelled by 800 8-node hexa elements. In this case, they are the NASTRAN CHEXA8 elements. The appropriate FE mesh consists of 1275 nodes. Boundary conditions need only be introduced at the ends of the tube. At the rear end, the boundary is either a rigid wall or an absorbing wall. Only the latter case needs an additional input. The absorbing wall is defined in the same way the coupling surface of the fluid (air) is defined, by 16 NASTRAN CQUAD4 plate elements. Both surfaces belong to the fluid model. The piston, combined with a spring, represents a flexible wall (coupling surface) at the front boundary of the tube. The finite element model of the spring-piston system consists of a central node with a CONM2 element, representing the mass of the piston, and connected to ground via the CELAS2 element. The remaining 24 nodes define

the piston surface and are connected to the center point by MPC conditions. Damping is provided by a CDAMP2 element.

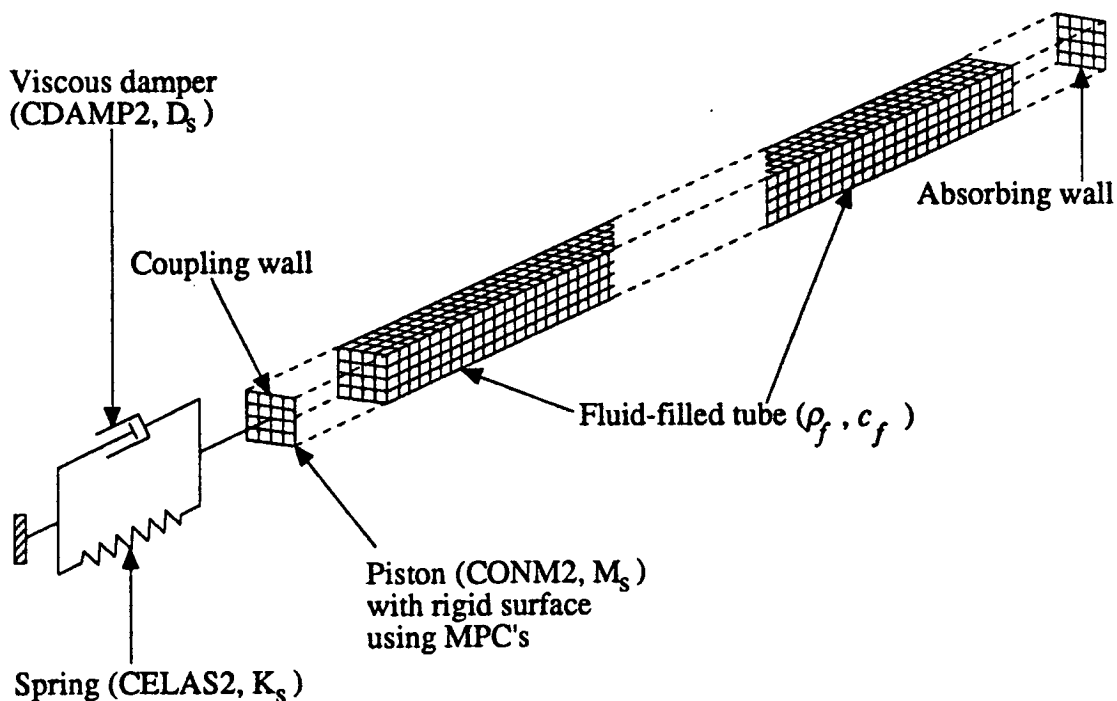


Figure 16. Finite element model of the spring-piston-tube system.

### 7.1.3.2 Uncoupled and coupled eigenanalysis

NASTRAN input decks are shown in Appendixes B1, B2. In tables 5 and 6 the analytically computed frequencies of the structure (spring-piston system without damping) and fluid (air-filled tube) are compared to FE results.

Table 5. Eigenfrequencies of the spring-piston system	
$v_s = \frac{1}{2\pi} \sqrt{\frac{K_s}{M_s}} \text{ (Hz)}$	(Hz)/ FE (NASTRAN)
137.6	137.6

<b>Table 6. Frequencies of the first four standing waves (longitudinal)</b>	
$v_f^{(n)} = n \frac{c_f}{2l}$ (Hz)	$v_f^{(n)}$ (Hz) / NASTRAN
137.6	137.6226
275.2	275.3812
412.8	413.4115
550.4	551.8498

Table 7 demonstrates the variation of frequencies with respect to different FE-model discretization. Frequencies of the first four longitudinal waves versus four different mesh sizes are shown. The analytic values are listed once again.

<b>Table 7 Frequencies of tubes with different mesh sizes</b>				
$v$ in Hz "analytic"	275 nodes 160 hexa	650 nodes 400 hexa	1275 nodes 800 hexa	2525 nodes 1600 hexa
137.6	138.1667	137.6907	137.6226	137.6057
275.2	279.7465	275.9251	275.3812	275.2452
412.8	428.1957	415.2490	413.4115	412.9529
550.4	586.9007	556.2116	551.8498	550.7625

Table 8 shows the frequencies of the coupled system calculated from equation (126) and from the finite element model using modal and direct coupling between the structure and fluid.

<b>Table 8. Frequencies of the coupled system</b>		
$v$ in Hz	$v$ in Hz/FE	
"theoretical"	direct coupled	modal coupled
128.3345	128.3430	128.4463
147.1835	147.1987	147.3315
	276.2529	276.2570
	413.9049	413.9070
	552.2022	552.2039



As mentioned in section 7.1.2, the coupling shifts the pressure node position and changes the pressure gradient at  $x = 0$  compared to the uncoupled case (rigid boundary at  $x = 0$ ), see figure 8. These effects can also be shown by using the finite elements to describe the dynamics of the coupled system. The quality of this approximation depends on the mesh size of the FE-model as well as the type of coupling.

Table 9 shows the dependence of the coupled frequencies on the mesh size of the FE-model. In this case only the mesh size of the fluid model was varied. Furthermore, the computations were carried out using only modal coupling with four fluid modes.

<b>Table 9. Air-filled tube coupled frequencies versus mesh size</b>				
<b>"theoretical" Results (Hz)</b>	<b>Finite Element Results (Hz)</b>			
	275 nodes 160 hexa	650 nodes 400 hexa	1275 nodes 800 hexa	2525 nodes 1600 hexa
128.3345	128.6230	128.4690	128.4463	128.4406
147.1835	147.6648	147.3728	147.3315	147.3212
	280.6546	276.8048	276.2570	276.1200
	428.7420	415.7506	413.9070	413.4470
	587.3251	556.5737	552.2039	551.1145

Assuming that the mesh size of the FE-model is "good enough," the best approximation is obtained by "direct coupling," which means that the structure and fluid are coupled in the physical coordinates before any modal transformation, see section 3.4. In realistic problems, like automobile interior acoustics, where the FE-models of a car body and the air in the passenger compartment are very large, modal reduction must be applied, (see also section 3.4), to reduce computation time. As a consequence of this action, the quality of the coupling approximation is reduced. The analyst has to select the number of structure and fluid modes needed for the analysis. That is, how many modes are required to obtain a sufficiently accurate approximation for the physics of the coupled problem? The user should be careful at all times in applying modal reduction.

The result of direct and modal coupling for the pressure distributions corresponding to the first two coupled modes is shown in figures 17 and 18. For the case of direct coupling, the deviation from the theoretical result (see figs. 17 and 18) is imperceptible. In comparison, the result based on modal coupling with a reduced fluid modal matrix shows a considerable deviation.

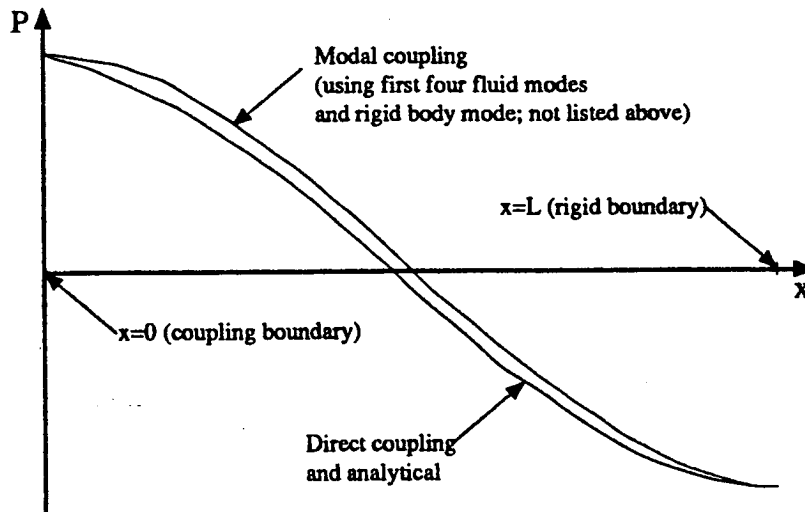


Figure 17. First coupled mode pressure distribution computed by using direct and modal coupling.

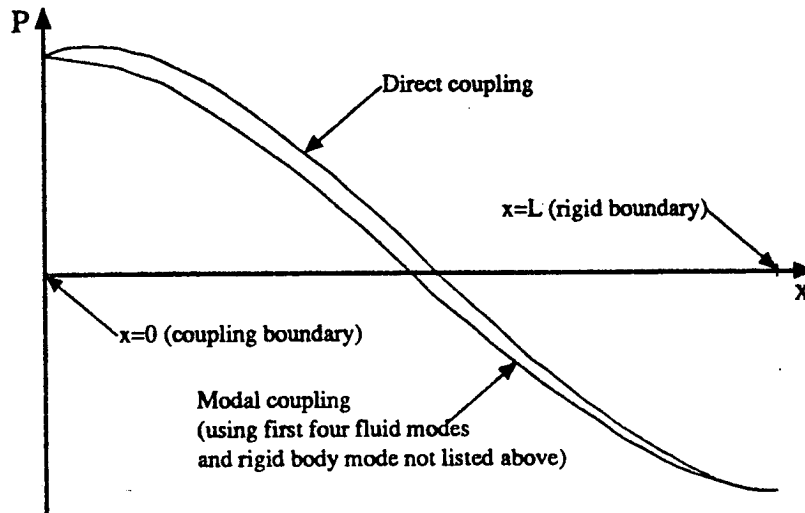


Figure 18. Second coupled mode pressure distribution computed by using direct and modal coupling.

### 7.1.3.3 Frequency response results

This section presents the results for the boundary value problem, equation (123). The results were calculated using the finite element method and compared to analytic results (see figs. 19, 20, and 21). See Appendix B3.1 for the NASTRAN input of the frequency response run.

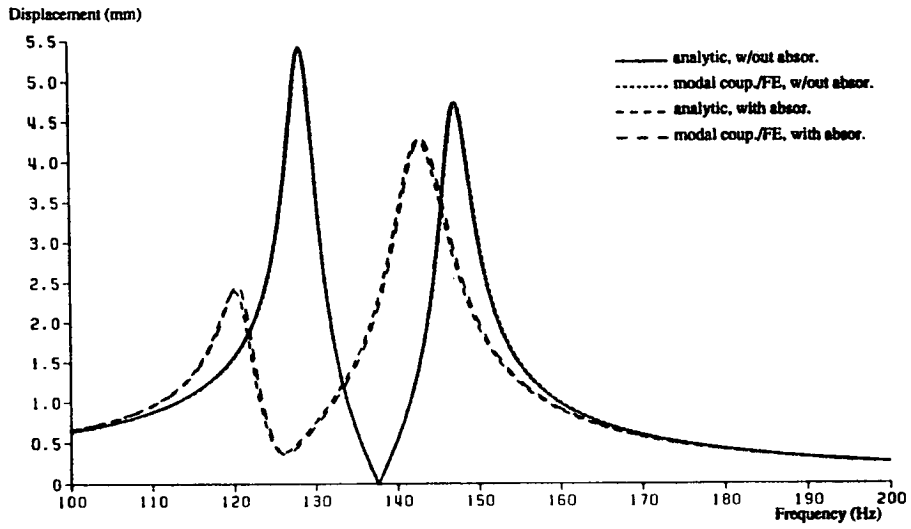


Figure 19. Piston displacement response.

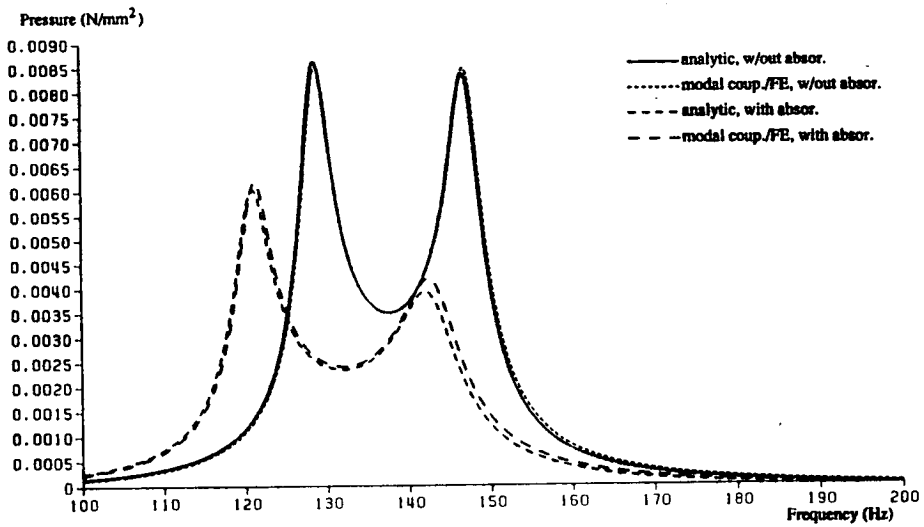


Figure 20. Pressure response at  $x = 0$ .

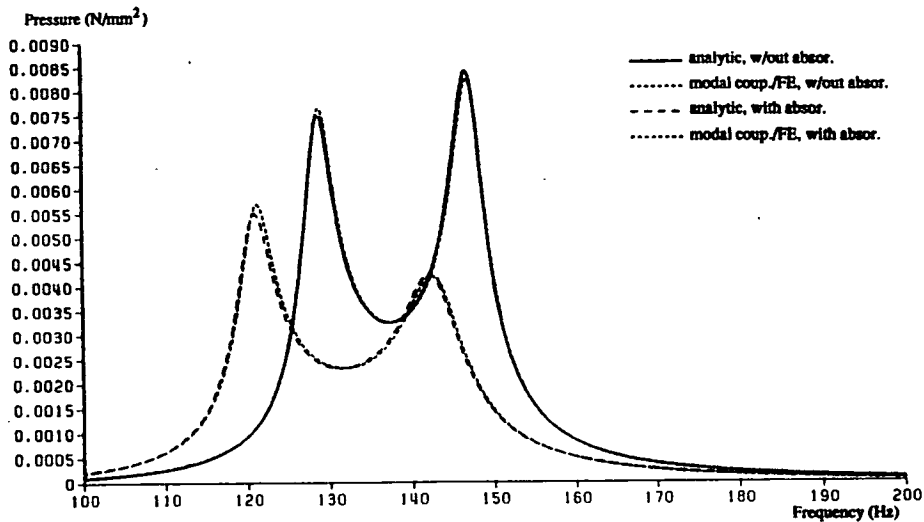


Figure 21. Pressure response at  $x = 0.15$  m.

#### 7.1.3.4 Acoustic contribution analysis

During this analysis the influence of the fluid surface, which is coupled to the surrounding structure, is determined. This is performed in Run 4, which is a restart of Run 3.1.

A description of the NASTRAN input deck can be found in section 6.7. The NASTRAN input for Run 4 of the coupled system, presented in figure 16, is listed in Appendix B4. Contribution of fluid surface points, which are coupled to structure, to the pressure at any interior fluid point "GID*i*" is only of formal interest so that the results of Run 4 can be shown. Description of the output and its interpretation is given in section 6.7.4.

The following figure shows the FE-model of the piston and the coupling surface of the fluid with numbered grid points. The numbers of the fluid coupling points (the so-called "participation points"  $PGP_i$  ( $i = 1, 2, \dots, 25$ ), see section 6.7.4 can be found in table 10. The "participation factors" of these grid points for frequencies  $\nu = 128$  Hz and  $\nu = 147$  Hz are listed in tables 10 and 11, respectively.

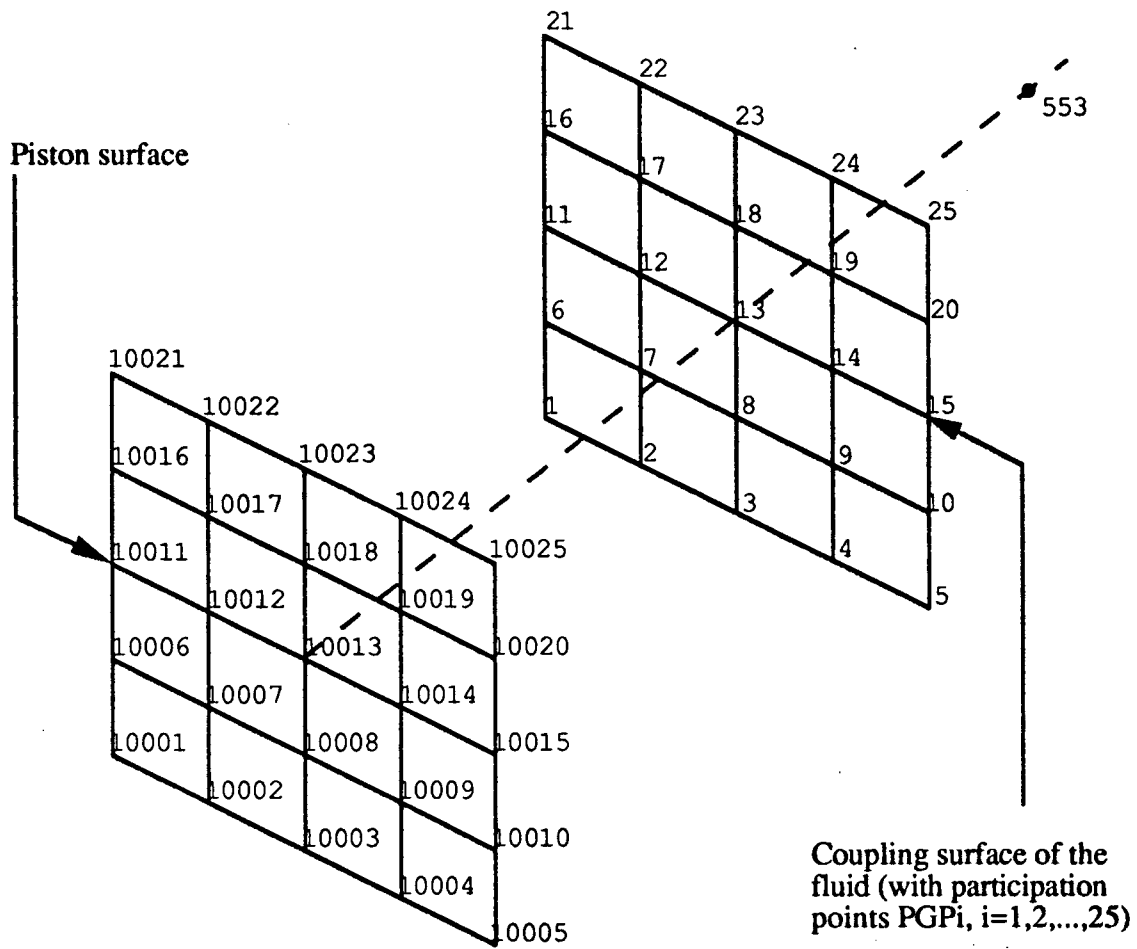


Figure 22. Coupling surface of the fluid and piston.

**Table 10. Participation factors for point 553 at 128Hz**

COMPLEX DISPLACEMENT VECTOR (REAL/IMAGINARY)					
POINT ID.	TYPE	T1	T2	T3	R1
1	G	-3.434522E-06 -1.172005E-04	1.172508E-04 2.710505E-20	1.562499E-02 3.612052E-18	2.499992E-01 0.0
2	G	-6.869054E-06 -2.344014E-04	2.345020E-04 0.0	3.125002E-02 0.0	4.999991E-01 0.0
3	G	-6.869051E-06 -2.344013E-04	2.345019E-04 5.421011E-20	3.125001E-02 7.224104E-18	4.999989E-01 0.0
4	G	-6.869055E-06 -2.344015E-04	2.345021E-04 2.710505E-20	3.125003E-02 3.612052E-18	4.999992E-01 0.0
5	G	-3.434528E-06 -1.172007E-04	1.172510E-04 1.355253E-20	1.562501E-02 1.806026E-18	2.499996E-01 0.0
6	G	-6.869044E-06 -2.344011E-04	2.345017E-04 2.710505E-20	3.124998E-02 3.612052E-18	4.999984E-01 0.0
7	G	-1.373808E-05 -4.688019E-04	4.690031E-04 5.421011E-20	6.249992E-02 7.224104E-18	9.999963E-01 0.0
8	G	-1.373806E-05 -4.688011E-04	4.690024E-04 0.0	6.249982E-02 0.0	9.999947E-01 0.0
9	G	-1.373808E-05 -4.688019E-04	4.690031E-04 5.421011E-20	6.249991E-02 7.224104E-18	9.999962E-01 0.0
10	G	-6.869044E-06 -2.344011E-04	2.345017E-04 5.421011E-20	3.124997E-02 7.224104E-18	4.999984E-01 0.0
11	G	-6.869044E-06 -2.344011E-04	2.345017E-04 2.710505E-20	3.124998E-02 3.612052E-18	4.999984E-01 0.0
12	G	-1.373805E-05 -4.688009E-04	4.690022E-04 0.0	6.249979E-02 0.0	9.999942E-01 0.0
13	G	-1.373803E-05 -4.688003E-04	4.690015E-04 5.421011E-20	6.249970E-02 7.224104E-18	9.999928E-01 0.0
14	G	-1.373805E-05 -4.688007E-04	4.690020E-04 5.421011E-20	6.249976E-02 7.224104E-18	9.999938E-01 0.0
15	G	-6.869036E-06 -2.344008E-04	2.345014E-04 5.421011E-20	3.124994E-02 7.224104E-18	4.999978E-01 0.0
16	G	-6.869063E-06 -2.344017E-04	2.345023E-04 5.421011E-20	3.125006E-02 7.224104E-18	4.999998E-01 0.0
17	G	-1.373812E-05 -4.688032E-04	4.690045E-04 5.421011E-20	6.250009E-02 7.224104E-18	9.999991E-01 0.0
18	G	-1.373813E-05 -4.688036E-04	4.690049E-04 0.0	6.250015E-02 0.0	1.000000E+00 0.0
19	G	-1.373812E-05 -4.688031E-04	4.690043E-04 5.421011E-20	6.250007E-02 7.224104E-18	9.999988E-01 0.0
20	G	-6.869055E-06 -2.344014E-04	2.345021E-04 0.0	3.125002E-02 0.0	4.999992E-01 0.0
21	G	-3.434535E-06 -1.172010E-04	1.172513E-04 1.355253E-20	1.562505E-02 1.806026E-18	2.500001E-01 0.0
22	G	-6.869094E-06 -2.344028E-04	2.345034E-04 2.710505E-20	3.125020E-02 3.612052E-18	5.000020E-01 0.0
23	G	-6.869106E-06 -2.344032E-04	2.345038E-04 2.710505E-20	3.125026E-02 3.612052E-18	5.000029E-01 0.0
24	G	-6.869093E-06 -2.344028E-04	2.345034E-04 0.0	3.125020E-02 0.0	5.000020E-01 0.0
25	G	-3.434535E-06 -1.172010E-04	1.172513E-04 1.355253E-20	1.562505E-02 1.806026E-18	2.500001E-01 0.0

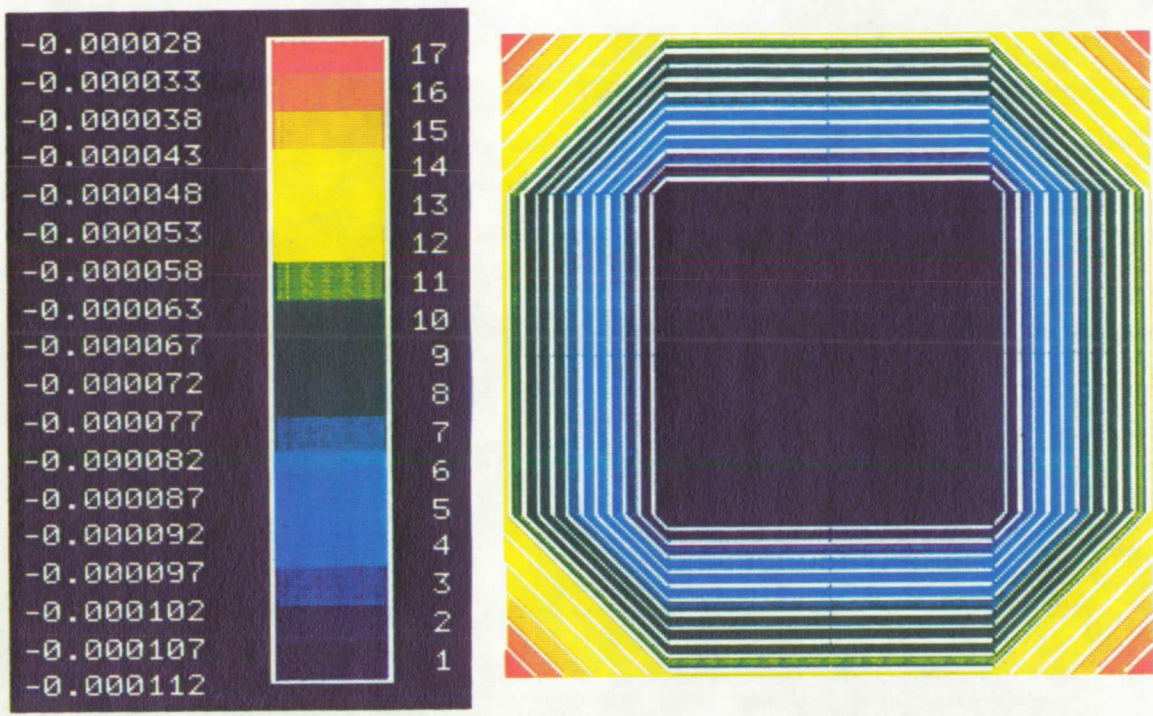


Figure 23. Grid point participation for fluid point 553 ( $x = 0.15$ ) at 128 Hz (Re(T3) from table 10).

**Table 11. Participation factors for point 553 at 147 Hz**

COMPLEX DISPLACEMENT VECTOR (REAL/IMAGINARY)					
POINT ID.	TYPE	T1	T2	T3	R1
1	G	-1.901086E-06	1.260271E-04	1.562499E-02	2.499992E-01
		1.260128E-04	1.423015E-19	1.764271E-17	0.0
2	G	-3.802178E-06	2.520546E-04	3.125002E-02	4.999991E-01
		2.520259E-04	2.710505E-19	3.360516E-17	0.0
3	G	-3.802177E-06	2.520545E-04	3.125001E-02	4.999989E-01
		2.520258E-04	2.710505E-19	3.360516E-17	0.0
4	G	-3.802179E-06	2.520546E-04	3.125003E-02	4.999992E-01
		2.520259E-04	2.574980E-19	3.192490E-17	0.0
5	G	-1.901090E-06	1.260273E-04	1.562501E-02	2.499996E-01
		1.260130E-04	1.287490E-19	1.596245E-17	0.0
6	G	-3.802173E-06	2.520542E-04	3.124997E-02	4.999984E-01
		2.520255E-04	2.846031E-19	3.528542E-17	0.0
7	G	-7.604342E-06	5.041081E-04	6.249991E-02	9.999963E-01
		5.040508E-04	5.421011E-19	6.721032E-17	0.0
8	G	-7.604330E-06	5.041073E-04	6.249981E-02	9.999947E-01
		5.040500E-04	5.692061E-19	7.057084E-17	0.0
9	G	-7.604342E-06	5.041081E-04	6.249991E-02	9.999962E-01
		5.040508E-04	5.421011E-19	6.721032E-17	0.0
10	G	-3.802173E-06	2.520542E-04	3.124997E-02	4.999984E-01
		2.520255E-04	2.710505E-19	3.360516E-17	0.0
11	G	-3.802173E-06	2.520542E-04	3.124997E-02	4.999984E-01
		2.520255E-04	2.439455E-19	3.024465E-17	0.0
12	G	-7.604326E-06	5.041071E-04	6.249979E-02	9.999942E-01
		5.040497E-04	5.421011E-19	6.721032E-17	0.0
13	G	-7.604316E-06	5.041064E-04	6.249970E-02	9.999928E-01
		5.040490E-04	5.692061E-19	7.057084E-17	0.0
14	G	-7.604323E-06	5.041069E-04	6.249976E-02	9.999938E-01
		5.040496E-04	5.963112E-19	7.393136E-17	0.0
15	G	-3.802169E-06	2.520539E-04	3.124994E-02	4.999978E-01
		2.520252E-04	2.981556E-19	3.696568E-17	0.0
16	G	-3.802183E-06	2.520549E-04	3.125006E-02	4.999997E-01
		2.520262E-04	2.574980E-19	3.192490E-17	0.0
17	G	-7.604363E-06	5.041096E-04	6.250009E-02	9.999991E-01
		5.040522E-04	5.421011E-19	6.721032E-17	0.0
18	G	-7.604370E-06	5.041100E-04	6.250015E-02	1.000000E+00
		5.040527E-04	5.421011E-19	6.721032E-17	0.0
19	G	-7.604361E-06	5.041094E-04	6.250007E-02	9.999988E-01
		5.040520E-04	5.692061E-19	7.057084E-17	0.0
20	G	-3.802179E-06	2.520546E-04	3.125002E-02	4.999992E-01
		2.520259E-04	2.710505E-19	3.360516E-17	0.0
21	G	-1.901094E-06	1.260276E-04	1.562505E-02	2.500001E-01
		1.260132E-04	1.355253E-19	1.680258E-17	0.0
22	G	-3.802200E-06	2.520560E-04	3.125020E-02	5.000020E-01
		2.520273E-04	2.846031E-19	3.528542E-17	0.0
23	G	-3.802207E-06	2.520565E-04	3.125026E-02	5.000029E-01
		2.520278E-04	2.710505E-19	3.360516E-17	0.0
24	G	-3.802200E-06	2.520560E-04	3.125020E-02	5.000020E-01
		2.520273E-04	2.846031E-19	3.528542E-17	0.0
25	G	-1.901094E-06	1.260276E-04	1.562504E-02	2.500001E-01
		1.260132E-04	1.423015E-19	1.764271E-17	0.0



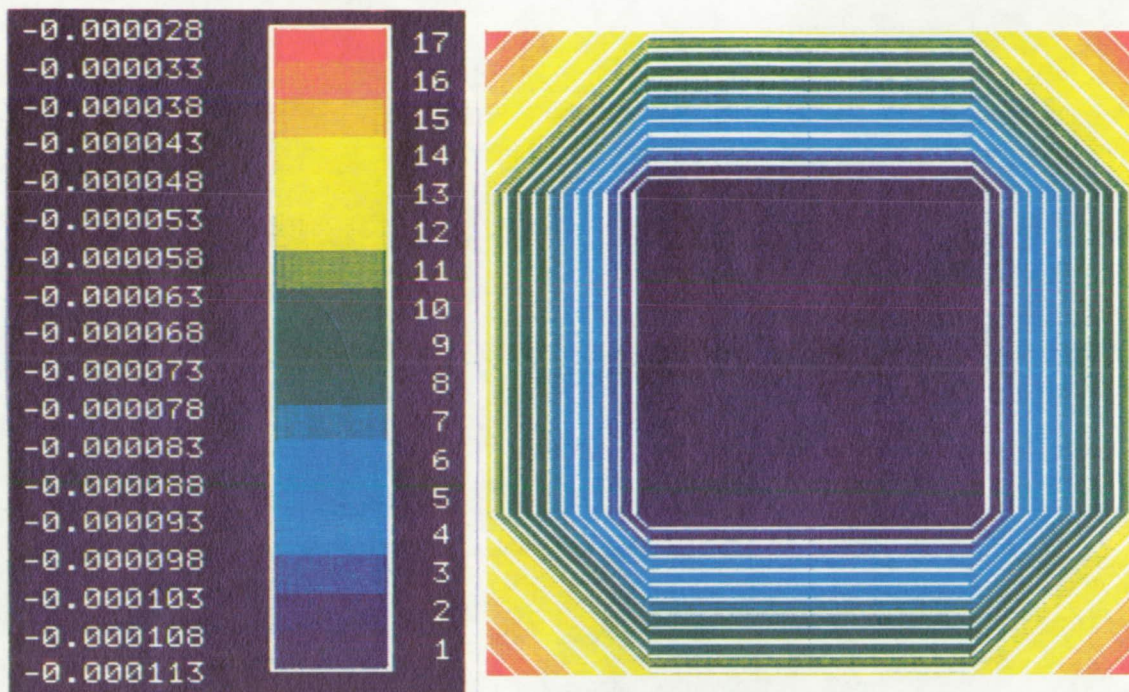


Figure 24. Grid point participation for fluid point 553 ( $x = 0.15$ ) at 147 Hz (Re(T3) from table 11).

It is very clear that grid points,  $PGP_i$  ( $i = 7,8,9,12,13,14,17,18,19$ ) (see figure 22), have the most influence on the pressure level at fluid interior point 553, ( $x = 0.15$ ). This is also shown by table 10 with figure 23 and table 11 with figure 24.

#### 7.1.3.4 Transient response

This analysis is not performed here. It can be easily done considering the remarks in section 6.6.

## 7.2 Two-dimensional fluid-structure system

In section 7.1 a one-dimensional, even though it was solved as three-dimensional, example problem was described in detail. In this section a simple two-dimensional system for which a solution exists will be used to illustrate all the capability in this development. Details of the theoretical solution can be found in reference 31. Although this problem is two-dimensional, all the capability is directly applicable to any three-dimensional system.

The unique aspect of this problem is the use of water as the fluid medium. In this particular case one can expect to see a greater effect of the fluid on the structure than in the previous example where the fluid medium was air. Through the use of these two sample problems one can observe that FSI is dependent on the type of the two interacting mediums. In practice, the structure will always have influence on the fluid, whereas the fluid may or may not have a significant effect on the structure. This effect depends, to some extent, on the fluid density, or the relative weight of the fluid and the structure.

### 7.2.1 Problem Description

A simply supported beam has one side in contact with a finite acoustic fluid, water, as shown in figure 20. A unit width of the fluid is considered.

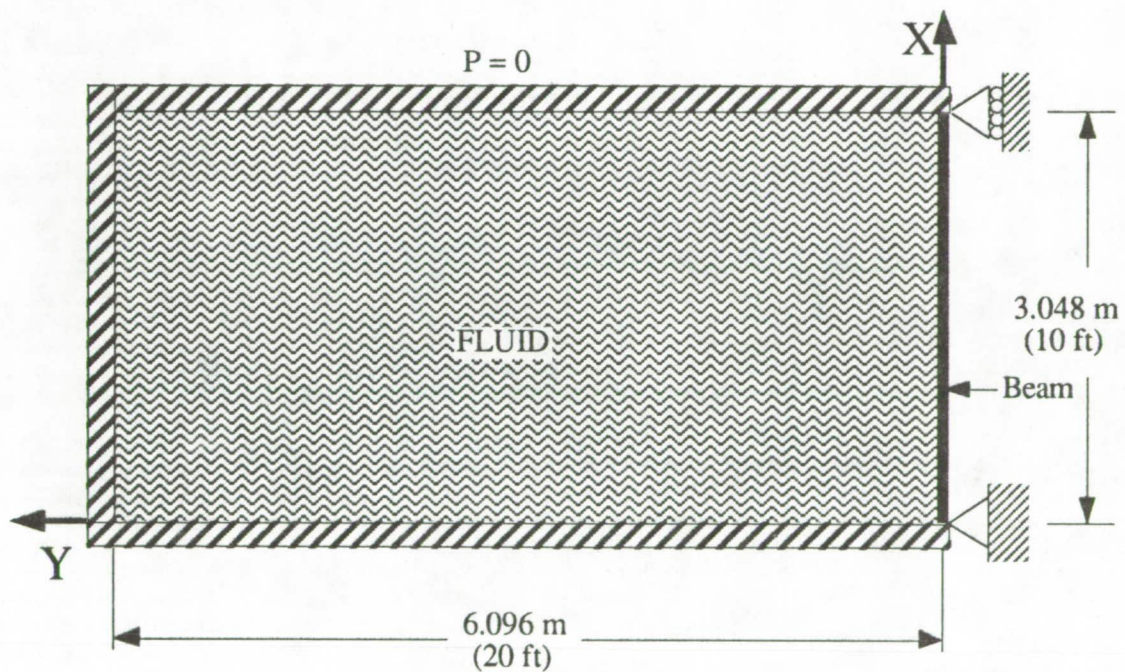


Figure 25. Beam with finite acoustic fluid



The physical properties of the beam and fluid used are listed in the following table.

Beam		
Weight Density ( $\rho_s$ )	7.682E4 N/m <sup>3</sup>	(0.283 lb/in <sup>3</sup> )
Young's Modulus (E)	2.068E11 Pa	(30E6 psi)
Moment of Inertia (I)	0.1675E-4 m <sup>4</sup>	(40.2412in <sup>4</sup> )
Length (L)	3.048 m	(10 ft)
Fluid		
Weight Density ( $\rho_f$ )	9802.25N/m <sup>3</sup>	(62.4 lb/ft <sup>3</sup> )
Acoustic Speed ( $c_f$ )	1524 m/sec	(5000 ft/sec)
Height of the Fluid (H)	6.096 m	(20 ft)

### 7.2.2 Theoretical solution

The coupled modal frequencies of the fluid-beam system are to be determined. The equation of motion of the beam is

$$m \frac{\partial^2 y}{\partial t^2} + EI \frac{\partial^4 y}{\partial x^4} = q(x, t)$$

where  $m$  is the mass of the beam per unit length,  $E$  is Young's modulus of the beam,  $I$  is the section moment of inertia, and  $q(x, t)$  is the distributed load on the beam.

The governing acoustic field equation in Cartesian coordinates can be written as

$$\frac{\partial^2 p}{\partial x^2} + \frac{\partial^2 p}{\partial y^2} + \frac{\partial^2 p}{\partial z^2} = \frac{1}{c_f^2} \frac{\partial^2 p}{\partial t^2} \quad (143)$$

The boundary conditions for the beam and fluid are

$$\text{Beam: } \left. \begin{array}{l} y = 0 \\ \frac{\partial^2 y}{\partial x^2} = 0 \end{array} \right\} \text{ at } x = 0 \text{ and } x = L \quad (144)$$

$$\text{Fluid: } p = 0 \quad \text{at } x = 0, L \text{ and } y = H \quad (145)$$

The fluid boundary condition implies that the fluid has a free surface on three sides. Of course, this is an impossible real condition, but it presents a solvable mathematical problem.

At the Beam-Fluid interface: 
$$\frac{\partial p}{\partial y} = -\rho_f \frac{\partial^2 y}{\partial t^2} \quad (146)$$

Solving equations (143) thru (146), the following frequency equations can be obtained:

for  $\alpha_n^2 = \frac{\omega_n^2}{c_f^2} - \left(\frac{n\pi}{L}\right)^2 > 0$ , 
$$\omega_n^2 \left\{ m + \frac{\rho_f \tanh(\alpha_n H)}{\alpha_n} \right\} = EI \left(\frac{n\pi}{L}\right)^4; \quad n = 1, 2, 3, \dots \quad (147)$$

for  $\alpha_n^2 = \frac{\omega_n^2}{c_f^2} - \left(\frac{n\pi}{L}\right)^2 < 0$ ; let  $\hat{\alpha}_n^2 = -\alpha_n^2$ , then

$$\omega_n^2 \left\{ m + \frac{\rho_f \tanh(\hat{\alpha}_n H)}{\hat{\alpha}_n} \right\} = EI \left(\frac{n\pi}{L}\right)^4; \quad n = 1, 2, 3, \dots \quad (148)$$

The mode shapes of the acoustic fluid pressure are expressed by

for  $\alpha_n^2 > 0$ , 
$$\Phi_n(x, y) = \frac{\rho_f \omega_n^2}{\alpha_n} \left( \sin \frac{n\pi x}{L} \right) (\sin \alpha_n y - \tan \alpha_n H \cos \alpha_n y) \quad (149)$$

for  $\alpha_n^2 > 0$ , and let  $\hat{\alpha}_n^2 = -\alpha_n^2$

$$\Phi_n(x, y) = \frac{\rho_f \omega_n^2}{\alpha_n} \left( \sin \frac{n\pi x}{L} \right) (\sinh \hat{\alpha}_n y - \tanh \hat{\alpha}_n H \cosh \hat{\alpha}_n y) \quad (150)$$

The frequency equations (147) and (148) are numerically solved for  $\omega_n$  and the acoustic fluid pressure modes are calculated with the given set of input data.

### 7.2.3 Two-dimensional Nastran finite element model

The two-dimensional finite element model for FSI analysis consists of the beam and the fluid. Owing to symmetry about the center of the beam and fluid, only half of the beam and the fluid are modeled, using 16 BAR elements and 128 QUAD8 elements, respectively. The fluid-beam finite element model is shown in figure 26. MSC/NASTRAN MSGMESH program was used to generate the finite element models and the listing of the input data deck is shown in Appendix C1.

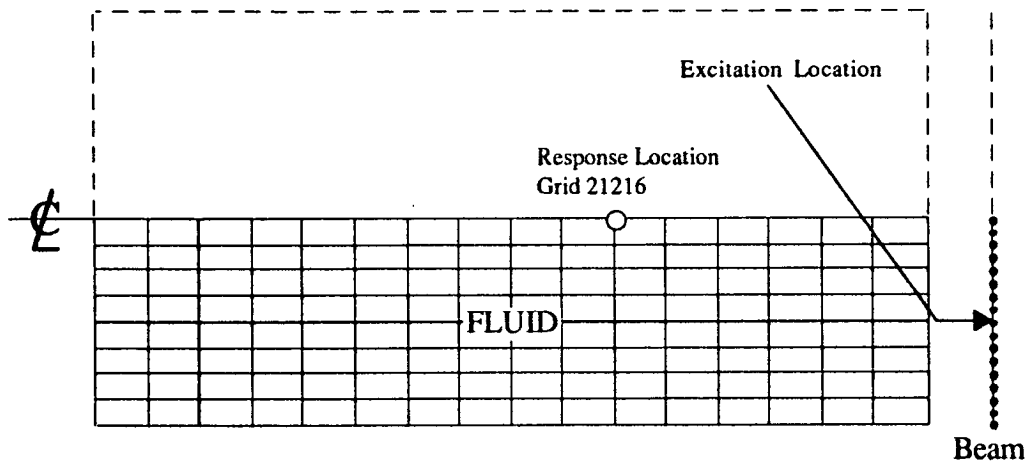


Figure 26. Beam/fluid - FE mesh.

To illustrate the use of superelements, the beam was modeled with one superelement and a residual structure. The grid point on the plane of symmetry is in the residual structure and all other points are in superelement 1.

#### 7.2.4 Normal Modes Analysis - SOL 63, 70

To understand the basic dynamic characteristics of the system and to compare with theoretical results, the normal mode analyses for the following cases were performed:

- normal modes of the structure only
- normal modes of the fluid only
- normal modes of the combined system

##### 7.2.4.1 Beam-only results

Five modes were computed below 5000 Hz. The first four natural frequencies and mode shapes are shown in figure 27. These are the typical mode shapes one would expect from a pinned-pinned beam.

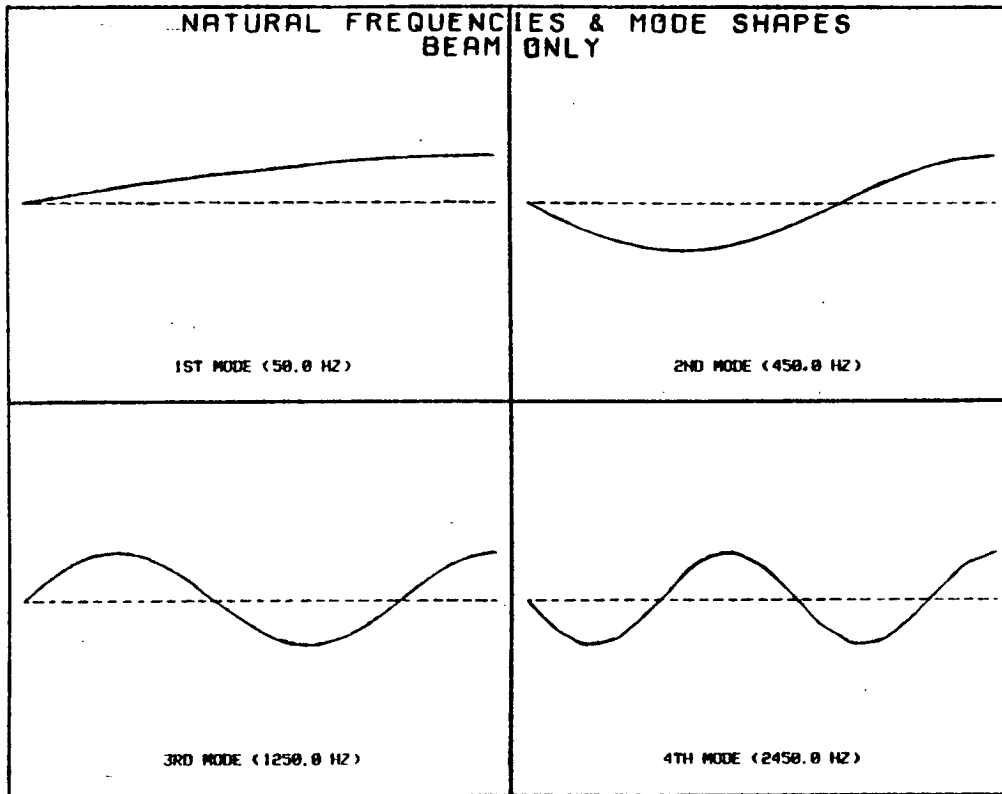


Figure 27. Mode shapes of the beam only.

#### 7.2.4.2 Fluid with rigid boundary results

Thirteen acoustic pressure modes were computed below 1000 Hz. The first four modes are displayed in figure 28, plotting the pressure variation along the  $x$ -axis. The first mode along the line of symmetry is identified as a vertical acoustic quarter wave mode, the second mode as a  $3/4$  wave mode, the third as  $1-1/4$  wave mode, etc.

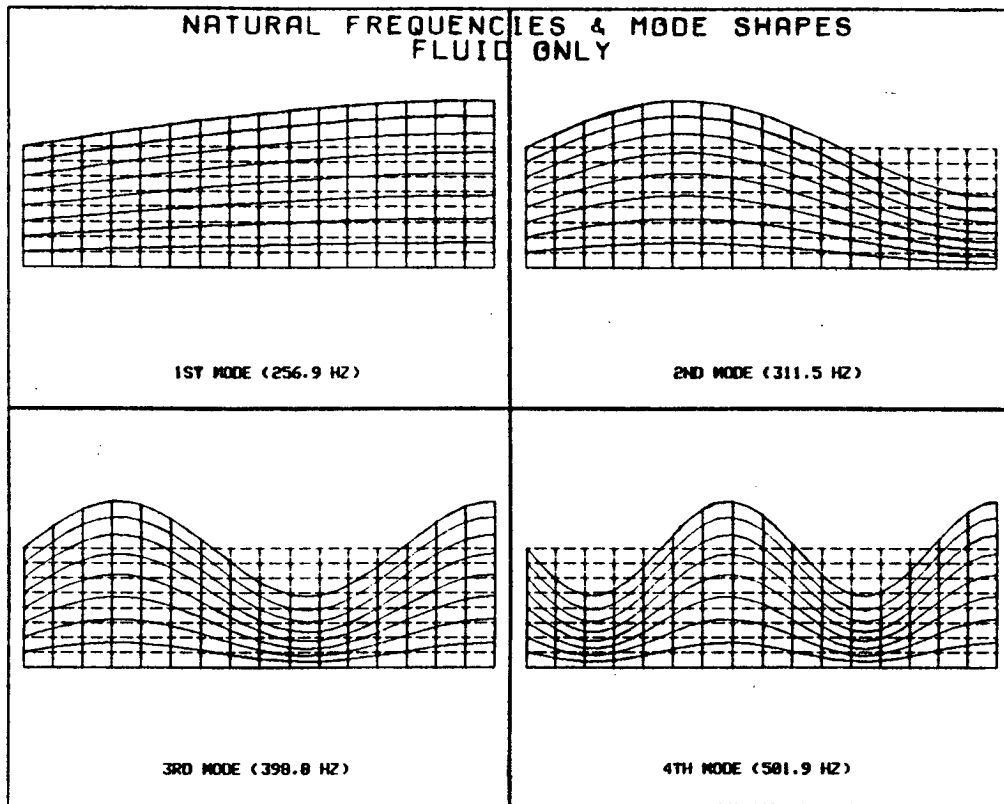


Figure 28. Mode shapes of the fluid only.

#### 7.2.4.3 Coupled fluid-structure modal results

This analysis was performed using SOL 70. The input deck is shown in Appendix C2.

Five dry structure modes and 13 fluid modes were included in the analysis of the coupled system. The lowest modes of the acoustic pressure are shown in figure 29. The second mode at 270.14 Hz is slightly longer than a quarter wave. The third, fifth, and sixth modes are close to 3/4, 1-1/4, and 1-3/4 waves, respectively. The results also indicate that the structural motion shifts the dominant acoustic frequencies. The finite element results are compared with the theoretical results based on the equations (147) and (148). Excellent agreement is obtained. The comparison of the natural frequencies is shown in table 12. Note that the fundamental beam frequency of 50 Hz has been shifted to 40.3 Hz in the coupled solution. This illustrates a significant effect of the fluid on the structural behavior.

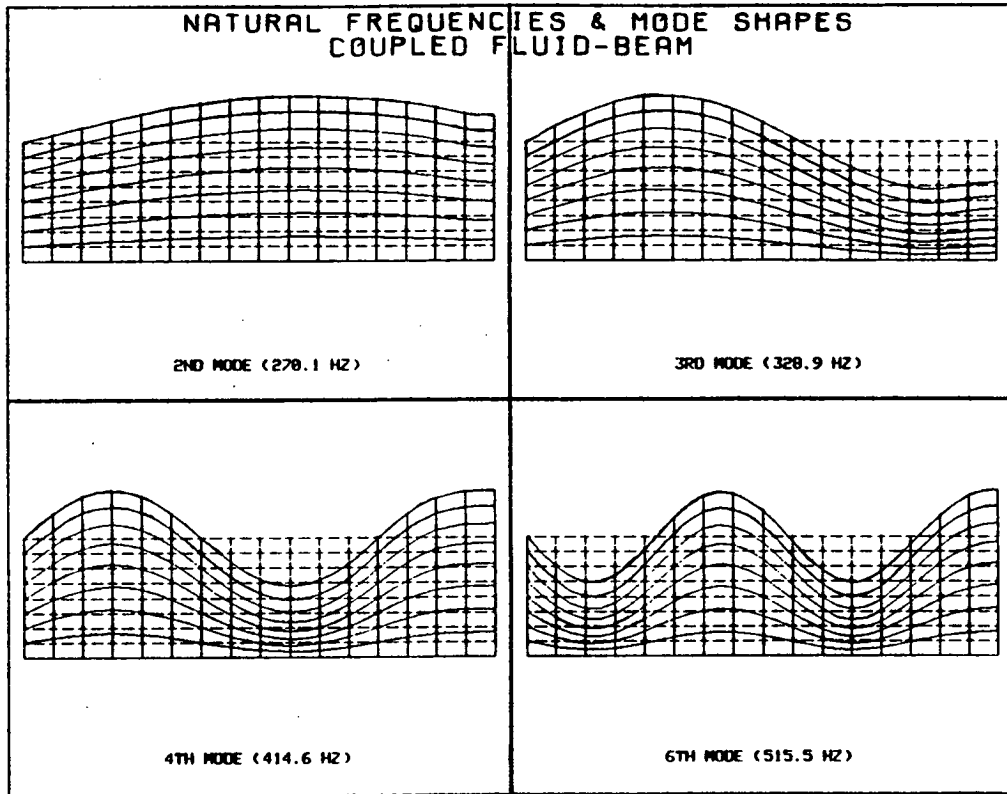


Figure 29. Mode shapes for the coupled fluid-beam system

<b>Table 12: Comparison of coupled natural frequencies between theoretical solution and finite element results</b>				
Mode no.	Structure only	Fluid only	Coupled NASTRAN	Coupled exact
1	5.0000E+01	2.5692E+02	4.0318E+01	3.9810E+01
2	4.5000E+02	3.1151E+02	2.7014E+02	2.6997E+02
3	1.2500E+03	3.9880E+02	3.2894E+02	3.2818E+02
4	2.4501E+03	5.0188E+02	4.1455E+02	4.0321E+02
5	4.0504E+03	6.1270E+02	4.2373E+02	4.1401E+02
6		7.2758E+02	5.1554E+02	5.1540E+02
7		7.4855E+02	6.2504E+02	6.2519E+02
8		7.6877E+02	7.3956E+02	7.3976E+02
9		8.0763E+02	7.5634E+02	7.5689E+02
10		8.4474E+02	7.8106E+02	7.7955E+02
12		8.6249E+02	8.2183E+02	
13		9.3032E+02	8.5742E+02	
14		9.6321E+02	8.7754E+02	



### 7.2.5 Modal frequency response analysis - SOL 71

It is difficult to obtain a frequency response theoretical solution for this problem. This calculation was performed only to further illustrate the Acoustic Procedure. Several different analyses were performed, each with the intent of demonstrating a different feature of the procedure. Two areas of absorption were defined on the interface of the beam and the fluid. Only the first area of absorption was considered in the following analyses. The first area started at  $x = 0$  and continued to  $x = l/4$ . The other area started at  $x = l/4$  and ended at  $x = l/2$ . The analyses that were performed and the respective inputs are listed below:

- Without absorption, with residual flexibility effects, Appendix C3.1
- Uniform absorption, without residual flexibility effects, Appendix C3.2
- Linearly varying absorption, without residual flexibility effects, Appendix C3.3
- Linearly varying absorption, with residual flexibility effects, Appendix C3.4

It should be noted that all these calculations were done as restarts from SOL 63 data base. Before each run, the Area Matrix Program was executed to create the appropriate input matrices.

The load was applied to the structure and its location is shown in figure 26. Because of assumed symmetrical boundary condition, there is a symmetric load implied on the right-hand side. Also note that the load is applied to the interior point of superelement 1. Owing to this fact, one must make use of the LOADSET card in the Case Control Deck and LSEQ card in the Bulk Data Deck. For further input details refer to Appendix C.

Some of the selected results are shown in figure 30 through 33. As can be expected, the peak pressure occurs at the first coupled mode (primarily a beam mode) and at the second coupled mode (primarily a fluid mode). From figures 30 and 31 it can be seen that absorption does not affect the response of the first mode whereas the second peak is significantly reduced.

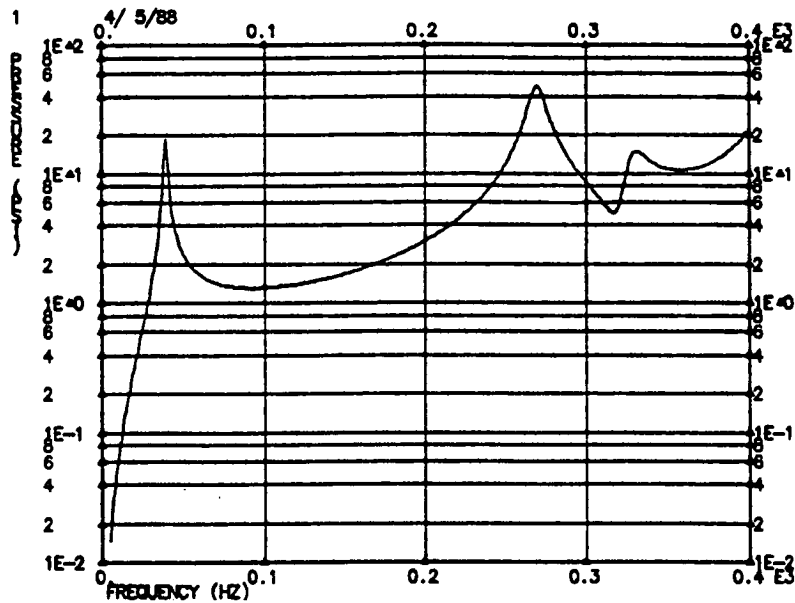


Figure 30. Fluid-beam system: no absorption damping - NORF=1.

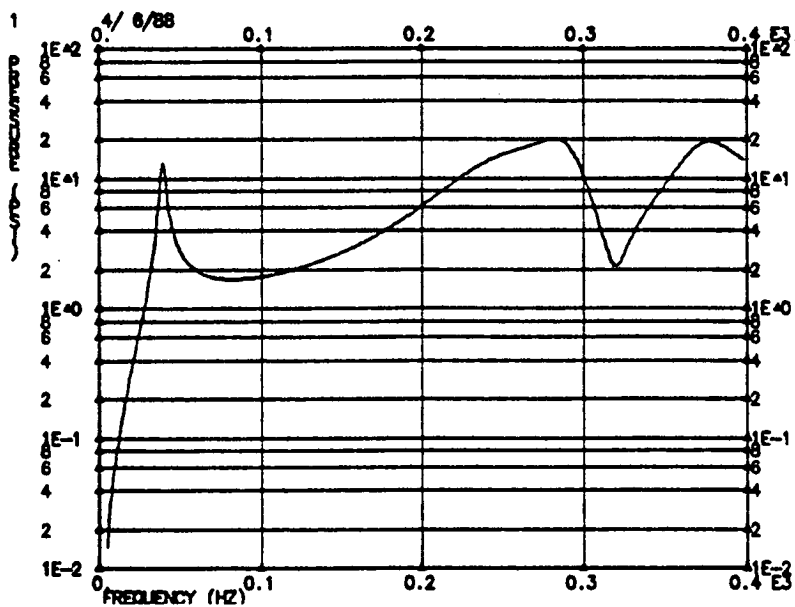


Figure 31. Fluid-beam system: uniform absorption damping - NORF=-1.

Since the calculations represented by figures 32 and 33 have the same damping, without and with residual flexibility effects, one can evaluate the effect of residual flexibility. In this case the effect is quite small and is only noticeable near the second peak. Unfortunately, it is very difficult to predict whether residual flexibility will have an important role. Since it is not expensive to calculate, it should be included in all cases.

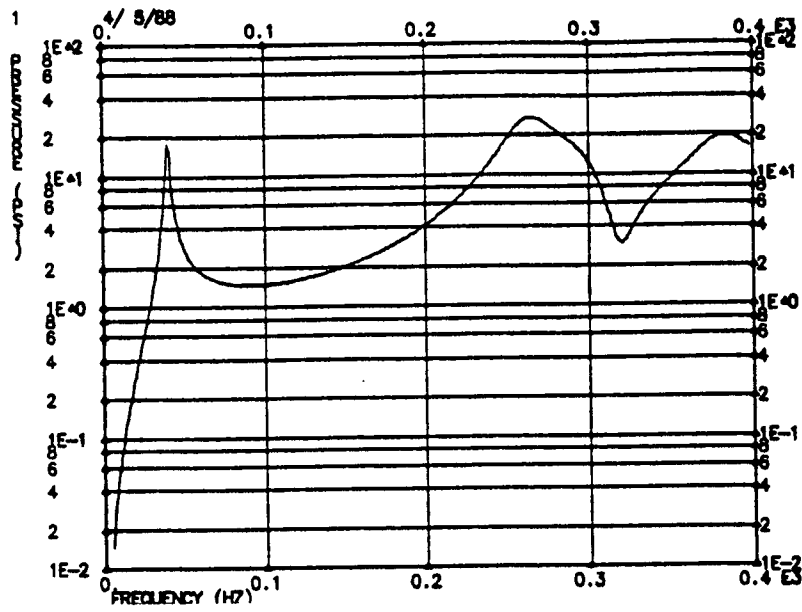


Figure 32. Fluid-beam system: linearly varying absorption damping - NORF=-1.

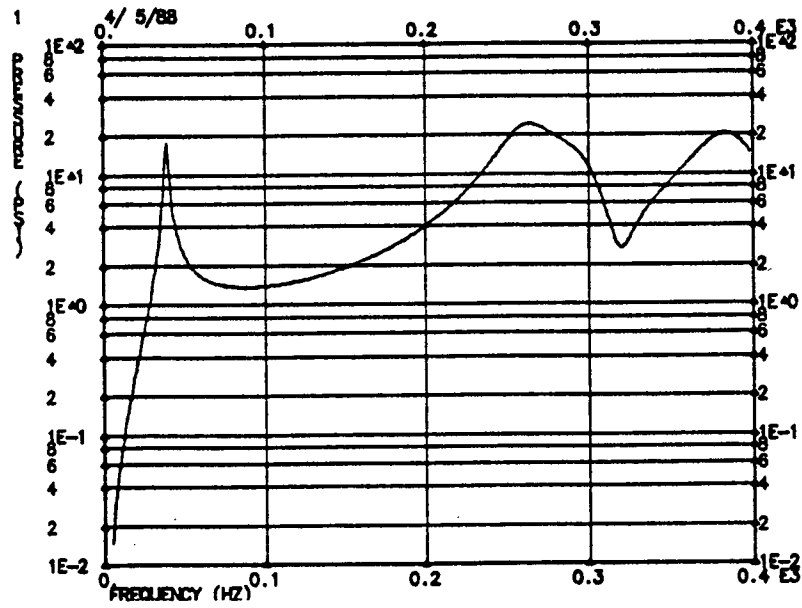


Figure 33. Fluid-beam system: linearly varying absorption damping - NORF=1

## 7.2.6 Fluid-beam grid participation factor calculation

To complete the last step in the analysis sequence, a sample grid point participation calculation was carried out for this problem. Following the instructions in section 6, the input data were prepared which essentially consisted only of selecting the fluid grid point for which the structural grid point participation was required. In this case, point 21216 was selected. Also the frequencies for which the calculation is to be made have to be selected. Only one frequency, 40 Hz, was chosen which corresponds to the first peak in the frequency response curves. The listing of the input deck can be found in Appendix C4. table 13 presents a selected output of points. As expected, the maximum contribution comes from the point closest to the middle of the beam since the first mode has a peak motion at the center.

**Table 13 Participation factors for point 21216 at 40 Hz**

COMPLEX DISPLACEMENT VECTOR (REAL/IMAGINARY)					
POINT ID.	TYPE	T1	T2	T3	R1
20001	G	-1.109855E-02	3.724580E-02	2.018416E-03	1.335892E-02
		3.555394E-02	1.053499E-04	5.709099E-06	0.0
20003	G	-9.526432E-02	3.198780E-01	1.733476E-02	1.147304E-01
		3.053643E-01	8.489896E-04	4.600826E-05	0.0
20005	G	-2.410586E-01	8.103863E-01	4.391628E-02	2.906606E-01
		7.737055E-01	1.851216E-03	1.003207E-04	0.0
20007	G	-4.124141E-01	1.389196E+00	7.528301E-02	4.982618E-01
		1.326569E+00	2.317275E-03	1.255773E-04	0.0
20009	G	-5.732617E-01	1.936381E+00	1.049359E-01	6.945202E-01
		1.849580E+00	1.558949E-03	8.448224E-05	0.0
20011	G	-6.990637E-01	2.368622E+00	1.283599E-01	8.495518E-01
		2.263113E+00	-3.561608E-04	-1.930099E-05	0.0
20013	G	-7.806732E-01	2.651931E+00	1.437129E-01	9.511660E-01
		2.534422E+00	-2.497307E-03	-1.353335E-04	0.0
20015	G	-8.196042E-01	2.788084E+00	1.510913E-01	1.000000E+00
		2.664897E+00	-3.828808E-03	-2.074899E-04	0.0

## 8. VEHICLE ACOUSTIC ANALYSIS

In recent years, the designers of airplane and automobile structures have been increasingly concerned with the noise in passenger compartments. These concerns occur because of government regulations and competitive pressures. In modern automotive designs, for example, there is a greater possibility of "boom" and "harshness" noises because of the use of lightweight structures and elimination of fully isolated chassis frames. In the past these problems were attacked by experimental testing methods alone. This process is time-consuming, expensive, and is performed only when the prototype models are available. It is also difficult to pinpoint the sources of the noise problems.

The main purpose of the development of the acoustic procedure is to provide the design engineer with a noise analysis program that can be used in the preliminary design stage. It is unlikely that an absolute quantitative noise prediction can be obtained for a particular design owing to the large number of uncertainties in the structure model and the attendant complications in finite element modeling of such structures. Nevertheless, using this procedure, a relative comparison can be made between two competing designs. The number of prototype tests will be significantly reduced by using this approach. Combining this procedure with testing should lead to an effective and timely method for solving these difficult problems.

This chapter is devoted to an example analysis of a realistic automobile structure. The choice of this particular example was motivated by the second author who spent most of his professional career at Daimler Benz. Most of the steps in the acoustic procedure have already been discussed in detail in previous sections. The main purpose in this section is to illustrate the practicality and simplicity of the procedure. One of the most important goals of this procedure is to present acoustic analysis as a simple extension of the typical structural dynamic analysis where the fluid domain is treated as if it were just another part of the structure with different properties. Therefore, the acoustic analysis can be performed early in the design process by a structural dynamic engineer rather than being treated as a stand-alone acoustic problem.

### 8.1 Structural Model

The hidden line plot of the structural model is shown in figure 34. The internal structural details could not be shown because most of the picture would be black due to the fineness of the finite element model. This structural model consists of 26144 grid points. In this particular case the whole model is subdivided into 36 superelements and one residual structure. In the MSC/NASTRAN terminology, this model consisted of three superelement levels. There are 33 tip superelements, 3 collector superelements, and one residual structure. For the purpose of normal modes calculation, the Guyan reduction method was used

to approximate the modal behavior of the grid points on the interior of each superelement. The number and the type of elements used in the structural model are shown in table 14.

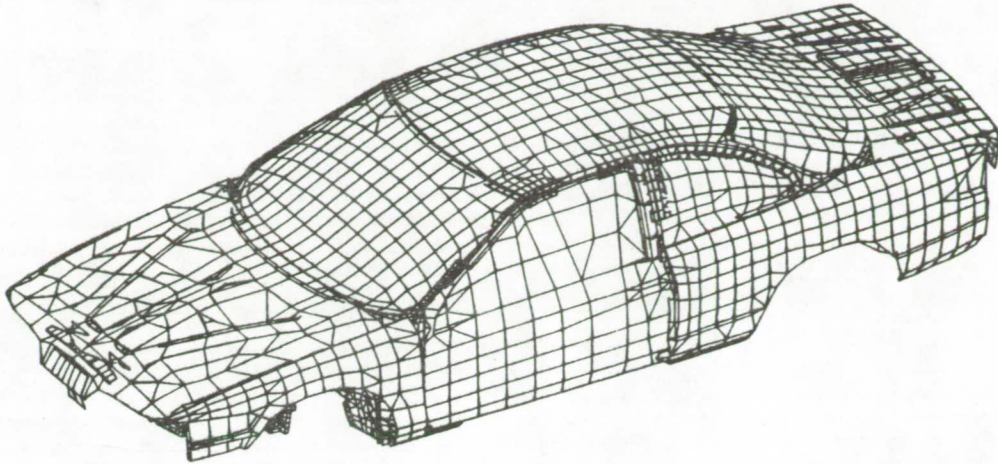


Figure 34. Vehicle structural model.

Table 14 Structural model	
Element Type	Number
CBAR	338
CELAS1	786
CQUAD4	19424
CTRIA3	8225

The total number of structural grid points in the residual structure is 663. From the acoustic analysis point of view the only additions to this model were the grid points and elements of the air in the passenger compartment.

An example of a different and smaller structural model is shown in figure 35. This example illustrates a coarser modelling approach for the structure. This problem was solved without the use of superelements.



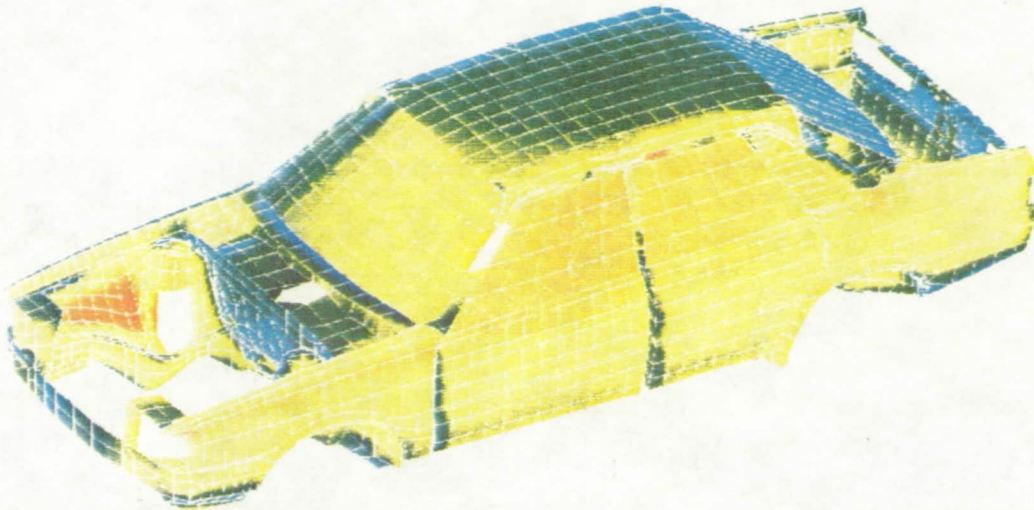


Figure 35. Coarse vehicle structural model.

## 8.2 Fluid Model of the Passenger Compartment

The model representing the air on the interior of the structure is shown in figure 36. This model consists of 973 fluid grid points, 394 CHEXA, and 494 CPENTA elements. Note that each fluid grid point has only one degree of freedom associated with each fluid grid point. It is easily seen that the fluid model is an extremely small addition to the total structural model. Clearly, the fluid model is much coarser than the structural model. The mesh size was determined based on the frequency of the fluid that had to be accurately represented. In this particular analysis, the maximum frequency of interest in the fluid model is only 200 Hz. In addition, it is known from previous experimental measurements that the structural model is capable of predicting reasonably accurate response only up to 100 Hz. Knowing the speed of sound in the air, and assuming a need for eight elements per wavelength, the resulting mesh is obtained.

The only additional required input for the fluid model is the application of the unit pressure to the outside surface of the fluid. This is used by the Area Matrix Program to determine the coupling points between the structure model and the fluid model. If absorption were to be specified, additional unit pressure loads would have to be applied to the fluid on the surfaces that are in contact with the absorbing materials.

The fluid model corresponding to the structural model in figure 35 is shown in figure 37. The size of this model is approximately the same as the one in figure 36. This points out the fact that even though the structural models can be significantly different in size, the fluid mesh is very similar since the volume that is modelled is approximately the same.

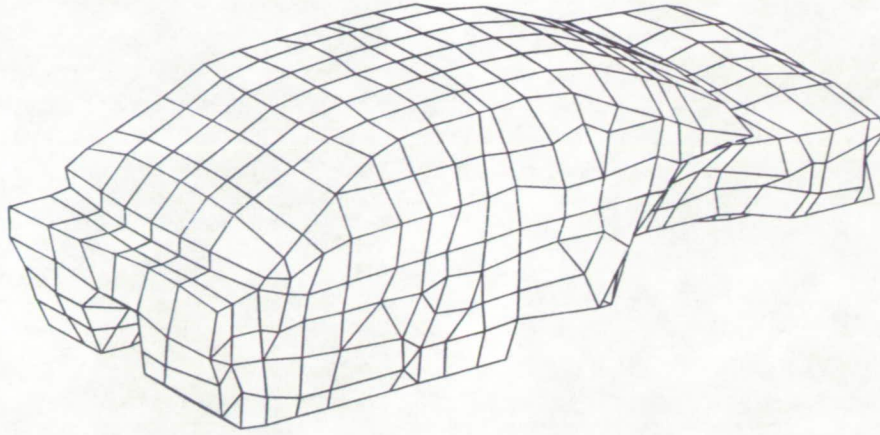


Figure 36. Vehicle fluid model.

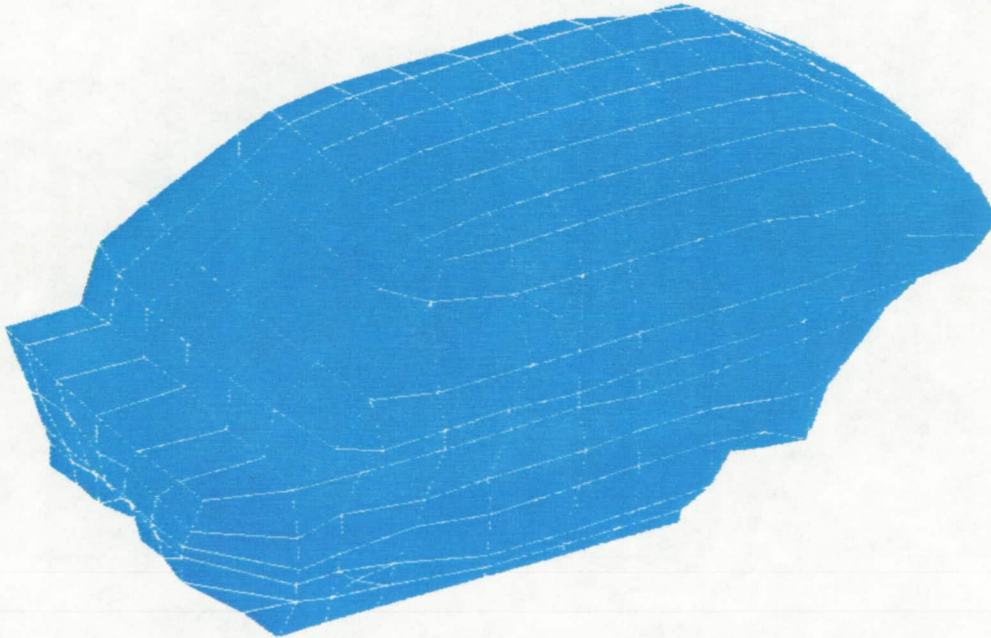


Figure 37. Vehicle fluid model (corresponding to coarse str. model).

### 8.3 Modal Analysis of the Complete Model, Structure and Fluid

This analysis is a standard SOL 63 in MSC/NASTRAN. Only the key portions of the input deck are shown in Appendix D1. The Bulk Data Deck could not be listed since it contains nearly 100,000 records. The only unusual aspect of this calculation is the use of two sub-cases for the residual structure in the Case Control Deck, otherwise it is the same as any other structural normal modes calculations. Note that the component modes were not



calculated for any superelement since there is no **METHOD** card request for any superelements. Guyan reduction was used for each superelement and only the modes of the residual structure were calculated. This is performed in two subcases. In the first, the modes of the residual for the structure model are calculated and in the second, the modes of the fluid model are calculated. A total of 200 modes were calculated for the structure with the first flexible mode at 7 Hz and the last mode at 150 Hz. Only 10 modes were extracted for the fluid with the highest mode at 200 Hz. For illustration purposes, figures 38 and 39 present several views of the first longitudinal fluid mode at approximately 70 Hz.

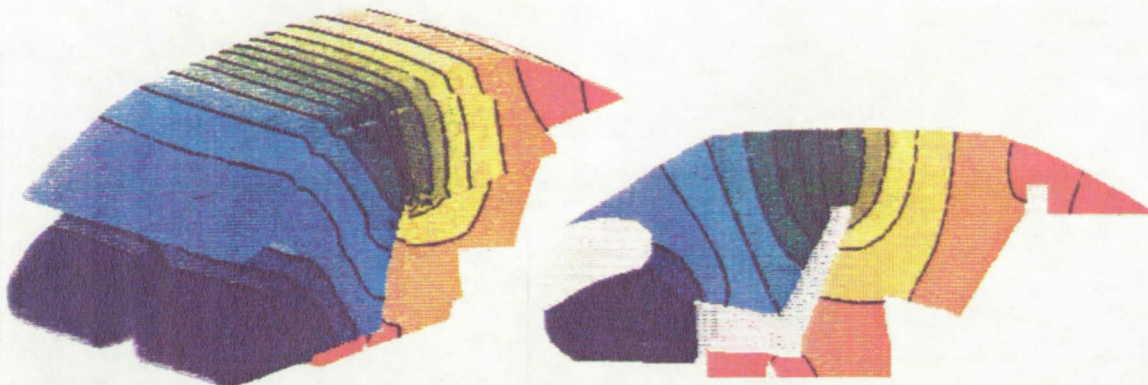


Figure 38. Orthographic and side views of the first longitudinal fluid mode (70Hz).

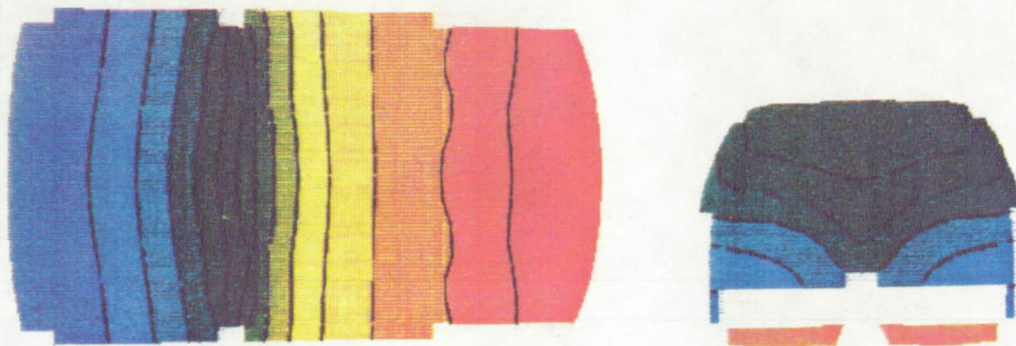


Figure 39. Top and front views of the first longitudinal fluid mode (70Hz).

The modes of the coupled model were not calculated for this example, simply because they were not required for any further calculation and there was no special interest in their eigenvalues.

## 8.4 Response Analysis During Harmonic Excitation

The loading conditions for a typical automobile structure are too numerous to list. Obviously, the input from the road is one of the interesting loading conditions. Input from the engine at the mounting points to the frame is another condition that can cause significant structurally borne noise in the passenger compartment.

In this section, a calculation of the acoustic response due to the drive shaft unbalance will be illustrated. Ultimately, the value of any analysis is directly related to its ability to correlate with actual measurements. A large number of variables can affect the comparison. Before any comparisons can be made for acoustical response, one must ensure that the structural responses, such as natural frequencies, accelerations response, etc., correlate with measured data.

For complex structures such as automobiles, that is a very difficult task. There is a significant existing effort, with a generic name of System Identification, whose goal is to assist the analyst in correlating analytical to experimental results. This is accomplished by adjusting the analytical model to better match the test data. Inherent in this approach is the assumption that the test results are correct. This assumption is not valid in many cases, but it is the best that can be done.

A condensed input deck for this particular analysis is listed in Appendix D3.1. Figure 39 presents the measured pressure versus the calculated pressure at the rear passenger's ear due to the drive shaft unbalance.

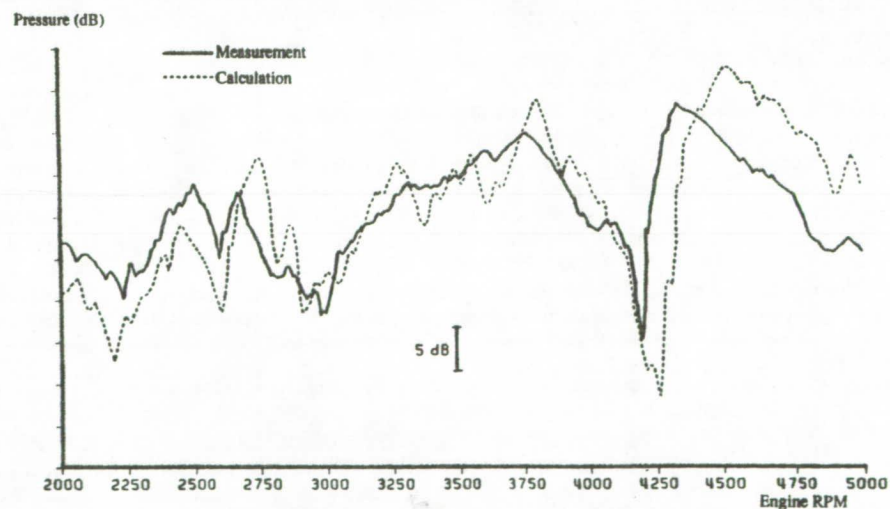


Figure 40. Comparison of the test and analysis pressure response at the rear passenger's ear - drive shaft unbalance.



Considering the above remarks, the comparison is very good. There is a 5dB difference in the results for frequencies above 70 Hz, but this is primarily due to the diminishing ability of the structural model to match the measured natural frequencies above 70 Hz.

Clearly data such as these are valuable to a design engineer in correcting any potential noise problems. As stated previously, even if the comparison were not very good, relative comparisons between different designs are useful in selecting the best design.

### 8.5 Grid Point Participation Factor Calculation

One of the most important aspects of the acoustic procedure is the ability to calculate the structural grid point participation in the generation of noise at a particular point in the fluid domain. With this information the design engineer can readily pinpoint the source of the structurally borne noise. Once the location of the disturbance is known, there are a number of available options for reducing the noise level. These include structural modifications, addition of absorbing materials, active noise suppression and other techniques. Participation factors change with excitation frequency and sometimes certain parts of the structure generate noise at one frequency and subtract from the total noise at another frequency. This leads to conflicting requirements that can make the ultimate solution difficult to find.

The ear locations of the driver and passenger are the points at which the pressure values were calculated during the harmonic response. Pressure responses at the rear passenger's and the driver's ear are shown in figures 41 and 42, respectively.

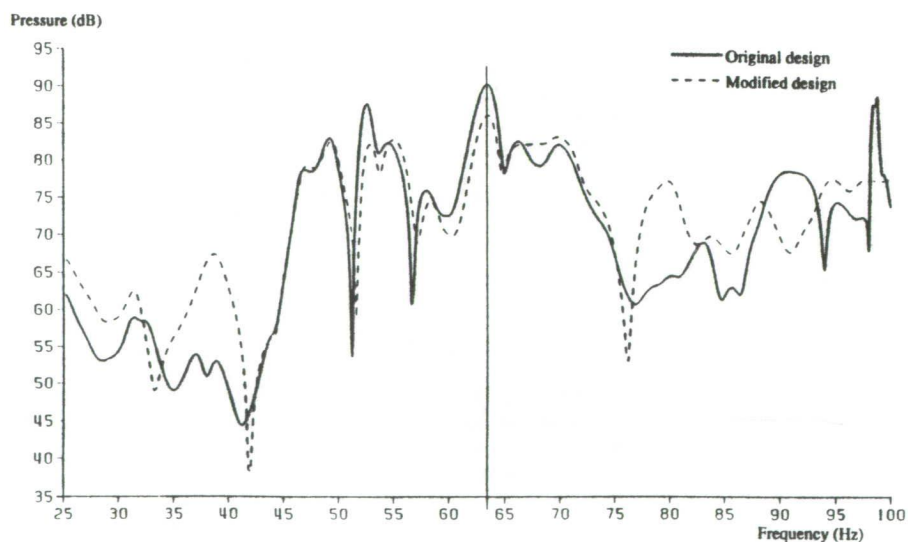


Figure 41. Pressure response at the rear passenger's ear.

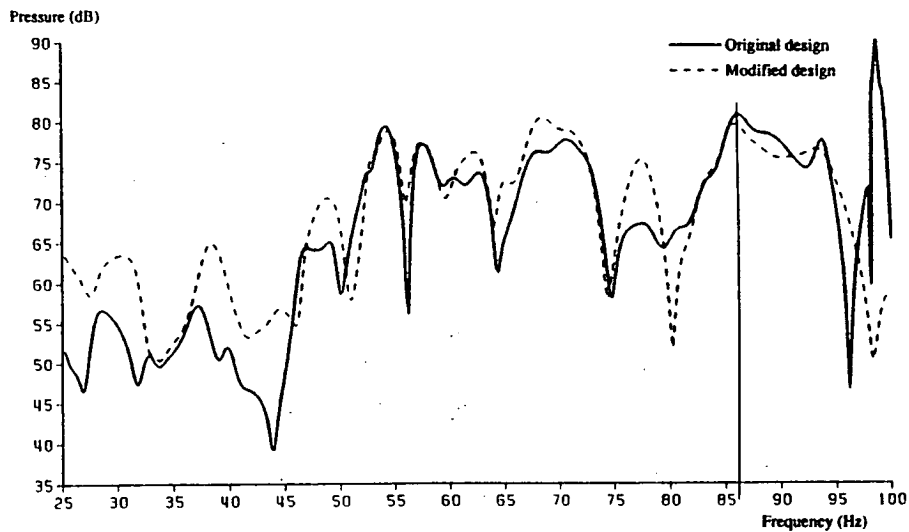


Figure 42. Pressure response at the driver's ear.

It can easily be seen from figure 41 that there is a significant pressure at 64 Hz for the rear passenger. Similarly, from figure 42, there is a pressure peak at 86 Hz for the driver. The peak near 100 Hz is ignored since the validity of the model is questionable in that range.

Therefore, to find the source of the pressure, grid participation factor calculation is carried out at 64 Hz for the rear passenger and for the driver at 86 Hz. For purpose of clarity, the contours of the participation factors are shown on the outside surface of the fluid (see section 6.7.4). The results are seen in figures 43 and 44. From figure 43 one can identify the source of noise for the rear passenger to be primarily the rear window. Clearly, the source of noise for the driver is the vibration of the front window.

For a typical design process, more plots of this kind would have to be generated for other peaks in the pressure response curves. Fortunately, it is very inexpensive in CPU time and man hours to generate large amounts of grid participation factor data. The more difficult and time-consuming task is to find a feasible solution from a number of inevitably conflicting results.

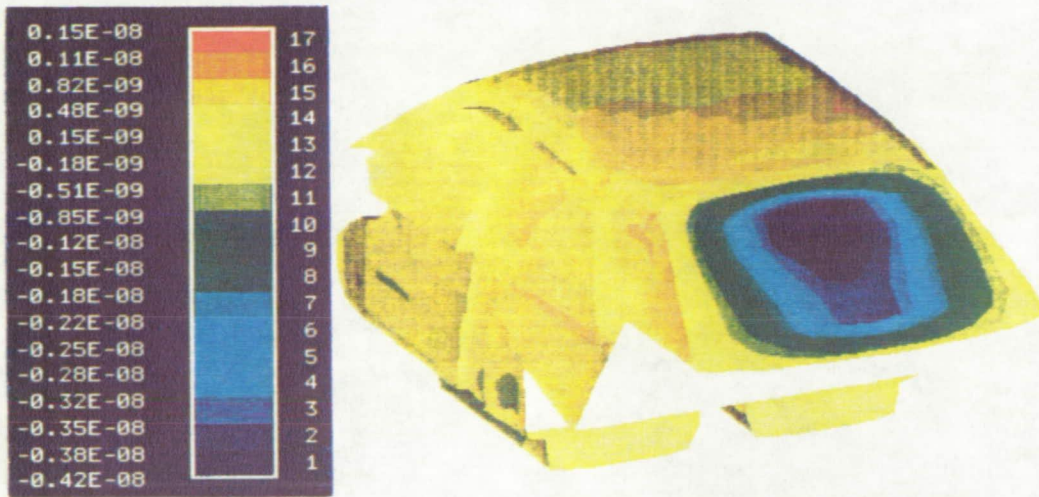


Figure 43. Grid participation factors for the rear passenger's ear at 64 Hz.

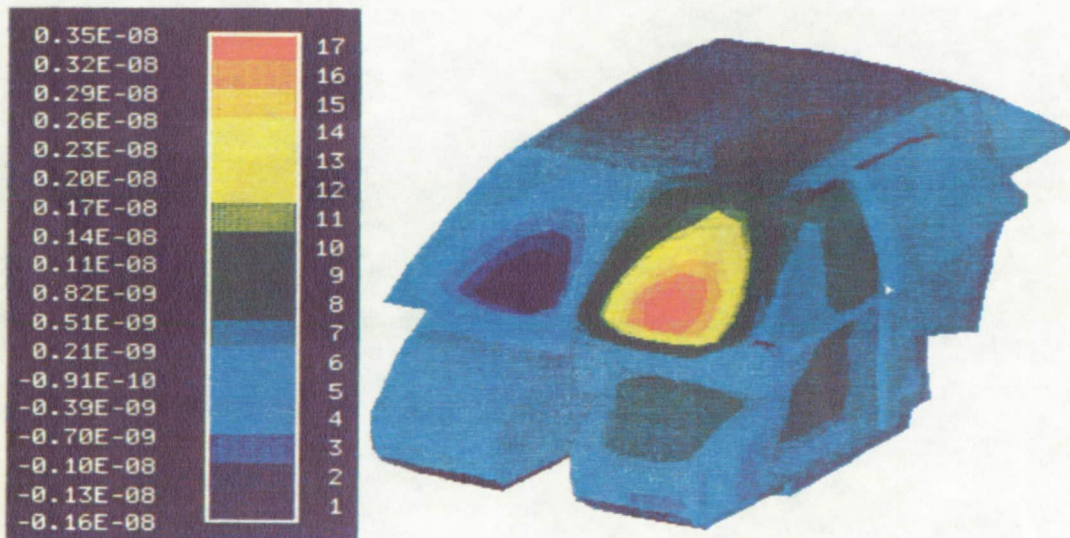


Figure 44. Grid participation factors for the driver's ear at 86 Hz.

## APPENDIX A : Notations

---

$A_z$	.....matrix representing absorbing parts of the fluid boundary $S$
$B_1, \dots, B_s$	.....fluid boundaries
$\underline{b}$	.....body force acting on the fluid
$C$	.....coupling matrix
$C_b$	.....submatrix of the coupling matrix due to boundary panel $b$
$c_f$	.....speed of sound
$d_B$	.....damping of the fluid on the boundary $B$
$d_f$	.....modal damping matrix of the fluid
$d_s$	.....modal damping matrix of the structure
$D_f$	.....damping matrix of the fluid
$D_s$	.....damping matrix of the structure
$D_z$	.....boundary absorption matrix (normal impedance $Z$ )
" $f$ "	.....index indicating fluid quantities
$\underline{E}$	.....total load on the structure
$\underline{E}_f$	.....load onto the fluid due to sources inside the fluid
$\underline{E}_p$	.....pressure-induced load onto the structure
$\underline{E}_s$	.....external load onto the structure
$f_s$	.....modal transformed structural load
$g_f$	.....modal transformed fluid load (symmetric form)
$i$	.....imaginary unit
$i, j$	.....indices
$I_f$	.....unit matrix (fluid)
$k$	.....wave number ( $k = \omega/c_f$ )
$k_f$	.....modal stiffness matrix of the fluid
$k_s$	.....modal stiffness matrix of the structure
$K_f$	.....fluid stiffness matrix
$K_s$	.....structure stiffness matrix
$L$	.....differential operator
$L_b$	.....fluid load vector due to body forces
$L_e$	.....fluid load vector due to external time-dependent pressure
$L_f$	.....structure load vector due to fluid interaction
$L_s$	.....fluid load vector due to structure interaction

$L_s^e$  .....structure load vector due to external time-dependent load  
 $L_q$  .....fluid load vector due to added fluid mass  
 $M_c$  .....Fluid-structure coupling mass matrix  
 $M_f$  .....fluid mass matrix  
 $M_s$  .....structure mass matrix  
 $m_f$  .....modal mass matrix of the fluid  
 $m_s$  .....modal mass matrix of the structure  
 $\underline{n}$  .....unit normal vector (components:  $n_x, n_y, n_z$ )  
 $n_b$  .....total number of boundary panels  
 $n_f$  .....total number of fluid modes  
 $n_s$  .....total number of structure modes  
 $N_f$  .....trial function in the fluid domain  
 $N_s$  .....trial function in the structure domain  
 $ND$  .....number of nodes required to discretize a wavelength  
 $\hat{p}$  .....fluid pressure, total value  
 $p_0$  .....fluid pressure, reference value  
 $p$  .....fluid pressure, ambient value  
 $p_e$  .....external time-dependent pressure  
 $P$  .....column vector of the nodal values of the pressure  
 $q$  .....added fluid mass per unit volume and time  
 $Q$  .....added fluid mass per unit volume,  $Q = qd$   
 $\underline{r}$  .....vector  $(x,y,z)$ ,  $x,y,z$  spatial coordinates  
"  $s$  " .....index indicating structural quantities  
 $S$  .....fluid boundary  
 $t$  .....time variable  
 $T$  .....transformation matrix for symmetry transforms  
 $[\cdot]^T$  .....transpose of matrix  
 $\underline{u}_f$  .....fluid displacement field,  $\underline{u}_f = (u_{fx}, u_{fy}, u_{fz})$   
 $\underline{u}_s$  .....structure displacement field,  $\underline{u}_s = (u_{sx}, u_{sy}, u_{sz})$   
 $u_{sf}$  .....structure displacement component perpendicular to the fluid boundary  
 $(u_{sf} = \underline{u}_f \cdot \underline{n})$   
 $U$  .....structure displacement vector  
 $\underline{v}$  .....fluid velocity field  
 $v_n$  .....fluid velocity component perpendicular to the fluid boundary  
 $V$  .....volume of the fluid domain

$w$ .....scalar test function  
 $Z_0$ .....wave resistance (for plane waves),  $Z_0 = \rho_f c_f$   
 $Z_n$ .....acoustic impedance  
 $Z_1$ .....specific acoustic resistance  
 $Z_z$ .....specific acoustic reactance  
 $Z_f', Z_f^{0t}$ .....residual flexibility terms of the fluid  
 $z_2$ .....acoustic modal frequency response function  
 $\beta$ .....specific acoustic admittance ( $\beta = \gamma + i\sigma$ )  
 $\epsilon_{xx}, \gamma_{xy}, \gamma_{yx}$ .....strain components in  $x$  direction  
 $\phi$ .....body force potential  
 $\phi_f$ .....fluid modal matrix  
 $\phi_s$ .....structure modal matrix  
 $\psi$ .....displacement potential field  
 $\hat{\rho}$ .....fluid density, total value  
 $\rho_f$ .....fluid density, reference value  
 $\rho$ .....fluid density, ambient value  
 $\sigma_{xx}, \tau_{xy}, \tau_{yx}$ .....stress components in  $x$  direction  
 $\zeta$ .....modal coupling matrix  
 $\xi_f$ .....fluid modal variable  
 $\xi_s$ .....structural modal variable  
 $\omega$ .....radian frequency (coupled system)  
 $\omega_f$ .....fluid radian frequency  
 $\int_V$ .....volume integral  
 $\int_S$ .....surface integral  
 $\int_{B_i}$ .....partial surface integrals ( $i=1, \dots, 5$ )  
 $\nabla$ .....gradient operator,  $\nabla = \left( \frac{\partial}{\partial x}, \frac{\partial}{\partial y}, \frac{\partial}{\partial z} \right)$   
 $\nabla_B$ .....gradient operator on the fluid boundary  
 $\nabla^2$ .....Laplace operator,  $\nabla^2 = \Delta$



**APPENDIX B : INPUT DECKS FOR SECTION 7.1**





```

SPC1    11      23456  11111
$
$
$ ***** SUPERELEMENT-ASSIGNMENT OF PISTON GRID POINTS *****
SESET   10      10001  THRU   10025
$
$
$ ***** THE SPRING - PISTON - SYSTEM *****
$ ***** (MATERIAL DATA, GEOMETRY AND TOPOLOGY) *****
$
$ MATERIAL DATA / PISTON
PSHELL  10      111    1.0    111      111
MAT1    111    2.06E5    .314    1.E-15
CONM2   101802  10013  0      0.01E-3
$
$ SPRING (STIFFNESS IN X1-DIRECTION)
CELAS2  101801  7.47474911111  1
$
CBAR    101803  88      11111  10013  0.      1.      0.
PBAR    88      111    1.E+2  1.E+4  1.E+4  2.E+4
$
$ VISCOUS DAMPING
CDAMP2  101804  5.E-4  11111  1
$
GRID    11111      0.0    0.0    0.0
$
$ GRID POINTS / PISTON SURFACE
GRID    10001      0.      0.      0.
GRID    10002      0.     -6.25   0.
GRID    10003      0.     -12.5   0.
GRID    10004      0.     -18.75  0.
GRID    10005      0.     -25.    0.
GRID    10006      0.      0.     6.25
GRID    10007      0.     -6.25  6.25
GRID    10008      0.     -12.5  6.25
GRID    10009      0.     -18.75 6.25
GRID    10010      0.     -25.   6.25
GRID    10011      0.      0.    12.5
GRID    10012      0.     -6.25  12.5
GRID    10013      0.     -12.5  12.5
GRID    10014      0.     -18.75 12.5
GRID    10015      0.     -25.   12.5
GRID    10016      0.      0.   18.75
GRID    10017      0.     -6.25  18.75
GRID    10018      0.     -12.5  18.75
GRID    10019      0.     -18.75 18.75
GRID    10020      0.     -25.   18.75
GRID    10021      0.      0.    25.
GRID    10022      0.     -6.25  25.
GRID    10023      0.     -12.5  25.
GRID    10024      0.     -18.75 25.
GRID    10025      0.     -25.   25.
$
$ RIGID BAR ELEMENTS / PISTON (RIGID PISTON SURFACE!)
RBE2    14001  10013  1  10001  10002  10003  10004
10005+XYZ1111

```











```

$
$ 4.145-7      => RHOC: WAVE RESISTANCE (FOR PLANE WAVES IN THE FLUID)
$              RHOC = CF * RHOF
$              CF: SPEED OF SOUND IN THE FLUID (HERE: AIR)
$              CF=3.44*EXP(5) MM/S
$              RHOF: DENSITY OF THE FLUID (HERE: AIR)
$              RHOF=1.205*EXP(-12) T/(MM*MM*MM)
$
$
$ 2.28-7,-1.456-6 => CR(I),CI(I) (REALS)
$              CR(I): REAL PART OF ACOUSTIC ADMITTANCE
$              CI(I): IMAGINARY PART OF ACOUSTIC ADMITTANCE
$
$              CR(I)=RHOC*ZR(I)/(ZR(I)*ZR(I)+ZI(I)*ZI(I))
$              CI(I)=-RHOC*ZI(I)/(ZR(I)*ZR(I)+ZI(I)*ZI(I))
$
$              ZR : REAL PART OF NORMAL IMPEDANCE
$              ZI : IMAGINARY PART OF NORMAL IMPEDANCE
$
$
$ ENDDATA
$ /EOF
$ 1.,0.
$ 1,1.
$ N
$ -1,-1
$ 1
$ 200.
$ 4.145-7
$ 2.28-7,-1.456-6

```

## APPENDIX B2 : Run 2 Input - One-Dimensional Piston/Tube Model

\*\*\*\*\*

\*\* R U N 2 \*\*

\*\*\*\*\*

```
NASTRAN SYSTEM(105)=2,BUFFSIZE=4609 $
NASTRAN DBSET 1=(DB01,DB15),DBSET 2=(DB01,DB15) $
NASTRAN DBSET 15=(DB15) $
ID FLUID STRUCTURE
SOL 70
TIME 999
DIAG 8,13,20
$
$$$$$$$$$$$
*READ CDMAP
$$$$$$$$$$$
$
CEND
TITLE =      XMPL02
SUBTITLE =   SPRING-PISTON-TUBE SYSTEM / COUPLED EIGENANALYSIS
ECHO =      NONE
$
SET 99 = 0
SEMG = 99
SPC = 11
$
$DISP=ALL
DISP(PLOT)=ALL
$
$ SELECTION OF STRUCTURAL POINTS FOR PLOTTING
$
$ SET 66 = 10001 THRU 10025
$ DISP = 66
$
SUPER = ALL
$
SUBCASE 11
  LABEL = RESIDUAL STRUCTURE
  METHOD = 11
$
$
BEGIN BULK
PARAM, LMODES, 7
PARAM, RESDUAL, -1
PARAM, DLOAD, -1
$
$ REAL EIGENANALYSIS
$
EIGR, 11, MGIV, , , , 7, , 1. -9, +E1
+E1, MAX
$
$ COMPLEX EIGENANALYSIS
$
```

EIGC,12,HESS,MAX,,,,,+EC1

+EC1,,,,,,7

\$

\$ -----

\$

\*READ DMI

\$

\$ -----

\$

ENDDATA

## APPENDIX B3.1 : Run 3.1 Input - One-Dimensional Piston/Tube Model

```
*****
** R U N  3.1 **
*****

NASTRAN SYSTEM(105)=2
NASTRAN SYSTEM(7)=10,BUFFSIZE=4609 $
NASTRAN DBSET 1=(DB01,DB15),DBSET 2=(DB01,DB15) $
NASTRAN DBSET 15=(DB15) $
ID FLUID STRUCTURE
SOL 71
TIME 60
DIAG 8,13,20
$
$$$$$$$$$$$
*READ CDMAP
$$$$$$$$$$$
$
CEND
$
TITLE =      XMPL03#1
SUBTITLE = SPRING-PISTON-TUBE SYSTEM / FREQUENCY RESPONSE
ECHO=SORT
$
SET 99=0,10
SELG = 99
SELR = 99
$
SPC = 11
$
$
$ SELECTION OF STRUCTURAL AND FLUID POINTS FOR PLOTTING
$
SET 60 = 10013
SET 61 = 13,553
$
DISP (SORT2,PHASE,PLOT) = 60
VELO (SORT2,PHASE,PLOT) = 61
$
$
LOADSET = 10
$
SUBCASE 1
SUPER = 10
$
SUBCASE 2
DLOAD = 1
FREQ = 2
SDAMPING = 3
$
$
OUTPUT (XYPLOT)
PLOTTER NAST
```

```

$
SEPLOT 0
PENSize = 4
XPAPER = 10.
YPAPER = 10.
XGRID = YES
YGRID = YES
UPPER TICS = -1
RIGHT TICS = -1
YVALUE PRINT SKIP = 1
XDIVISIONS = 12
YDIVISIONS = 10
XTITLE = FREQUENCY (HZ)
YTITLE = PRESSURE
$
TCURVE = PRESSURE AT FLUID GRID POINT 13
XYPLOT, XYPUNCH VELO / 13(T1RM)
$
TCURVE = PRESSURE AT FLUID GRID POINT 553
XYPLOT, XYPUNCH VELO / 553(T1RM)
$
$
SEPLOT 10
PENSize = 4
XPAPER = 10.
YPAPER = 10.
XGRID = YES
YGRID = YES
UPPER TICS = -1
RIGHT TICS = -1
YVALUE PRINT SKIP = 1
XDIVISIONS = 12
YDIVISIONS = 10
XTITLE = FREQUENCY (HZ)
YTITLE = AMPLITUDE IN MM
$
TCURVE = PISTON DISPLACEMENT / GRID POINT 10013
XYPLOT, XYPUNCH DISP/10013(T1RM)
$
$
BEGIN BULK
PARAM, NORF, -1
PARAM, SMALL, 0.
PARAM, LMODES, 7
PARAM, DLOAD, -1
$PARAM, RESDUAL, -1
$
$ EXCITATION AT PISTON CENTER 10013
$
FORCE, 11, 10013, , 2.1885, 1.0, ,
RLOAD1 1 12 13
LSEQ, 10, 12, 11
$
TABLED1 13
+TAB
+TAB 100. 1. 300. 1. ENDT
$
$ MODAL DAMPING INPUT

```

```
$
TABDMP1      3
+CF2
+CF2   -1000.  .0      0.      .0      .1      .0      1000.  .0
+CF3
+CF3   ENDT
$
$ FREQUENCY DOMAIN
$
FREQ1  2      100.    0.1    1000
$
-----
$
*READ DMI
$
-----
$
ENDDATA
```

**APPENDIX B3.2 : Run 3.2 Input - One-Dimensional Piston/Tube Model**

\*\*\*\*\*  
\*\* R U N 3.2 \*\*  
\*\*\*\*\*

NASTRAN SYSTEM(105)=2  
NASTRAN SYSTEM(7)=10,BUFFSIZE=4609 \$  
NASTRAN DBSET 1=(DB01,DB15),DBSET 2=(DB01,DB15) \$  
NASTRAN DBSET 15=(DB15) \$  
ID FLUID STRUCTURE  
SOL 72  
TIME 60  
DIAG 8,13,20  
\$  
\$\$\$\$\$\$\$\$\$\$  
\*READ CDMAP  
\$\$\$\$\$\$\$\$\$\$  
\$  
CEND  
\$  
TITLE = XMPLO3#2  
SUBTITLE = SPRING-PISTON-TUBE SYSTEM / TRANSIENT RESPONSE  
ECHO = SORT  
\$  
SET 99=0,10  
SELG = 99  
SELR = 99  
\$  
SPC = 11  
\$  
\$  
\$ SELECTION OF STRUCTURAL AND FLUID POINT FOR PLOTTING  
\$  
SET 60 = 10013  
SET 61 = 13,553  
\$  
DISP(SORT2,PHASE,PLOT) = 60  
VELO(SORT2,PHASE,PLOT) = 61  
\$  
\$  
SUBCASE 1  
SUPER = 10  
\$  
SUBCASE 2  
DLOAD = 1  
TSTEP = 2  
\$  
\$  
OUTPUT(XYPLOT)  
PLOTTER NAST  
\$  
SEPLOT 0  
PENSIZE = 4

```

XPAPER = 10.
YPAPER = 10.
XGRID = YES
YGRID = YES
UPPER TICS = -1
RIGHT TICS = -1
YVALUE PRINT SKIP = 1
XDIVISIONS = 12
YDIVISIONS = 10
$
XTITLE = FREQUENCY (HZ)
YTITLE = PRESSURE
$
TCURVE = PRESSURE AT FLUID GRID POINT 13 (X=0.0)
XYPLOT, XYPUNCH VELO / 13(T1RM)
$
TCURVE = PRESSURE AT FLUID GRID POINT 553 (X=150MM)
XYPLOT, XYPUNCH VELO / 553(T1RM)
$
$
SEPLOT 10
PENSIZE = 4
XPAPER = 10.
YPAPER = 10.
XGRID = YES
YGRID = YES
UPPER TICS = -1
RIGHT TICS = -1
YVALUE PRINT SKIP = 1
XDIVISIONS = 12
YDIVISIONS = 10
XTITLE = FREQUENCY (HZ)
YTITLE = AMPLITUDE IN MM
$
TCURVE = PISTON DISPLACEMENT / GRID POINT 10013
XYPLOT, XYPUNCH DISP/10013(T1RM)
$
$
BEGIN BULK
PARAM, NORF, -1
PARAM, SMALL, 0.
PARAM, LMODES, 7
PARAM, DLOAD, -1
$PARAM, RESDUAL, -1
$
$
$ EXCITATION AT GRID POINT 11111
DLOAD 1 1.0 1.0 11
$
TLOAD1, 11, 111, ,, 112
DAREA 111 11111 1 1.E+0
$
TABLED1, 112, ,, ,, +TABL1
+TABL1, -1.0, 0.0, 0.0, 0.0, 0.005, 1.0, 0.0195, 1.0, +TABL2
+TABL2, 0.02, 0.0, 1.0, 0.0, ENDT
$
$ TIME DOMAIN
TSTEP, 2, 2000, 1.0-4, 1

```



```
$  
$ -----  
$  
$ *READ DMI  
$  
$ -----  
$  
$ ENDDATA
```



```

$   THE REST OF THE CASE CONTROL DECK MUST BE THE SAME AS THAT   $
$   IN SOLUTION 71 RUN.  I.E. THE SUBCASE STRUCTURE FOR THE     $
$   RESIDUAL MUST BE THE SAME.                                   $
$                                                                 $
$   BULK DATA DECK -                                           $
$                                                                 $
$   DMIG,PDOF,0,9,1,0,,,1                                        $
$   DMIG,PDOF,1,1,,GIDi,CID,1.0                                  $
$                                                                 $
$   IF ONE WANTS ONLY THE REAL DISPLACEMENT OUTPUT SET THE     $
$   PARAM,REAL,0                                                 $
$                                                                 $
$$$$$$$$$$$$$$$$$$$$$$$$$$$$$$$$$$$$$$$$$$$$$$$$$$$$$$$$$$$$$$$
$
PARAM,REAL,-1
$
DMIG,PDOF,0,6,1,0
DMIG,PDOF,553,1,,553,1,1.0
$
ENDDATA

```

**APPENDIX C : INPUT DECKS FOR SECTION 7.2**



```

TITLE = FLUID-STRUCTURE INTERACTION
SUBTITLE = NORMAL MODES ANALYSIS
ECHO = NONE
SEALL = ALL
SPC = 1
LOADSET = 11
$
$ DEFINE THE PARTITION VECTOR FOR THE FLUID
$
SET 66 = 20000 THRU 30000
$
DISP(PLOT) = ALL
SUBCASE 1
  SUPER = 1
  METHOD = 1
SUBCASE 11
  LABEL = STRUCTURE MODEL
  PARTN = 66
  METHOD = 2
SUBCASE 12
  LABEL = FLUID MODEL
  METHOD = 3
BEGIN BULK
$$$$$$$$$$$$$$$$$$$$$$$$$$$$$$$$$$$$$$$$$$$$$$$$$$$$$$$$$$$$
$$$$$$$$$$$$$$$$$$$$$$$$$$$$$$$$$$$$$$$$$$$$$$$$$$$$$$$$$$$$
$
$ DEFINE THE STRUCTURE MODEL
$
EGRID,1
EGRID,2,,60.
$
GRIDG,1,,1345,16,-1,-2
CBARG,1,1,1,,,1.
PBAR,1,1,7.845,40.24
MAT1,1,3,+7,,.3,7.324-4
$
SPC1,1,12,10000
SPC1,1,6,10016
$
$ DEFINE THE EIGENVALUE EXTRACTION DATA FOR THE
$ STRUCTURE
$
EIGRL,1,,,8
EIGR,2,MGIV,,,,5,,1.-8,+E1
+E1,MAX
$
$ DEFINE THE SUPERELEMENT FOR THE STRUCTURE
$
SESET,1,10000,THRU,10015
SPOINT,11001,THRU,11020
SEQSET1,1,0,11001,THRU,11020
$
$$$$$$$$$$$$$$$$$$$$$$$$$$$$$$$$$$$$$$$$$$$$$$$$$$$$$$$$$$$$
$$$$$$$$$$$$$$$$$$$$$$$$$$$$$$$$$$$$$$$$$$$$$$$$$$$$$$$$$$$$
$
$ DEFINE THE FLUID MODEL
$
EGRID,3,,60.,240.

```

```

EGRID,4,,0.,240.
GRIDG,2,,23456,16,-1,-2,-3,,+G2
+G2,32,-4
CGEN,QUAD8,101,1,2
PSHELL,1,11,1.
MAT2,11,1.060+4,0.,0.,1.060+4,0.,1.060+4,2.96-6
SPCG,1,2,1,AD,CD
PARAM,COUPMASS,1
$
$ DEFINE THE LOAD ON THE FLUID TO CALCULATE
$ THE AREAS
$
FORCE,1,20000,,1.250,,1.
FORCE,1,20001,,5.000,,1.
FORCE,1,20002,,2.500,,1.
FORCE,1,20003,,5.000,,1.
FORCE,1,20004,,2.500,,1.
FORCE,1,20005,,5.000,,1.
FORCE,1,20006,,2.500,,1.
FORCE,1,20007,,5.000,,1.
FORCE,1,20008,,2.500,,1.
FORCE,1,20009,,5.000,,1.
FORCE,1,20010,,2.500,,1.
FORCE,1,20011,,5.000,,1.
FORCE,1,20012,,2.500,,1.
FORCE,1,20013,,5.000,,1.
FORCE,1,20014,,2.500,,1.
FORCE,1,20015,,5.000,,1.
FORCE,1,20016,,1.250,,1.
$
$ THE FOLLOWING TWO LOAD SETS DEFINE THE AREAS
$ FOR ABSORPTION DAMPING
$
FORCE,2,20000,,1.250,,1.
FORCE,2,20001,,5.000,,1.
FORCE,2,20002,,2.500,,1.
FORCE,2,20003,,5.000,,1.
FORCE,2,20004,,2.500,,1.
FORCE,2,20005,,5.000,,1.
FORCE,2,20006,,2.500,,1.
FORCE,2,20007,,5.000,,1.
FORCE,2,20008,,2.500,,1.
$
FORCE,3,20008,,2.500,,1.
FORCE,3,20009,,5.000,,1.
FORCE,3,20010,,2.500,,1.
FORCE,3,20011,,5.000,,1.
FORCE,3,20012,,2.500,,1.
FORCE,3,20013,,5.000,,1.
FORCE,3,20014,,2.500,,1.
FORCE,3,20015,,5.000,,1.
FORCE,3,20016,,1.250,,1.
$
LSEQ,11,101,1
LSEQ,11,102,2
LSEQ,11,103,3
$
$ DEFINE THE EIGENVALUE EXTRACTION DATA

```

```
$ FOR THE FLUID
$
EIGRL,3,,,13
$
ENDDATA
$
$$$$$$$$$$$$$$$$$$$$$$$$$$$$$$$$$$$$$$$$$$$$$$$$$$$$$$$$$$$$
$$$$$ AREA MATRIX PROGRAM - USER INPUT $$$$$
$$$$$$$$$$$$$$$$$$$$$$$$$$$$$$$$$$$$$$$$$$$$$$$$$$$$$$$$$$$$
$
$ TOL1,TOL2
  1.,0.
$ IFF,FF
  1,1.
$ SEARCH REGION
  N
$ SELECT ABSORPTION AREAS
  -1,-1
$
$$$$$$$$$$$$$$$$$$$$$$$$$$$$$$$$$$$$$$$$$$$$$$$$$$$$$$$$$$$$
```





\$ INSERT DMI.DAT HERE

\$

DMI*	DMI0000				2	123	1.250000000E+00		
DMI	DMI0000	0	2	1	0		2624	2624	
DMI*	DMI0001				2	27	1.250000000E+00		
DMI*	DMI0001				8	33	5.000000000E+00		
DMI*	DMI0001				14	39	2.500000000E+00		
DMI*	DMI0001				20	45	5.000000000E+00		
DMI*	DMI0001				26	51	2.500000000E+00		
DMI*	DMI0001				32	57	5.000000000E+00		
DMI*	DMI0001				38	63	2.500000000E+00		
DMI*	DMI0001				44	69	5.000000000E+00		
DMI*	DMI0001				50	75	2.500000000E+00		
DMI*	DMI0001				56	81	5.000000000E+00		
DMI*	DMI0001				62	87	2.500000000E+00		
DMI*	DMI0001				68	93	5.000000000E+00		
DMI*	DMI0001				74	99	2.500000000E+00		
DMI*	DMI0001				80	105	5.000000000E+00		
DMI*	DMI0001				86	111	2.500000000E+00		
DMI*	DMI0001				92	117	5.000000000E+00		
DMI	DMI0001	0	2	1	0		2624	122	
DMI	SUPER	0	2	1	0		2	1	
DMI*	SUPER				1	1	0.000000000E+00		
*	1.000000000E+00								

ENDDATA

## APPENDIX C3.1 : Run 3.1 Input - Two-Dimensional Fluid/Beam Model

```

$$$$$$$$$$$$$$$$$$$$$$$$$$$$$$$$$$$$$$$$$$$$$$$$$$$$$$$$$$$$
$$$$$$ AREA MATRIX PROGRAM - USER INPUT $$$$$$
$$$$$$$$$$$$$$$$$$$$$$$$$$$$$$$$$$$$$$$$$$$$$$$$$$$$$$$$$$$$
$
$ TOL1,TOL2
$ 1.,0.
$ IFF,FF
$ 1,1.
$ SEARCH REGION
$ N
$ SELECT ABSORPTION AREAS
$ -1,-1
$
$$$$$$$$$$$$$$$$$$$$$$$$$$$$$$$$$$$$$$$$$$$$$$$$$$$$$$$$$$$$

NASTRAN DBSET 1=(DB01,DB15),DBSET 2=(DB01,DB15) $
NASTRAN DBSET 15=(DB15) $
NASTRAN REAL=0,HICORE=300000 $
ID FLUID STRUCTURE
SOL 71
TIME 30
DIAG 8,13
$$$$$$$$$$$$$$$$$$$$$$$$$$$$$$$$$$$$$$$$$$$$$$$$$$$$$$$$$$$$
$$$$$$$$$$$$$$$$$$$$$$$$$$$$$$$$$$$$$$$$$$$$$$$$$$$$$$$$$$$$
$
$ USER INSTRUCTIONS:
$
$ 1. THE USER MUST INSERT THE DMAP.DAT DATA GENERATED BY THE
$ AREA MATRIX FORTRAN PROGRAM IN THE DMAP SEQUENCE. THE
$ LOCATION IS SHOWN BELOW.
$
$ 2. ALSO THE USER MUST INSERT THE DMI.DAT DATA GENERATED BY
$ THE AREA MATRIX FORTRAN PROGRAM IN THE BULK DATA DECK.
$ THE LOCATION IS SHOW IN THE BULK DATA DECK.
$
$ 3. IF ABSORPTION DAMPING DATA, DMIG.DAT, GENERATED BY THE
$ AREA MATRIX PROGRAM EXIST THE USER MUST ALSO INCLUDE
$ THIS DATA IN THE BULK DATA DECK. THE LOCATION IS SHOW
$ IN THE BULK DATA DECK.
$
$$$$$$$$$$$$$$$$$$$$$$$$$$$$$$$$$$$$$$$$$$$$$$$$$$$$$$$$$$$$
$
$ ***** BEGIN OF THE ALTER PACKAGE FOR FSI ANALYSIS *****
$
$$$$$$$$$$$$$$$$$$$$$$$$$$$$$$$$$$$$$$$$$$$$$$$$$$$$$$$$$$$$
$
$ INSERT THE DMAP.DAT HERE
```

```

$
$ INSERT THE DMAP ALTER HERE
$
CEND
TITLE = COUPLED FLUID-STRUCTURE FREQUENCY RESPONSE
SUBTITLE = 3% BEAM, 2% FLUID DAMPING
LABEL = NO ABSORPTION - NORF=1
$
SET 99 = 1,0
SET 67 = 21216
SET 65 = 0
$
SELG = ALL
SELR = ALL
SEDR = 65
$
SPC = 1
VELO = 67
FREQ = 1
SDAMPING = 1
$
SUBCASE 1
  SUPER = 99
  LOADSET = 11
  DLOAD = 21
$
OUTPUT (XYPLOT)
CSCALE 4.0
XPAPER = 105.
YPAPER = 80.
XAXIS = YES
YAXIS = YES
XGRIDLINES = YES
YGRIDLINES = YES
XMIN = 0.
XMAX = 400.
XTITLE = FREQUENCY (HZ)
YTITLE = PRESSURE (PSI)
TCURVE = PRESSURE AT GRID 21216
XYPLOT VELO / 21216(T1RM)
BEGIN BULK
$
$ DEFINE PARAMETERS
$
PARAM,NORF,1          $ RESIDUAL FLEXIBILITY FOR FLUID
PARAM,SMALL,0.
PARAM,LMODES,100
PARAM,DLOAD,-1
$
$ DEFINE THE DYNAMIC LOADS
$
FREQ1,1,5.,1.,395
$
FORCE,1,10008,,1000.,,1.
LSEQ,11,101,1
$
RLOAD1,21,101,,,1
$

```

```

TABLED1,1,,,,,,,,+TD1
+TD1,0.,1.,1000.,1.,ENDT
$
$ DEFINE MODAL DAMPING FOR FLUID AND BEAM
$ 2% FOR FLUID AND 3% FOR THE BEAM
$ NOTE: THE FLUID MODAL DAMPING IS DEFINED IN
$ THE THIRD QUADRANT, i.e. -FREQ AND -DAMPING
$
TABDMP1,1,,,,,,,,+TAB1
+TAB1,-1000.,-.04,0.,-.04,1.,+.06,1000.,+.06,+TAB2
+TAB2,ENDT
$
$ INSERT DMI.DAT HERE
$
DMI*      DMI0000      2      123 1.250000000E+00
DMI      DMI0000 0      2      1      0      2624      2624
DMI*      DMI0001      2      27 1.250000000E+00
DMI*      DMI0001      8      33 5.000000000E+00
DMI*      DMI0001     14      39 2.500000000E+00
DMI*      DMI0001     20      45 5.000000000E+00
DMI*      DMI0001     26      51 2.500000000E+00
DMI*      DMI0001     32      57 5.000000000E+00
DMI*      DMI0001     38      63 2.500000000E+00
DMI*      DMI0001     44      69 5.000000000E+00
DMI*      DMI0001     50      75 2.500000000E+00
DMI*      DMI0001     56      81 5.000000000E+00
DMI*      DMI0001     62      87 2.500000000E+00
DMI*      DMI0001     68      93 5.000000000E+00
DMI*      DMI0001     74      99 2.500000000E+00
DMI*      DMI0001     80     105 5.000000000E+00
DMI*      DMI0001     86     111 2.500000000E+00
DMI*      DMI0001     92     117 5.000000000E+00
DMI      DMI0001 0      2      1      0      2624      122
DMI      SUPER 0      2      1      0      2      1
DMI*      SUPER      1      1 0.000000000E+00
*      1.000000000E+00
ENDDATA

```



DMI*	DMI0001			8		33	5.000000000E+00
DMI*	DMI0001			14		39	2.500000000E+00
DMI*	DMI0001			20		45	5.000000000E+00
DMI*	DMI0001			26		51	2.500000000E+00
DMI*	DMI0001			32		57	5.000000000E+00
DMI*	DMI0001			38		63	2.500000000E+00
DMI*	DMI0001			44		69	5.000000000E+00
DMI*	DMI0001			50		75	2.500000000E+00
DMI*	DMI0001			56		81	5.000000000E+00
DMI*	DMI0001			62		87	2.500000000E+00
DMI*	DMI0001			68		93	5.000000000E+00
DMI*	DMI0001			74		99	2.500000000E+00
DMI*	DMI0001			80		105	5.000000000E+00
DMI*	DMI0001			86		111	2.500000000E+00
DMI*	DMI0001			92		117	5.000000000E+00
DMI	DMI0001	0	2	1	0		2624 122
DMI	SUPER	0	2	1	0		2 1
DMI*	SUPER				1		1 0.000000000E+00
*							1.000000000E+00
\$							
ENDDATA							

**APPENDIX C3.3 : Run 3.3 Input - Two-Dimensional Fluid/Beam Model**

```

$$$$$$$$$$$$$$$$$$$$$$$$$$$$$$$$$$$$$$$$$$$$$$$$$$$$$$$$$$$$
$$$$$$ AREA MATRIX PROGRAM - USER INPUT $$$$$$
$$$$$$$$$$$$$$$$$$$$$$$$$$$$$$$$$$$$$$$$$$$$$$$$$$$$$$$$$$$$
$
$ TOL1,TOL2
  1.,0.
$ IFF,FF
  1,1.
$ SEARCH REGION
  N
$ SELECT ABSORPTION AREAS
  -1,1
$ INPUT THE NUMBER OF FREQ AT WHICH THE
$ ABSORPTION WILL BE SPECIFIED
  3
$ INPUT THE FREQUENCIES
  2.,3.,600.
$ INPUT THE RHO*SPEED OF SOUND FOR FLUID
  5.645
$ INPUT THE REAL AND IMAGINARY COMPONENTS
$ FOR THE SPECIFIC ADMITTANCE - REGION 1
  2.E-3,3.E-3
  3.E-3,6.E-3
  6.E-1,1.2
$$$$$$$$$$$$$$$$$$$$$$$$$$$$$$$$$$$$$$$$$$$$$$$$$$$$$$$$$$$$

```

PARAM,NORF,-1 \$ NO RESIDUAL FLEXIBILITY FOR THE FLUID

```

$
$ INSERT DMI.DAT HERE
$
DMIG    DAMP101 0      6      3      0
DMIG    DAMP102 0      6      3      0
DMIG    DAMP103 0      6      3      0
DMIG*   DAMP101          20008          1
*                20008          1 8.857396315E-04 1.771479263E-03
DMIG*   DAMP101          20009          1
*                20009          1 1.771479263E-03 3.542958526E-03
DMIG*   DAMP101          20010          1
*                20010          1 8.857396315E-04 1.771479263E-03
DMIG*   DAMP101          20011          1
*                20011          1 1.771479263E-03 3.542958526E-03
DMIG*   DAMP101          20012          1
*                20012          1 8.857396315E-04 1.771479263E-03
DMIG*   DAMP101          20013          1
*                20013          1 1.771479263E-03 3.542958526E-03
DMIG*   DAMP101          20014          1

```



*		20014	1	8.857396315E-04	1.771479263E-03
DMIG*	DAMP101		20015	1	
*		20015	1	1.771479263E-03	3.542958526E-03
DMIG*	DAMP101		20016	1	
*		20016	1	4.428698157E-04	8.857396315E-04
DMIG*	DAMP102		20008	1	
*		20008	1	1.328609418E-03	2.657218836E-03
DMIG*	DAMP102		20009	1	
*		20009	1	2.657218836E-03	5.314437672E-03
DMIG*	DAMP102		20010	1	
*		20010	1	1.328609418E-03	2.657218836E-03
DMIG*	DAMP102		20011	1	
*		20011	1	2.657218836E-03	5.314437672E-03
DMIG*	DAMP102		20012	1	
*		20012	1	1.328609418E-03	2.657218836E-03
DMIG*	DAMP102		20013	1	
*		20013	1	2.657218836E-03	5.314437672E-03
DMIG*	DAMP102		20014	1	
*		20014	1	1.328609418E-03	2.657218836E-03
DMIG*	DAMP102		20015	1	
*		20015	1	2.657218836E-03	5.314437672E-03
DMIG*	DAMP102		20016	1	
*		20016	1	6.643047091E-04	1.328609418E-03
DMIG*	DAMP103		20008	1	
*		20008	1	2.657218874E-01	5.314437747E-01
DMIG*	DAMP103		20009	1	
*		20009	1	5.314437747E-01	1.062887549E+00
DMIG*	DAMP103		20010	1	
*		20010	1	2.657218874E-01	5.314437747E-01
DMIG*	DAMP103		20011	1	
*		20011	1	5.314437747E-01	1.062887549E+00
DMIG*	DAMP103		20012	1	
*		20012	1	2.657218874E-01	5.314437747E-01
DMIG*	DAMP103		20013	1	
*		20013	1	5.314437747E-01	1.062887549E+00
DMIG*	DAMP103		20014	1	
*		20014	1	2.657218874E-01	5.314437747E-01
DMIG*	DAMP103		20015	1	
*		20015	1	5.314437747E-01	1.062887549E+00
DMIG*	DAMP103		20016	1	
*		20016	1	1.328609437E-01	2.657218874E-01

DTI, AERO, 0, 1

DTI, AERO, 1, 0, 0, 1., 0, 0, ENDREC

DTI	AERO	2	1.0	12.566	1.0	18.850	1.03769.911
DMI*	DMI0000			2		123	1.250000000E+00
DMI	DMI0000	0	2	1	0		2624 2624
DMI*	DMI0001			2		27	1.250000000E+00
DMI*	DMI0001			8		33	5.000000000E+00
DMI*	DMI0001			14		39	2.500000000E+00
DMI*	DMI0001			20		45	5.000000000E+00
DMI*	DMI0001			26		51	2.500000000E+00
DMI*	DMI0001			32		57	5.000000000E+00
DMI*	DMI0001			38		63	2.500000000E+00
DMI*	DMI0001			44		69	5.000000000E+00
DMI*	DMI0001			50		75	2.500000000E+00
DMI*	DMI0001			56		81	5.000000000E+00
DMI*	DMI0001			62		87	2.500000000E+00
DMI*	DMI0001			68		93	5.000000000E+00

DMI*	DMI0001				74		99	2.500000000E+00
DMI*	DMI0001				80		105	5.000000000E+00
DMI*	DMI0001				86		111	2.500000000E+00
DMI*	DMI0001				92		117	5.000000000E+00
DMI	DMI0001	0	2	1	0			
DMI	SUPER	0	2	1	0			
DMI*	SUPER				1			
*	1.000000000E+00							
\$								
ENDDATA								

**APPENDIX C3.4 : Run 3.4 Input - Two-Dimensional Fluid/Beam Model**

```

$$$$$$$$$$$$$$$$$$$$$$$$$$$$$$$$$$$$$$$$$$$$$$$$$$$$$$$$$$$$
$$$$$ AREA MATRIX PROGRAM - USER INPUT $$$$$
$$$$$$$$$$$$$$$$$$$$$$$$$$$$$$$$$$$$$$$$$$$$$$$$$$$$$$$$$$$$
$
$ TOL1,TOL2
  1.,0.
$ IFF,FF
  1,1.
$ SEARCH REGION
  N
$ SELECT ABSORPTION AREAS
  -1,1
$ INPUT THE NUMBER OF FREQ AT WHICH THE
$ ABSORPTION WILL BE SPECIFIED
  3
$ INPUT THE FREQUENCIES
  2.,3.,600.
$ INPUT THE RHO*SPEED OF SOUND FOR FLUID
  5.645
$ INPUT THE REAL AND IMAGINARY COMPONENTS
$ FOR THE SPECIFIC ADMITTANCE - REGION 1
  2.E-3,3.E-3
  3.E-3,6.E-3
  6.E-1,1.2
$$$$$$$$$$$$$$$$$$$$$$$$$$$$$$$$$$$$$$$$$$$$$$$$$$$$$$$$$$$$

```

```

NASTRAN DBSET 1=(DB01,DB15),DBSET 2=(DB01,DB15) $
NASTRAN DBSET 15=(DB15) $
NASTRAN REAL=0,HICORE=300000 $
ID FLUID STRUCTURE
SOL 71
TIME 30
DIAG 8,13

```

```

$$$$$$$$$$$$$$$$$$$$$$$$$$$$$$$$$$$$$$$$$$$$$$$$$$$$$$$$$$$$
$$$$$$$$$$$$$$$$$$$$$$$$$$$$$$$$$$$$$$$$$$$$$$$$$$$$$$$$$$$$
$
$ USER INSTRUCTIONS:
$
$ 1. THE USER MUST INSERT THE DMAP.DAT DATA GENERATED BY THE
$ AREA MATRIX FORTRAN PROGRAM IN THE DMAP SEQUENCE. THE
$ LOCATION IS SHOWN BELOW.
$
$ 2. ALSO THE USER MUST INSERT THE DMI.DAT DATA GENERATED BY
$ THE AREA MATRIX FORTRAN PROGRAM IN THE BULK DATA DECK.
$ THE LOCATION IS SHOW IN THE BULK DATA DECK.
$
$ 3. IF ABSORPTION DAMPING DATA, DMIG.DAT, GENERATED BY THE
$

```

```

$      AREA MATRIX PROGRAM EXIST THE USER MUST ALSO INCLUDE      $
$      THIS DATA IN THE BULK DATA DECK.  THE LOCATION IS SHOW  $
$      IN THE BULK DATA DECK.                                     $
$                                                                 $
$$$$$$$$$$$$$$$$$$$$$$$$$$$$$$$$$$$$$$$$$$$$$$$$$$$$$$$$$$$$$$$$
$                                                                 $
$      ***** BEGIN OF THE ALTER PACKAGE FOR FSI ANALYSIS ***** $
$                                                                 $
$$$$$$$$$$$$$$$$$$$$$$$$$$$$$$$$$$$$$$$$$$$$$$$$$$$$$$$$$$$$$$$$
$
$  INSERT THE DMAP.DAT HERE
$
$  INSERT THE DMAP ALTER HERE
$
CEND
TITLE = COUPLED FLUID-STRUCTURE FREQUENCY RESPONSE
SUBTITLE = 3% BEAM, 2% FLUID DAMPING
LABEL = LINEARLY VARYING ABSORPTION - NORF=1
$
SET 99 = 1,0
SET 67 = 21216
SET 65 = 0
$
SELG = ALL
SELR = ALL
SEDR = 65
$
SPC = 1
VELO = 67
FREQ = 1
SDAMPING = 1
$
SUBCASE 1
  SUPER = 99
  LOADSET = 11
  DLOAD = 21
$
OUTPUT(XY PLOT)
CSCALE 4.0
XPAPER = 105.
YPAPER = 80.
XAXIS = YES
YAXIS = YES
XGRIDLINES = YES
YGRIDLINES = YES
XMIN = 0.
XMAX = 400.
YMIN = -30.
YMAX = 30.
XTITLE = FREQUENCY (HZ)
YTITLE = PRESSURE (PSI)
TCURVE = PRESSURE AT GRID 21216
XY PLOT VELO / 21216(T1RM)
BEGIN BULK
$
$  DEFINE PARAMETERS
$
PARAM,NORF,1          $  RESIDUAL FLEXIBILITY FOR FLUID

```

```

PARAM, SMALL, 0.
PARAM, LMODES, 100
PARAM, DLOAD, -1
$
$ DEFINE THE DYNAMIC LOADS
$
FREQ1, 1, 5., 1., 395
$
FORCE, 1, 10008., 1000., 1.
LSEQ, 11, 101, 1
$
RLOAD1, 21, 101., 1
$
TABLED1, 1., 1000., 1., ENDT
+TD1, 0., 1., 1000., 1., ENDT
$
$ DEFINE MODAL DAMPING FOR FLUID AND BEAM
$ 2% FOR FLUID AND 3% FOR THE BEAM
$ NOTE: THE FLUID MODAL DAMPING IS DEFINED IN
$ THE THIRD QUADRANT, i.e. -FREQ AND -DAMPING
$
TABDMP1, 1., 1000., -0.04, 0., -0.04, 1., +0.06, 1000., +0.06, +TAB2
+TAB1, -1000., -0.04, 0., -0.04, 1., +0.06, 1000., +0.06, +TAB2
+TAB2, ENDT
$
$ INSERT DMI.DAT HERE
$
DMIG    DAMP101 0      6      3      0
DMIG    DAMP102 0      6      3      0
DMIG    DAMP103 0      6      3      0
DMIG*   DAMP101      20008      1
*        1 8.857396315E-04 1.771479263E-03
DMIG*   DAMP101      20009      1
*        1 1.771479263E-03 3.542958526E-03
DMIG*   DAMP101      20010      1
*        1 8.857396315E-04 1.771479263E-03
DMIG*   DAMP101      20011      1
*        1 1.771479263E-03 3.542958526E-03
DMIG*   DAMP101      20012      1
*        1 8.857396315E-04 1.771479263E-03
DMIG*   DAMP101      20013      1
*        1 1.771479263E-03 3.542958526E-03
DMIG*   DAMP101      20014      1
*        1 8.857396315E-04 1.771479263E-03
DMIG*   DAMP101      20015      1
*        1 1.771479263E-03 3.542958526E-03
DMIG*   DAMP101      20016      1
*        1 4.428698157E-04 8.857396315E-04
DMIG*   DAMP102      20008      1
*        1 1.328609418E-03 2.657218836E-03
DMIG*   DAMP102      20009      1
*        1 2.657218836E-03 5.314437672E-03
DMIG*   DAMP102      20010      1
*        1 1.328609418E-03 2.657218836E-03
DMIG*   DAMP102      20011      1
*        1 2.657218836E-03 5.314437672E-03
DMIG*   DAMP102      20012      1
*        1 1.328609418E-03 2.657218836E-03

```

DMIG*	DAMP102		20013		1				
*				1	2.657218836E-03	5.314437672E-03			
DMIG*	DAMP102		20014		1				
*				1	1.328609418E-03	2.657218836E-03			
DMIG*	DAMP102		20015		1				
*				1	2.657218836E-03	5.314437672E-03			
DMIG*	DAMP102		20016		1				
*				1	6.643047091E-04	1.328609418E-03			
DMIG*	DAMP103		20008		1				
*				1	2.657218874E-01	5.314437747E-01			
DMIG*	DAMP103		20009		1				
*				1	5.314437747E-01	1.062887549E+00			
DMIG*	DAMP103		20010		1				
*				1	2.657218874E-01	5.314437747E-01			
DMIG*	DAMP103		20011		1				
*				1	5.314437747E-01	1.062887549E+00			
DMIG*	DAMP103		20012		1				
*				1	2.657218874E-01	5.314437747E-01			
DMIG*	DAMP103		20013		1				
*				1	5.314437747E-01	1.062887549E+00			
DMIG*	DAMP103		20014		1				
*				1	2.657218874E-01	5.314437747E-01			
DMIG*	DAMP103		20015		1				
*				1	5.314437747E-01	1.062887549E+00			
DMIG*	DAMP103		20016		1				
*				1	1.328609437E-01	2.657218874E-01			

DTI, AERO, 0, 1

DTI, AERO, 1, 0, 0, 1., 0, 0, ENDREC

DTI	AERO	2		1.0	12.566		1.0	18.850		1.03769.911
DMI*	DMI0000				2			123	1.250000000E+00	
DMI	DMI0000	0	2	1	0				2624	2624
DMI*	DMI0001				2			27	1.250000000E+00	
DMI*	DMI0001				8			33	5.000000000E+00	
DMI*	DMI0001				14			39	2.500000000E+00	
DMI*	DMI0001				20			45	5.000000000E+00	
DMI*	DMI0001				26			51	2.500000000E+00	
DMI*	DMI0001				32			57	5.000000000E+00	
DMI*	DMI0001				38			63	2.500000000E+00	
DMI*	DMI0001				44			69	5.000000000E+00	
DMI*	DMI0001				50			75	2.500000000E+00	
DMI*	DMI0001				56			81	5.000000000E+00	
DMI*	DMI0001				62			87	2.500000000E+00	
DMI*	DMI0001				68			93	5.000000000E+00	
DMI*	DMI0001				74			99	2.500000000E+00	
DMI*	DMI0001				80			105	5.000000000E+00	
DMI*	DMI0001				86			111	2.500000000E+00	
DMI*	DMI0001				92			117	5.000000000E+00	
DMI	DMI0001	0	2	1	0				2624	122
DMI	SUPER	0	2	1	0				2	1
DMI*	SUPER				1			1	0.000000000E+00	
*									1.000000000E+00	

\$

ENDDATA



BEGIN BULK  
PARAM, EQUAL, 0  
DMIG, PDOF, 0, 6, 1, 0  
DMIG, PDOF, 21216, 1, , 21216, 1, 1.  
ENDDATA



**APPENDIX D : INPUT DECKS FOR SECTION 8**

**APPENDIX D1 : Run 1 Input - Vehicle Acoustic Analysis**

---

```
*****
** R U N 1 **
*****

ID FLUID STRUCTURE
SOL 63
TIME 500
DIAG 8,13
READ 9 $ FSI.63 !!! NOTE !!! THIS MUST BE IMMEDIATELY BEFORE CEND
CEND
TITLE = FLUID-STRUCTURE INTERACTION
SUBTITLE = NORMAL MODES ANALYSIS
SEALL = ALL
SPC = 111
$
$ DEFINE ALL THE SUPERELEMENT ID'S EXCEPT 0
$
SET 65 =
DISP(PLOT) = ALL
SUBCASE 1
  SUPER = 1
  METHOD = 1
$
$ DEFINE THE PARTITION VECTOR FOR THE FLUID
$
SET 66 = 100000 THRU 101000
$
SUBCASE 11
  LABEL = RESIDUAL STRUCTURE MODEL
  LOADSET = 11
  PARAM,COUPMASS,1
  PARTN = 66
  METHOD = 11
SUBCASE 12
  LABEL = FLUID MODEL
  METHOD = 12
BEGIN BULK
$
$ DEFINE THE STRUCTURE MODEL
$
=====
$
$ DEFINE THE FLUID MODEL
$
LSEQ,11,101,1
LSEQ,11,102,2
LSEQ,11,103,3
LSEQ,11,104,4
$
$ DEFINE THE EIGENVALUE EXTRACTION DATA FOR THE
$ FLUID
```

```

$
EIGRL,12,-1.,,10,1
SPC1      111      23456 100000      THRU 101000
$ MN12 EP2 ACOUSTIC MODEL UPDATE 2
PSOLID 100001 100001      2
PSOLID 100002 100002      2
PSOLID 100003 100002      2
MAT9      100001 8317.E8
+MMT1A
+MMT1A
+MMT1B
+MMT1B      8317.E8      8317.E8 7.058+3
MAT9      100002 7994.E7
+MMT2A
+MMT2A
+MMT2B
+MMT2B      7994.E7      7994.E7 7.058+3
GRID      100001      2023.15 443.730 519.240
.
.
.
GRID      100947      2912.00 400.000 460.590
CPENTA 100001 100001 100207 100212 100508 100203 100216 100585
+EACU674 100109 100120
.
.
.
CHEXA      100675 100001 100107 100102 100947 100946 100109
100104+EACU675
+EACU675 100122 100120
CPENTA 100676 100001 100947 100102 100103 100122 100104 100105
$
$
$ DEFINE THE PRESSURE LOAD ON THE FLUID TO
$ CALCULATE THE AREAS
$
PLOAD4      1 100001      1.      100212 100203
.
.
.
PLOAD4      1 100676      1.      100122
$
$ THIS PRESSURE LOAD DEFINES THE ABSORPTION AREA FOR THE ROOF
$
PLOAD4      2 100002      1.      100207 100190
.
.
.
PLOAD4      2 100569      1.      100236 100413
$
$ THIS PRESSURE LOAD DEFINES THE ABSORPTION AREA FOR THE FLOOR
$
PLOAD4      3 100084      1.      100302 100299
.
.
.
PLOAD4      3 100676      1.      100103 100104
$

```

```
$ THIS PRESSURE LOAD DEFINES THE ABSORPTION AREA FOR THE TRUNK LID
$
PLOAD4      4 100041    1.                100353 100555
.
.
.
PLOAD4      4 100605    1.                100465 100390
ENDDATA
```

## APPENDIX D3.1 : Run 3.1 Input - Vehicle Acoustic Analysis

---

\*\*\*\*\*  
\*\* R U N 3.1 \*\*  
\*\*\*\*\*

```
NASTRAN DBSET 1=(DB01,DB02),DBSET 2=(DB01,DB02) $
NASTRAN DBSET 15=(DB02) $
BUFFSIZE=9217 $
ID ACUSTIC, TWO
TIME 1000
DIAG 8
$
$ *** INSERT SOL71 DMAP ALTER HERE
$
READ 9 $ FSI.71 !!! NOTE !!! THIS MUST BE IMMEDIATELY BEFORE CEND
CEND
TITLE = FREQUENCY RESPONSE CALCULATION
SUBTITLE = 3% MODAL DAMPING
$
SET 99 = 0
SELG = 99
SEDR = 99
$
SET 66 = 100597
VELO(PHASE) = 66
$
FREQ = 1
SDAMP = 1
$
SUBCASE 11
  LABEL = DRIVE SHAFT UNBALANCE
  LOADSET = 33
  DLOAD = 201
OUTPUT(XYPLOT)
SEPLOT 0
CSCALE 4.0
XPAPER=105.
YPAPER=80.
XAXIS=YES
YAXIS=YES
XGRID LINES=YES
YGRID LINES=YES
YLOG = YES
XDIVISIONS = 9
XTITLE = FREQUENCY (HZ)
YTITLE = PRESSURE
TCURVE = PRESSURE AT DRIVERS EAR (GRID 100597)
XYPLOT VELO / 100597(T1RM)
BEGIN BULK
$
$ DEFINE PARAMETERS
$
PARAM, SMALL, 0.
```

```

PARAM,LMODES,2000
PARAM,DLOAD,-1
PARAM,RESDUAL,-1
$
$ DEFINE LOADS
$
FREQ1,1,10.,1.,90
$
DAREA,201,32818,3,1.
DAREA,202,9261,3,1.
DAREA,203,35174,3,1.
DAREA,204,11927,3,1.
$
RLOAD1,21,201,,,1
RLOAD1,22,202,,,1
RLOAD1,23,203,,,1
RLOAD1,24,204,,,1
$
DLOAD,201,1.,1.,21.1.,22.1.,23
+,1.,24
DLOAD,202,1.,-1.,21.1.,22.1.,23
+,-1.,24
TABLED1,1
+,0.,3.536+10,1000.,3.536+10,ENDT
$
$ DEFINE DAMPING
$
TABDMP1,1
+,-1000.,-.06,0.,-.06,1.-6,+0.06,1000.,+.06
+,ENDT
$
$ INSERT DMI.DAT HERE
$
include(DMI)
ENDDATA

```

## APPENDIX D4 : Run 4 Input - Vehicle Acoustic Analysis

\*\*\*\*\*

\*\* R U N 4 \*\*

\*\*\*\*\*

```
NASTRAN DBSET 1=(DB01,DB02,DB15),DBSET 2=(DB01,DB02,DB15) $
NASTRAN DBSET 15=(DB02,DB15) $
NASTRAN BUFFSIZE=9217 $
ID FLUID STRUCTURE
TIME 30
DIAG 8,13
READ 9 $ FSI.71R !!! NOTE !!! THIS MUST BE IMMEDIATELY BEFORE CEND
CEND
TITLE = AUTOMOBILE ACOUSTIC ANALYSIS - MODAL DAMPING ONLY
SUBTITLE = PARTICIPATION FACTOR CALCULATION FOR DRIVERS EAR
$
$ INSERT SET.DAT HERE
$
include(SET)
DISP = 911
SET 912 = 64., 86.
OFREQ = 912
SUBCASE 11
    LABEL = DRIVE SHAFT UNBALANCE
BEGIN BULK
DMIG,PDOF,0,6,1,0
DMIG,PDOF,100597,1,,100597,1,1.
ENDDATA
```

## References

---

1. Zienkiewics, O. C.: *Finite Elements in Fluid Mechanics - A Decade of Progress. Finite Elements in Fluids*, Volume 5, Gallagher, R.H. et al., eds., 1984, J.Wiley.
2. Gallagher, R. H. et al., eds.: *Finite Elements in Fluids*, Volumes 1 - 5, J. Wiley 1985.
3. Gladwell, G.M.L.; and Zimmermann, G.: *On Energy and Complementary Energy Formulations of Acoustic and Structural Vibration Problems*. J. Sound and Vibration, vol. 3, no. 3, 1966, pp. 233-241.
4. Gladwell, G.M.L.: *A Variational Formulation of Damped Acousto-Structural Vibration Problems*. J. Sound and Vibration, vol. 4, no. 2, 1966, pp. 172-186.
5. Craggs, A.: *The Transient Response of Coupled Plate Acoustic Systems Using Plate and Acoustic Finite Elements*. J. Sound and Vibration, vol. 15, no. 4, 1971, pp. 509-528.
6. Craggs, A.: *The Use of Simple Three-Dimensional Acoustic Finite Elements for Determining the Natural Modes and Frequencies of Complex Shaped Enclosures*. J. Sound and Vibration, vol. 23, no. 2, 1972, pp. 231-339.
7. Craggs, A.: *An Acoustic Finite Element Approach for Studying Boundary Flexibility and Sound Transmission Between Irregular Enclosures*. J. Sound and Vibration, Volume 30, no. 3, pp. 347-357, 1973.
8. Everstine, G.C.: *Structural Analogies for Scalar Field Problems*. Int. J. Numerical Methods in Engineering, vol. 17, no. 3, 1981, pp. 471-476.
9. Kalinowski, A.J.: *Fluid-Structure Interaction Problems Using Finite Elements*, Proceedings of the Fifth Navy-NASTRAN Colloquium, CMD-32-74, Naval Ship Research and Development Center, Bethesda, Maryland, DDC Rep. ADA 004604, 1974, pp. 71-86.
10. Wolf, J.A.; and Nefske, D.J.: *NASTRAN Modeling and Analysis of Rigid and Flexible Walled Acoustic Cavities*. Fourth NASTRAN User's Colloquium, Langley Research Center, Hampton, Virginia, Sept. 1975.



11. Raasch, I.: *Procedures to Solve Acoustic Problems with MSC/NASTRAN*. MSC/NASTRAN User's Conference, Munich, West Germany, June, 1981.
12. Nefske, D.J.; Wolf, J.A.; and Howell, L.J.: *Structural-Acoustic Finite Element Analysis of the Automobile Passenger Compartment: A Review of Current Practice*. J. Sound and Vibration, vol. 80, no. 2, 1982, pp. 247-266.
13. Nefske, D.J.; and Sung, S.H.: *Automobile Interior Noise Prediction Using a Coupled Structural Acoustic Finite Element Model*. Proceedings of the 11th Congress on Acoustics, Paris, 1983.
14. Nefske, D.J.; and Sung, S.H.: *Vehicle Interior Acoustic Design Using Finite Element Methods*. Int. J. Vehicle Design, vol. 6, no. 1, 1985, pp. 24-40.
15. Burfeindt, H.; Kluczynski, G.; Zimmer, H.; and Sarfeld, W.: *Akustik-Berechnungen auf der Basis der Finite Elemente Methode*. Automobil-Industrie, vol. 5, 1986, pp. 589-597.
16. Bliss, D.B.: *Study of Bulk Reacting Porous Sound Absorbers and a New Boundary Condition for Thin Porous Layers*. J. Acoustical Society of America, vol. 71, no. 3, 1982, pp. 533-545.
17. Craggs, A.: *A Finite Element Model for Rigid Porous Absorbing Materials*. J. Sound and Vibration, vol. 61, no. 1, 1978, pp. 101-111.
18. Craggs, A.: *A Finite Element Method for Modelling Dissipative Mufflers with a Locally Reactive Lining*. J. Sound and Vibration, vol. 54, no. 2, 1977, pp. 285-296.
19. Cole, R.H.: *Underwater Explosions*, Princeton University Press, 1948.
20. Sandberg, G.: *Finite Element Modelling of Fluid-Structure Interaction*. Lund Inst. of Tech., Rep. TVSM-1002, Lund 1986.
21. Zienkiewicz, O.C.; and Newton, R.E.: *Coupled Vibration of a Structure Submerged in a Compressible Fluid*. ISD International Ship Structure Congress on FEM, Stuttgart, 1969.
22. Irons, B.M.: *Role of Part-Inversion in Fluid-Structure Problems with Mixed Variables*. AIAA Journal, vol. 8, no. 3, 1970, p. 568.
23. MacNeal, R.H.: *Three Dimensional Acoustic Analysis With MSC/NASTRAN*, MSC Internal Memo No. RHM-70, Dec. 20, 1978.

24. MacNeal, R.H.; Citerley, R.; and Chargin, M.: *A New Method for Analyzing Fluid-Structure Interaction Using MSC/NASTRAN*. Trans. 5th Int. Conf. on Structural Mechanics in Reactor Technology, Paper B4/9, Aug. 13-17, 1979.
25. MacNeal, R.H.; Citerley, R.; and Chargin, M.: *A Symmetric Modal Formulation of Fluid-Structure Interaction, Including a Static Approximation to Higher Order Fluid Modes*. ASME 80-C2/PVP 116, ASME Century 2 Pressure Vessel and Piping Conf., San Francisco, California, Aug. 12-15, 1980.
26. Jeanpierre, F.; Gilbert, R.F.; Hoffman, A.; and Livolant, M.: *Description of a General Method to Compute the Fluid-Structure Interaction*. Trans. 5th Int. Conf. on Structural Mechanics in Reactor Technology, Paper B4/1, Aug. 13-17, 1979.
27. Morand, H.; and Ohayon, R.: *Substructure Variational Analysis of the Vibrations of Coupled Fluid Structure Systems, Finite Element Results*. Int. J. Numerical Methods in Engineering, vol. 14, no. 5, 1979, pp. 741-755.
28. Everstine, G.C.: *A Symmetric Potential Formulation for Fluid-Structure Interaction*. J. Sound and Vibration, vol. 79, no. 1, 1981, pp. 157-160.
29. Sandberg, G.; and Göransson, P.: *A Symmetric Finite Element Formulation for Acoustic Fluid Structure Interaction Analysis*. J. Sound and Vibration, vol. 123, no. 3, 1988, pp. 507-515.
30. Herting, D.N.: *Formulation of Hydroelastic Analysis Using Fluid Model Residuals*, MSC Internal Memo No. DNH-49, Jan. 22, 1988.
31. Izadpaneh, K.; Kansakar, R.; Reymond, M.; and Wallerstein, D.: *Coupled Fluid-Structure Interaction Analysis using MSC/NASTRAN*. Proceedings of the 16th MSC/NASTRAN European User's Conference, London, UK, 1989.
32. Göransson, P.: *ASKA Acoustics, Theory and Applications*, FFA TN 1988-13, Stockholm.
33. Shin, Y.S.; and Chargin, M.: *Acoustic Responses of Coupled Fluid-Structure System by Acoustic-Structural Analogy*. Shock and Vibration Bulletin, vol. 53, 1983, pp. 11-21.
34. Everstine, G.C.; Schroeder, E.A.; and Marcus, M.S.: *The Dynamic Analysis of Submerged Structures NASTRAN: Users' Experiences*. NASA TM X-3278, 1975.

35. Everstine, G.C.: *NASTRAN Implementation of the Doubly Asymptotic Approximation for Underwater Shock Responses*. NASA TM X-3428, 1976.
36. Nefske, D.J.: *Acoustic Finite Element Analysis of Automobile Passenger Compartment With Absorption Materials*. Noise-Con 85, June 3-5, 1985, Ohio State University.



# Report Documentation Page

1. Report No. NASA TM-102857	2. Government Accession No.	3. Recipient's Catalog No.	
4. Title and Subtitle A Finite Element Procedure for Calculating Fluid-Structure Interaction Using MSC/NASTRAN		5. Report Date December 1990	6. Performing Organization Code
		7. Author(s) Mladen Chargin and Otto Gartmeier (Daimler-Benz AG, Stuttgart, Germany)	8. Performing Organization Report No. A-90262
9. Performing Organization Name and Address Ames Research Center Moffett Field, CA 94035-1000		10. Work Unit No. 505-63-01	11. Contract or Grant No.
		13. Type of Report and Period Covered Technical Memorandum	
12. Sponsoring Agency Name and Address National Aeronautics and Space Administration Washington, DC 20546-0001		14. Sponsoring Agency Code	
		15. Supplementary Notes Point of Contact: Mladen Chargin, Ames Research Center, MS 213-3, Moffett Field, CA 94035-1000 (415) 604-6248 or FTS 464-6248	
16. Abstract <p>This report is intended to serve two purposes. The first is to give a survey of the theoretical background of the dynamic interaction between a non-viscid, compressible fluid and an elastic structure. Section 1 presents a short survey of the application of finite element method (FEM) to the area of fluid-structure-interaction (FSI). Section 2 describes the mathematical foundation of the structure and fluid with special emphasis on the fluid. The main steps in establishing the finite element (FE) equations for the fluid structure coupling are discussed in section 3. The second purpose of this report is to demonstrate the application of MSC/NASTRAN to the solution of FSI problems. Some specific topics, such as fluid structure analogy, acoustic absorption, and acoustic contribution analysis are described in section 4. Section 5 deals with the organization of the Acoustic Procedure implemented in MSC/NASTRAN. Steps which have to be performed for a complete acoustic analysis are illustrated by a flowchart. Section 6 includes the most important information that a user needs for applying the Acoustic Procedure to practical FSI problems. Beginning with some rules concerning the FE modelling of the coupled system, the NASTRAN USER DECKS for the different steps are described. The goal of section 7 is to demonstrate the use of the Acoustic Procedure with some examples. This demonstration includes an analytic verification of selected FE results. The analytical description considers only some aspects of FSI and is not intended to be mathematically complete. Finally, section 8 presents an application of the Acoustic Procedure to vehicle interior acoustic analysis with selected results.</p>			
17. Key Words (Suggested by Author(s)) Acoustics Vibration analysis Finite element analysis		18. Distribution Statement Unclassified-Unlimited  Subject Category - 39	
19. Security Classif. (of this report) Unclassified	20. Security Classif. (of this page) Unclassified	21. No. of Pages 190	22. Price A09